



Letter

Observation of $t\bar{t}\gamma\gamma$ production at $\sqrt{s} = 13$ TeV with the ATLAS detectorThe ATLAS Collaboration¹

ARTICLE INFO

Editor: Dr. M. Doser

Keywords:

Top-quark pair production in association with two photons

ABSTRACT

This paper presents the first observation of top-quark pair production in association with two photons ($t\bar{t}\gamma\gamma$). The measurement is performed in the single-lepton decay channel using proton-proton collision data collected by the ATLAS detector at the Large Hadron Collider. The data correspond to an integrated luminosity of 140 fb^{-1} recorded during Run 2 at a centre-of-mass energy of 13 TeV. The $t\bar{t}\gamma\gamma$ production cross section, measured in a fiducial phase space based on particle-level kinematic criteria for the lepton, photons, and jets, is found to be $2.42^{+0.58}_{-0.53} \text{ fb}$, corresponding to an observed significance of 5.2 standard deviations. Additionally, the ratio of the production cross section of $t\bar{t}\gamma\gamma$ to top-quark pair production in association with one photon is determined, yielding $(3.30^{+0.70}_{-0.65}) \times 10^{-3}$.

1. Introduction

Measurements of top-quark pair production ($t\bar{t}$) in association with neutral vector bosons (γ , Z boson) allow a direct probe of the electroweak couplings of the top quark. In particular, the associated production of top quarks with photons is a probe of the top-quark-photon coupling. These measurements provide access to the electric charge and the electroweak dipole moments of the top quark and, more generally, allow constraints on modifications of the structure of these couplings relative to the Standard Model predictions [1–4].

The production of $t\bar{t}$ in association with a single photon ($t\bar{t}\gamma$), for which evidence was first reported by the CDF Collaboration [5], has been studied in detail by the ATLAS and CMS Collaborations. Inclusive and differential production cross-section measurements were performed at centre-of-mass energies (\sqrt{s}) ranging from 7 to 13 TeV, in both the dilepton and single-lepton $t\bar{t}$ decay channels [6–12]. Recent measurements by the ATLAS Collaboration focus specifically on the production of $t\bar{t}\gamma$ events, where the photon arises from initial-state radiation or an off-shell top quark, measuring inclusive and differential cross sections [13] and the $t\bar{t}$ charge asymmetry in $t\bar{t}\gamma$ events [14]. However, the associated production of $t\bar{t}$ events with two photons ($t\bar{t}\gamma\gamma$), a much rarer process with an expected production cross section at the per mille level compared to $t\bar{t}\gamma$, was not specifically studied. In $t\bar{t}\gamma\gamma$ final states, the photons can be emitted by any charged particle: the initial-state partons, the top quarks or the top quark decay products (including the W boson and W boson decay products). Example Feynman diagrams for $t\bar{t}\gamma\gamma$ production are shown in Fig. 1. The $t\bar{t}\gamma\gamma$ process has been discussed in several recent calculations with stable top quarks and including the decays at parton level [15–17]. It represents a relevant irreducible background for the measurements of the production of the Higgs boson in associa-

tion with $t\bar{t}$ ($t\bar{t}H$), where the Higgs boson decays into two photons. It could additionally be a handle to further constrain the anomalous chromomagnetic and chromoelectric dipole moments [18]. The ratio of the cross section between the $t\bar{t}\gamma\gamma$ and $t\bar{t}\gamma$ processes is also proposed as an observable to constrain the anomalous dipole moments.

This paper presents the first measurement of the $t\bar{t}\gamma\gamma$ fiducial cross section and the ratio of the $t\bar{t}\gamma\gamma$ and $t\bar{t}\gamma$ cross sections. Processes such as $t\bar{t}\gamma$ and $t\bar{t}\gamma\gamma$, including photons radiated from any charged particles in the initial or final states, cannot currently be simulated at high-order accuracy using matrix-element (ME) generators interfaced with parton shower (PS) simulations. Moreover, the previously mentioned $t\bar{t}\gamma\gamma$ theoretical calculations cannot be directly compared with measurements. Therefore, the main goal of this paper is to provide a first reference measurement for future theoretical developments, instead of putting the emphasis on comparisons with the existing simulations. The measurements are performed by selecting $t\bar{t}$ single-lepton final states, characterised by one high-transverse-momentum (p_T) lepton and at least four jets, two of which arise from b -quarks (b -jets), and by requiring the presence of exactly two high- p_T photons. They are measured using the full data set recorded by the ATLAS detector at the Large Hadron Collider (LHC) between 2015 and 2018 at $\sqrt{s} = 13$ TeV, corresponding to an integrated luminosity of 140 fb^{-1} [19]. The background processes comprise events with genuine photons and events with fake photons. These processes are estimated by using a combination of simulation and data-driven methods. The output of a boosted decision tree (BDT) classifier, trained to separate signal and background processes, is used as the observable for the measurements. In particular, the cross section is measured in a fiducial phase space at particle level using a profile likelihood fit to the BDT output. The fiducial phase space is defined by requiring exactly two photons, one electron or muon, and at least four jets, in-

Contact: atlas.publications@cern.ch.¹ Authors are listed at the end of this paper.

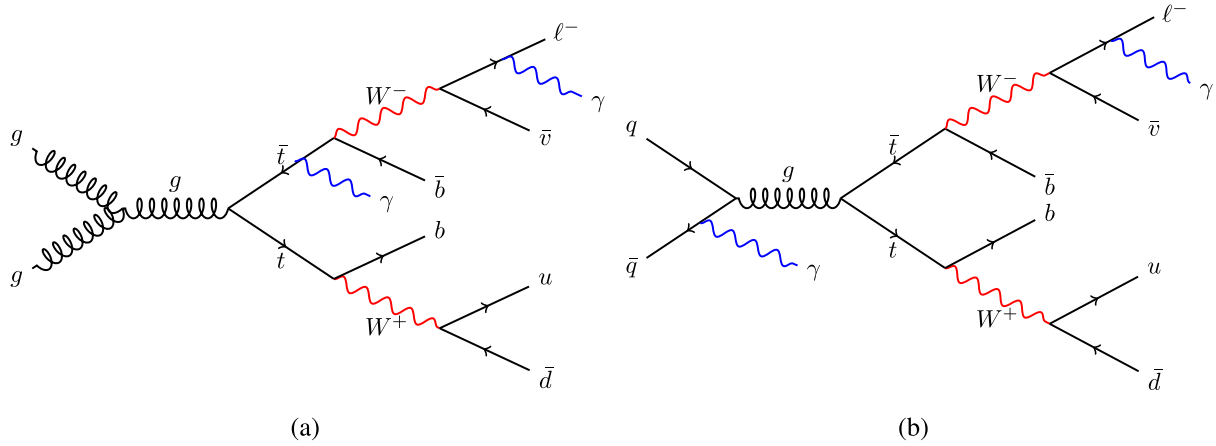


Fig. 1. Examples of leading-order Feynman diagrams for $t\bar{t}\gamma\gamma$ production in the single-lepton $t\bar{t}$ final state, where the photons are radiated by (a) an off-shell top quark and the charged lepton and (b) an initial-state quark and the charged lepton, respectively.

cluding at least one b -jet, closely following the kinematic requirements at reconstruction level. Additionally, the ratio of the $t\bar{t}\gamma\gamma$ to $t\bar{t}\gamma$ cross sections is extracted from a simultaneous measurement, incorporating data and simulation inputs from the $t\bar{t}\gamma$ analysis described in Ref. [13]. This measurement is expected to yield better precision than the cross section owing to the cancellation of normalisation uncertainties.

2. ATLAS detector

The ATLAS experiment [20] at the LHC is a multipurpose particle detector with a forward-backward symmetric cylindrical geometry and a near 4π coverage in solid angle.¹ It consists of an inner tracking detector (ID) surrounded by a thin superconducting solenoid providing a 2 T axial magnetic field, electromagnetic and hadronic calorimeters, and a muon spectrometer. The inner tracking detector covers the pseudorapidity range $|\eta| < 2.5$. It consists of silicon pixel, silicon microstrip, and transition radiation tracking detectors. Lead/liquid-argon (LAr) sampling calorimeters provide electromagnetic (EM) energy measurements with high granularity within the region $|\eta| < 3.2$. A steel/scintillator-tile hadronic calorimeter covers the central pseudorapidity range ($|\eta| < 1.7$). The endcap and forward regions are instrumented with LAr calorimeters for EM and hadronic energy measurements up to $|\eta| = 4.9$. The muon spectrometer surrounds the calorimeters and is based on three large superconducting air-core toroidal magnets with eight coils each. The field integral of the toroids ranges between 2.0 and 6.0 Tm across most of the detector. The muon spectrometer includes a system of precision tracking chambers up to $|\eta| = 2.7$ and fast detectors for triggering up to $|\eta| = 2.4$. The luminosity is measured mainly by the LUCID-2 [21] detector, which is located close to the beampipe. A two-level trigger system is used to select events [22]. The first-level trigger is implemented in hardware and uses a subset of the detector information to accept events at a rate below 100 kHz. This is followed by a software-based trigger that reduced the accepted rate of complete events to 1.25 kHz on average in Run 2 depending on the data-taking conditions. A software suite [23] is used in data simulation, in the reconstruction and analysis of real and simu-

lated data, in detector operations, and in the trigger and data acquisition systems of the experiment.

3. Modelling of signal and background processes

The signal and background processes are modelled using Monte Carlo (MC) simulation samples. The ATLAS detector response is simulated [24] with GEANT4 [25], and some alternative samples for evaluating systematic uncertainties are processed with a fast simulation (ATLFAST-II) relying on calorimeter response parameterisation. All the MC samples described in the following that were generated with either POWHEG-BOX [26–29] or MADGRAPH5_AMC@NLO [30] were interfaced to PYTHIA 8 [31] to simulate the PS, fragmentation, and underlying event. The A14 set of tuned parameters (tune) [32] and the NNPDF2.3LO parton distribution function (PDF) set [33] were used in PYTHIA. The heavy-flavour hadron decays were modelled by EvtGen [34]. Samples generated with SHERPA [35,36] used the SHERPA parton shower with a dedicated tune provided by the authors [37].

The top quark mass was set to 172.5 GeV in the samples. Pile-up effects, additional pp collisions in the same or neighbouring bunch crossings, were simulated by overlaying minimum bias events using PYTHIA 8 [38] with the A3 tune [39]. The MC events were reweighted to match the observed number of interactions per bunch crossing. Additionally, corrections for trigger, reconstruction and selection efficiencies, and energy scales are applied to MC events to improve the description of the data.

The signal $t\bar{t}\gamma\gamma$ process was simulated as a $2 \rightarrow 8$ process² with MADGRAPH5_AMC@NLO 2.9.9 at leading-order (LO) in quantum chromodynamics (QCD) with the NNPDF3.0NLO set of PDFs [40]. Diagrams where photons are radiated from the initial state, the top quarks, or their charged decay products are considered. The event generation is interfaced to PYTHIA 8.306 [41]. The renormalisation and factorisation scales were set to $0.5 \times \sum_i \sqrt{m_i^2 + p_{T,i}^2}$, where m_i and $p_{T,i}$ are the masses and transverse momenta of the particles generated from the ME calculation. Photons were required to have $p_T > 15$ GeV and to be isolated according to a smooth-cone hadronic isolation criterion with $\delta_0 = 0.1$, $\epsilon_\gamma = 0.1$ and $n = 2$, defined in Ref. [42], to avoid infrared divergences. Leptons and quarks at the ME level are required to have a minimum transverse momentum of 4 GeV and 1 GeV respectively. The normalisation of the LO $2 \rightarrow 8$ $t\bar{t}\gamma\gamma$ sample is rescaled using a K -factor calculated from two $pp \rightarrow$

¹ ATLAS uses a right-handed coordinate system with its origin at the nominal interaction point (IP) in the centre of the detector and the z -axis along the beam pipe. The x -axis points from the IP to the centre of the LHC ring, and the y -axis points upwards. Polar coordinates (r, ϕ) are used in the transverse plane, ϕ being the azimuthal angle around the z -axis. The pseudorapidity is defined in terms of the polar angle θ as $\eta = -\ln \tan(\theta/2)$ and is equal to the rapidity $y = \frac{1}{2} \ln \left(\frac{E+p_z}{E-p_z} \right)$ in the relativistic limit. Angular distance is measured in units of $\Delta R \equiv \sqrt{(\Delta y)^2 + (\Delta \phi)^2}$.

² The 8 final-state particles correspond to the 6 decay products of the $t\bar{t}$ system and the 2 photons.

$t\bar{t}\gamma\gamma$ samples ($2 \rightarrow 4$), in which photons are emitted from either off-shell top quarks or initial-state particles. This process can also be simulated at next-to-leading-order (NLO) in QCD with MADGRAPH5_AMC@NLO, unlike the $2 \rightarrow 8 t\bar{t}\gamma\gamma$ sample. The NLO and LO $2 \rightarrow 4 t\bar{t}\gamma\gamma$ samples are simulated using MADGRAPH5_AMC@NLO interfaced with PYTHIA 8, with the same parameters as the nominal sample. The expected cross sections in the fiducial phase space at particle level described in Section 6 are $0.733^{+0.073}_{-0.080}(\text{scale})^{+0.016}_{-0.008}(\text{PDF})$ fb and $0.423^{+0.070}_{-0.090}(\text{scale})^{+0.009}_{-0.004}(\text{PDF})$ fb for the NLO and LO $2 \rightarrow 4$ simulations, respectively, corresponding to a K -factor of 1.7.

Top-quark-related processes constitute a background to the $t\bar{t}\gamma\gamma$ signal, as their final states result in topologies with a lepton, jets, b -jets, and either genuine photons or fake photons from misreconstructed objects. The production of vector bosons in association with photons constitutes a background as well, as these events may include b -jets from initial-state radiation. These processes are simulated as described below.

The $t\bar{t}\gamma$ events were simulated as two complementary samples using also the MADGRAPH5_AMC@NLO generator. The first, referred to as ‘ $t\bar{t}\gamma$ production sample’, models photon production from the off-shell top quark or initial-state radiation in a $2 \rightarrow 3$ process at NLO in QCD, with top quark decays at LO using MADSPIN [43,44]. The second, the ‘ $t\bar{t}\gamma$ decay sample’, simulates photon production from on-shell top quarks and their decay products as a $2 \rightarrow 2$ process at LO. Both samples use the NNPDF3.0NLO PDF set. The same photon requirements and renormalisation and factorisation scales as in the $t\bar{t}\gamma\gamma$ sample are set in these samples. The $t\bar{t}\gamma$ production sample is normalised to the NLO cross section given by the MC simulation, while the normalisation of the $t\bar{t}\gamma$ decay sample is corrected by an NLO/LO inclusive K -factor of 1.5, as obtained in Ref. [14].

The production of $t\bar{t}$ and single-top-quark events (t - and s -channels) was modelled at NLO in QCD using POWHEG-BOX [26–29]. For the $t\bar{t}$ sample, the h_{damp} parameter, which controls the p_T of the first additional emission, was set to 1.5 times the top quark mass [45]. The $t\bar{t}$ and single-top-quark simulation samples are normalised to the cross sections calculated at next-to-next-to-leading-order (NNLO) in QCD including the resummation of next-to-next-to-leading-logarithmic (NNLL) soft-gluon terms [46] at NNLO or approximated NNLO [47–49], respectively. The $tW\gamma$ events were generated at LO with MADGRAPH5_AMC@NLO in the five-flavour scheme as two samples: one as a $2 \rightarrow 3$ process with a stable top quark and the other as a $2 \rightarrow 2$ process with photon radiation from final-state charged particles. To avoid infrared divergences, the photon was required to have $p_T > 15$ GeV and $|\eta| < 5.0$ and to be separated by $\Delta R > 0.2$ from any parton. Both $tW\gamma$ samples use the NNPDF2.3LO PDF set and are normalised to MC-predicted cross sections. Events with a $t\bar{t}$ pair produced in association with a W or Z boson ($t\bar{t}V$) were simulated at NLO in QCD with MADGRAPH5_AMC@NLO using the NNPDF3.0NLO PDF set. The simulation of $t\bar{t}H$ events, with the Higgs boson decaying into two photons, was also performed at NLO in QCD with MADGRAPH5_AMC@NLO using the NNPDF3.0NLO PDF set and interfaced to PYTHIA 8.230. The sample is normalised to the total $t\bar{t}H$ NLO cross section times the branching fraction of Higgs boson decays into two photons [50].

Events with V (Z and W) bosons produced in association with one or two photons simulated at ME level, $V\gamma$ and $V\gamma\gamma$, and the production of V + jets and diboson processes were simulated with different versions of SHERPA [35,36] at NLO in QCD using the NNPDF3.0NNLO PDF set. The simulations of $V\gamma\gamma$ and $V\gamma$ are normalised to the cross section provided by the MC simulations, the diboson processes are normalised to cross sections at NLO accuracy in QCD [51], while the V boson samples are normalised to cross sections at NNLO accuracy in QCD [52].

The analysis combines multiple MC samples where the photons are generated either at the ME or the PS step. In particular, the $t\bar{t}\gamma\gamma$ and $V\gamma\gamma$ samples include two photons generated at the ME level with certain kinematic requirements on the photons. A second set of samples — $t\bar{t}\gamma$ production and decay, $tW\gamma$, and $V\gamma$ — contain one photon simulated at the ME level and the second one at PS. Additionally, inclusive sam-

ples are used in which photons are generated only during the PS step. To avoid the double-counting of events among samples corresponding to the same physics process, the overlapping events in the samples without explicit photon inclusion at ME are removed. The overlap among events is considered for those with photons at parton level with $p_T > 15$ GeV and separated by $\Delta R > 0.2$ from any charged lepton, referred to as the *overlap region*. First, events from the inclusive samples without any photons at ME ($t\bar{t}$, V + jets) are vetoed if there is only one candidate photon which falls into the overlap region. No events from those samples are found in the overlap region with the samples with two photons at ME. Events from samples with one photon simulated at ME ($t\bar{t}\gamma$ production and decay and $V\gamma$) are discarded if both photons fall into the overlap region with $t\bar{t}\gamma\gamma$ and $V\gamma\gamma$. This approach removes the overlap among events with photons generated in the same phase space, while keeping the events from such samples that might satisfy the event selection at reconstruction level because a candidate object is a fake photon. For instance, an event from the $V\gamma$ samples with a genuine photon at ME in the overlap region and a fake photon at reconstruction level would not be removed.

4. Event selection and background estimate

The measurement is performed using the proton–proton collision data collected at the LHC between 2015 and 2018 at $\sqrt{s} = 13$ TeV with the ATLAS detector, which corresponds to an integrated luminosity of 140 fb^{-1} [19]. The event reconstruction, object identification and event selection follow closely that of the $t\bar{t}\gamma$ cross-section measurement [13]. In the following, a brief description of the event selection and background estimate is given. Further details can be found in Ref. [13] and references therein.

Single-lepton triggers with electron and muon p_T thresholds between 20 and 27 GeV depending on the data-taking period and various identification and isolation criteria [53–56] are used to select the events. Events are required to have at least one reconstructed collision vertex with two or more associated tracks with $p_T > 0.5$ GeV. The primary vertex is defined as the vertex with the largest $\sum p_T^2$ of the associated tracks [57] and consistent with the average beamspot position.

Photon candidates are reconstructed from energy deposits (clusters) in the electromagnetic calorimeter. Photons are required to satisfy a *tight* identification criterion and fulfil calorimeter and track isolation criteria [13,58] defined as $E_T^{\text{iso}} \Big|_{\Delta R=0.4} < 0.022 \cdot E_T(\gamma) + 2.45 \text{ GeV}$ and $p_T^{\text{iso}} \Big|_{\Delta R=0.2} < 0.05 \cdot E_T(\gamma)$. Here, $E_T^{\text{iso}} \Big|_{\Delta R=0.4}$ corresponds to the calorimeter isolation within a cone of radius $\Delta R = 0.4$ in the direction of the photon candidate. The term $p_T^{\text{iso}} \Big|_{\Delta R=0.2}$ is the track isolation within $\Delta R = 0.2$ and $E_T(\gamma)$ represents the transverse energy of a photon. Photon candidates are selected if they satisfy $E_T(\gamma) > 20$ GeV, $|\eta_{\text{cluster}}| < 2.37$, excluding those in the transition region between the barrel and the endcap calorimeters ($|\eta_{\text{cluster}}| \notin [1.37, 1.52]$). Photon candidates are classified as unconverted if the cluster is not matched to any reconstructed track in the ID system, or as converted if the cluster is matched to reconstructed tracks that are consistent with originating from a photon conversion and have a reconstructed conversion vertex.

Electron candidates are reconstructed from energy deposits in the electromagnetic calorimeter associated with reconstructed tracks from the ID system. They are identified with a combined likelihood technique and required to satisfy the *MediumLH* identification criteria [58] and have a pseudorapidity of $|\eta_{\text{cluster}}| < 2.47$, excluding candidates in the transition region ($|\eta_{\text{cluster}}| \notin [1.37, 1.52]$). Muon candidates are reconstructed by combining track segments in various layers of the muon spectrometer and tracks in the ID system. Muons are required to satisfy the *Medium* identification quality criteria and to have $|\eta| < 2.5$ [59]. Both electron and muon candidates are required to have $p_T > 7$ GeV and meet the loose working point (WP) requirement of the prompt-lepton isolation discriminant [60]. The transverse impact parameter divided by its estimated uncertainty is required to be less

than five (three) for electron (muon) candidates and the longitudinal impact parameter must be smaller than 0.5 mm for both lepton flavours.

Jets are reconstructed based on particle-flow objects using the anti- k_r algorithm [61] based on the FASTJET implementation [62] with a radius parameter $R = 0.4$ [63]. The jet energy scale (JES) and resolution are calibrated using simulations with in situ corrections obtained from data [64]. They are required to have $p_T > 25$ GeV and $|\eta| < 2.5$. To reject jets from pile-up or other primary vertices, a *jet vertex tagger* (JVT) discriminant [65] is required to be larger than 0.59 for jets with $p_T < 60$ GeV and $|\eta| < 2.4$. Jets arising from b -quark hadronisation, are identified using the DLL1r b -tagging algorithm [66]. The b -tagged jets are required to satisfy a WP that corresponds to a 70% per-jet efficiency for identifying b -quark-initiated jets in $t\bar{t}$ simulated events.

The missing transverse momentum vector, with magnitude E_T^{miss} , corresponds to the negative sum of the transverse momenta of the reconstructed and calibrated physical objects, with a ‘soft term’ built from all other tracks associated with the primary vertex but not matched to a reconstructed object [67].

Events are selected if they have exactly two isolated photons and exactly one isolated electron or muon that must be matched to the corresponding trigger-level object. The p_T thresholds for the matched leptons are 25 GeV for 2015 data, 27 GeV for 2016 data, and 28 GeV for 2017 and 2018 data. Events are rejected if additional lepton candidates with $p_T > 7$ GeV are present. Furthermore, events where the invariant mass of the electron and any photon is within the range 86.19–96.19 GeV are removed, to suppress the background from $Z \rightarrow ee$ events, where an electron is misidentified as a photon. The last requirement for retaining an event is that it must contain at least four reconstructed jets, with at least one of them tagged as a b -jet.

After applying the full event selection, the background contribution accounts for roughly 50% of the total events. Based on the photon origin, the background processes are divided into prompt photon background, where both photons are prompt, and fake photon background, where at least a photon is mimicked by another object, such as a misreconstructed hadron or electron. The contribution from events with misidentified leptons or leptons from heavy flavour decays is negligible and not further considered.

The prompt photon background is estimated by using MC simulations. The fraction of these background events is about 15% of the total expected events. The largest prompt photon background contribution arises from V boson events with two photons, and $t\bar{t}H$ events. In the following, $t\bar{t}\gamma$ events passing the overlap removal are referred to as ‘ $t\bar{t}\gamma$ (prompt γ)’ and prompt photon background events from the single-top quark, single and diboson samples, $t\bar{t}V$, $t\bar{t}H$ and $t\bar{t}$ simulated samples as the ‘Other $\gamma\gamma$ ’ background category. The largest contributions to this category arise from V boson events with two photons (35%), and $t\bar{t}H$ events (22%).

In this paper, the MC estimate of events with fake photons is corrected using the data-driven scale factors measured in dedicated control regions in Ref. [13]. The contribution from processes with at least one electron mimicking a photon signature, ‘e-fake’, originates mainly from dilepton $t\bar{t}\gamma$ events where an electron from a top-quark decay is identified as a photon yielding the same signature as the single-lepton $t\bar{t}\gamma\gamma$ channel. In particular, those events amount to 80% of the total events in this category. The e-fake background is estimated in data from the fraction of electron–positron candidates from $Z \rightarrow e^+e^-$ decays that are reconstructed as $e\gamma$ pairs [68]. The ratio of the e-fake rates in data and simulation is used to correct the e-fake background predicted by the simulation in the signal region. The scale factors are applied per photon as a function of the fake photon p_T and η , separately for converted and unconverted photons. After applying the data-driven corrections, this background category represents about 20% of the total number of selected events. The background contribution from events where at least one photon candidate arises from misidentified hadrons or from hadron decays, referred to as ‘h-fake’, was estimated from data using the ‘ABCD’

data-driven method [69] in Ref. [13]. It is also measured as a function of photon p_T , η and conversion type. This category corresponds to about 10% of the events, where 80% of them correspond to $t\bar{t}\gamma$ events with a fake photon. The contribution of events with one e-fake and one h-fake photon represents about 1% of the events and is included in the e-fake contribution. Example variables illustrating the description of the data by the simulation after the event selection are shown in Section 6.

5. Systematic uncertainties

The measurements are affected by systematic uncertainties owing to theoretical assumptions and detector effects and uncertainties arising from the limited number of events in the MC simulations. The determination of the modelling and normalisation uncertainties associated with the background samples and the experimental uncertainties follows the same prescriptions as in Ref. [13].

The signal and background modelling uncertainties include effects due to the choice of renormalisation and factorisation scales, PDF set, parton shower, amount of QCD initial-state radiation (ISR) and final-state radiation (FSR). Modelling uncertainties are treated as uncorrelated sources of uncertainty between different processes because they are simulated using different generators or at different accuracy in QCD. The effect of the QCD scale uncertainty for the $t\bar{t}\gamma\gamma$, $t\bar{t}\gamma$ production and decay, $tW\gamma$ and $t\bar{t}$ processes is evaluated independently by separately halving and doubling the renormalisation and factorisation scales relative to the nominal scale choice. The uncertainty in the PDFs for the $t\bar{t}\gamma\gamma$ signal and the main background processes, $t\bar{t}\gamma$ production and decay, are obtained using the 30 PDF variations of the PDF4LHC15 prescription [70]. The uncertainty from the parton shower and hadronisation for $t\bar{t}\gamma\gamma$, $t\bar{t}\gamma$ production and decay, $tW\gamma$ and $t\bar{t}$ processes is estimated by comparing the nominal simulated samples interfaced with PYTHIA 8 with alternative samples interfaced to HERWIG 7.2.1 [71,72]. Uncertainties due to the value of α_s used in the ISR parton shower modelling are estimated by comparing the nominal $t\bar{t}\gamma\gamma$, $t\bar{t}\gamma$, and $t\bar{t}$ simulations to alternative samples generated with varied radiation parameter settings in the A14 tune, controlled by the *var3c* parameter implemented in PYTHIA 8 [32]. This parameter is varied within its uncertainties corresponding to variation of $\alpha_s(m_Z)$ between 0.115 and 0.140. The impact of the FSR uncertainties in $t\bar{t}\gamma\gamma$ is evaluated by varying the renormalisation scale for QCD emission in the FSR in PYTHIA 8 by factors of 0.5 and 2.0, respectively. For the $t\bar{t}$ process, an additional ISR uncertainty is obtained by comparing the nominal sample with an additional one with the h_{damp} parameter varied by a factor of two [73] and the impact of the ME corrections applied to all emissions is evaluated by comparing the nominal $t\bar{t}$ sample to a dedicated POWHEG + PYTHIA 8 sample with the corrections turned off.

Additionally, normalisation uncertainties are considered for the different prompt-photon background processes. A normalisation uncertainty of 7% is considered separately for the $t\bar{t}\gamma$ production and $t\bar{t}\gamma$ decay samples, which is based on the measured uncertainties for those processes in Ref. [13]. A 6% normalisation uncertainty is assigned to the $t\bar{t}$ simulation [46], which corresponds to the uncertainty of the NNLO in perturbative QCD, including soft-gluon resummation to next-to-next-to-leading-log. A 10% uncertainty is assigned to the $t\bar{t}H$ process based on the calculations from Ref. [50]. For $V\gamma\gamma$ and $V\gamma$ events a 50% normalisation uncertainty is assigned. While the processes are measured with a 20% precision or better [74], this normalisation uncertainty accounts for the possible mismodelling of the heavy flavour jets. The value is based on the differences between data and simulation observed in dedicated $W\gamma$ validation regions in Ref. [14]. For the small background processes, single top quark (t- and s-channel), $t\bar{t}V$, $V\gamma$, $V + \text{jets}$, $tW\gamma$ and diboson processes, a 50% uncertainty is assigned, following the prescription of the latest $t\bar{t}\gamma$ cross-section measurement [13]. For the backgrounds estimated with data-driven methods, i.e., e-fakes and h-fakes, the corresponding uncertainties of the scale factors applied to the simulation are considered [13]. The sources of systematic uncertainty in

the e-fake background estimate are related to the choice of the function describing the Z boson mass peak, the mass range considered, and from the assumed function used to describe the background. The systematic uncertainties in the h-fake background include the modelling of the $t\bar{t}$ process, which accounts for most of the h-fake events in the dedicated control regions in the $t\bar{t}\gamma$ measurement, and the normalisation of the e-fake and prompt background processes.

The experimental systematic uncertainties account for uncertainties related to the reconstruction and identification of the physics objects, the integrated luminosity and the simulation of pile-up events. Photon and lepton identification and isolation efficiencies, momentum scale and resolution [58,59,68], and lepton trigger efficiencies in the simulation are corrected using scale factors to improve the description of the data. The associated systematic uncertainties are obtained by varying the corrections within their uncertainties.

The JES uncertainty is derived from a combination of simulations, test-beam data and in situ measurements [64] resulting in 30 uncorrelated JES uncertainty subcomponents, which take into account effects from jet-flavour composition, η -intercalibration, punch-through, single-particle response, calorimeter response to different jet flavours, and pile-up. The jet energy resolution in simulation is smeared by its corresponding uncertainty [64] split into 13 uncorrelated sources. The uncertainty associated with the JVT discriminant for pile-up jet rejection is obtained by varying the efficiency correction factors [65].

The uncertainties in the b -jet tagging calibration are determined separately for b -jets, c -jets and light-flavour jets [75–77]. For each jet category, the uncertainties are decomposed into several uncorrelated components. Additionally, a 50% normalisation uncertainty is applied to events with high- p_T jets above the p_T limit where the b -jet tagging algorithm is calibrated.

The uncertainty in E_T^{miss} results from the propagation of the uncertainties in the energy scales and resolutions of photons, leptons and jets, and the modelling of its soft term [67].

The uncertainty in the total integrated luminosity, using the LUCID-2 detector [21] for the primary luminosity measurements, is estimated to be 0.83% [19]. The uncertainty arising from the modelling of pile-up is determined by varying the pile-up reweighting applied to correct the simulation to better describe the data within its uncertainties.

6. Measurement of the $t\bar{t}\gamma\gamma$ cross section and $t\bar{t}\gamma\gamma/t\bar{t}\gamma$ cross-section ratio

A multivariate analysis using a BDT is performed to separate the $t\bar{t}\gamma\gamma$ signal from the background processes. The training is performed with the eXtreme Gradient Boosting classifier from the XGBoost library [78]. A 4-fold cross-validation was performed, where the events were randomly split into four equally sized subsets. For each fold, three subsets were used for training the BDT configuration, and the remaining one was used for testing. The event weights are applied to the events in the training and testing samples. Events with negative weights in samples generated at NLO are included in the training using the absolute value of their weights. It was verified that the shape of the input variables is not significantly affected. The training uses simulated events from the $t\bar{t}\gamma\gamma$, $t\bar{t}\gamma$ production and decay and $V\gamma\gamma$ samples, with the corresponding data-driven scale factors applied to the fake photon events. The $t\bar{t}\gamma\gamma$ signal and the total background contributions are rescaled to be equally represented in the training. A total of 19 variables are selected for the training based on their good agreement between data and MC simulation, balanced correlations among them, yielding good separation and best expected significance. They are related to the properties of the photons, such as photon conversion type, p_T and η , invariant masses and angular separations of different objects in the event (e.g. to the invariant mass and ΔR of the two photons, the lepton and each photon and the photons and the closest b -tagged jet), to the E_T^{miss} and to the jet properties, such as the number of b -tagged jets. It was checked that the simulation accurately describes the data within the uncertainties for all input variables. Example variables with the most separation power are shown in Fig. 2 before the fit.

The measurements are performed at particle level in a fiducial phase space, which is defined based on the requirements used in Ref. [13] and closely follows the kinematic requirements at reconstruction level. Photons are required to not originate from a hadron decay, to have $p_T > 20$ GeV and $|\eta| < 2.37$ and to be isolated such that the sum of transverse momenta of all charged particles surrounding the photon within $\Delta R \leq 0.2$ must be smaller than 5% of its p_T . Electrons and muons are dressed with nearby photons, which do not originate from hadrons, in a $\Delta R < 0.1$ cone around the lepton. Only leptons not originating from

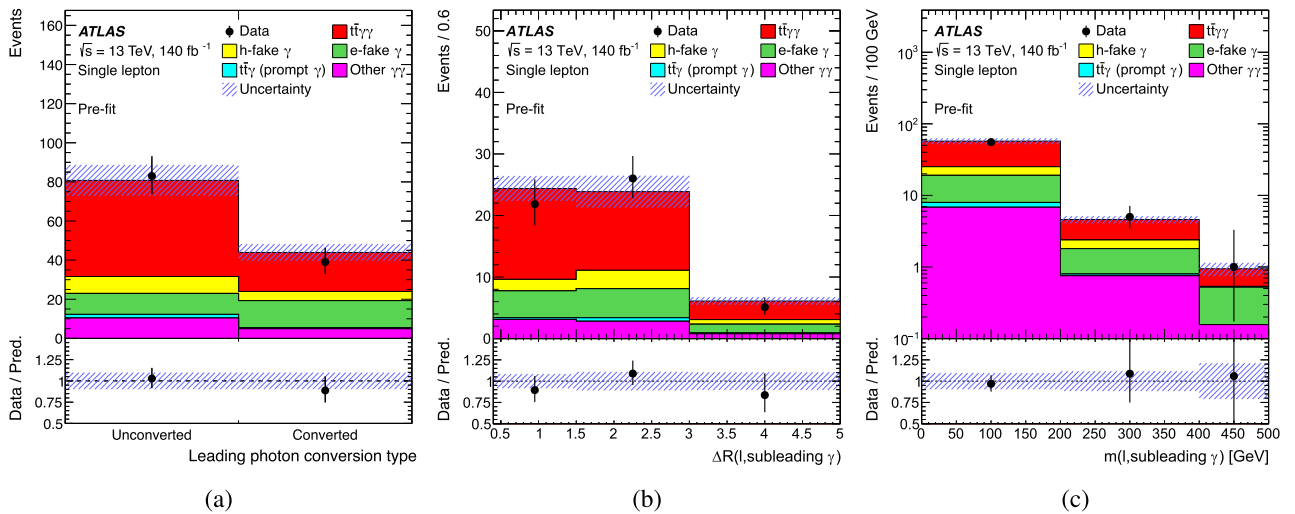


Fig. 2. Example of input variables with large separation power, before the fit to data: (a) conversion type of the photon leading in p_T , (b) ΔR between the lepton and the subleading photon in p_T and (c) their invariant mass. The uncertainty band corresponds to the total uncertainties before the fit to data. The lower part of the plot shows the ratio of the data to the prediction. If present, overflow events are included in the last bin of the distribution. The ‘Other $\gamma\gamma$ ’ category includes simulated events with two prompt photons from single-top quark, single and diboson processes, $t\bar{t}V$, $t\bar{t}H$, and $t\bar{t}$ samples. The normalisation of the $t\bar{t}\gamma\gamma$ sample is rescaled using the NLO/LO K -factor described in Section 3.

hadron decays are selected. Jets are clustered with the anti- k_r algorithm with a radius of $R = 0.4$. All stable particles are considered in the clustering, except for the selected electrons, muons and photons, and the neutrinos originating from the top quarks. A particle-level jet is identified as a b -jet if a hadron with $p_T > 5$ GeV containing a b -quark is matched to the jet through a ghost-matching method [79]. Lepton and jets are required to have $p_T > 25$ GeV and $|\eta| < 2.5$. Additionally, leptons within $\Delta R < 0.4$ from a jet are excluded and jets are removed if they are within $\Delta R = 0.4$ of an isolated photon candidate. Events are additionally required to satisfy that the ΔR distance between the lepton and any photon and between the photons is larger than 0.4. The fiducial phase space is defined by requiring exactly two photons, exactly one electron or muon, and at least four jets among which at least one is a b -jet. Events are rejected if there are additional leptons with $p_T > 7$ GeV. The fraction of simulated $t\bar{t}\gamma\gamma$ signal events that pass the event selection at reconstruction level over the number of events in the fiducial region at particle level is 19% and the fraction of signal events that fulfil the selection at reconstruction level and the particle-level requirements is 79%.

The fiducial cross section at particle level is measured using a profile likelihood fit to the BDT output that profiles nuisance parameters and minimises the negative log-likelihood [80]. The normalisation of the $t\bar{t}\gamma\gamma$ signal template is treated as the parameter of interest in the fit. The resulting normalisation factor is then used to extract the observed cross section by scaling the predicted cross section in the fiducial phase space at particle level. Background processes are modelled using MC simulation and data-driven methods, with normalisation and shape uncertainties included as nuisance parameters in the likelihood fit. All MC samples used to evaluate signal modelling uncertainties are scaled to the same cross section in the fiducial phase space. Each source of systematic uncertainty, including those affecting the signal, is incorporated as a Gaussian prior in the likelihood function. The variations are symmetrised, taking half the difference between the upward and downward variations as the uncertainty. If both variations have the same sign, the average of the difference between each variation and the nominal value is chosen as the two-sided uncertainty. If only one variation is available (e.g. the uncertainty from the parton shower or the PDF uncertainties) the difference between the nominal and alternative prediction is taken as the size of the uncertainty. A pruning procedure is implemented to remove uncertainties that are too small to meaningfully impact the results, improving the fit's convergence and reducing computing time. In addition, a smoothing procedure is applied, where necessary, to reduce the impact of statistical fluctuations in the systematic templates. The impact of these procedures on the precision of the results is negligible. The output of the BDT after the fit is shown in Fig. 3. The binning is optimised to enhance signal-to-background separation while ensuring smooth templates for the small background contributions. The fraction of background events after the fit corresponds to 47%. Good agreement is observed between the data and the prediction. The global goodness of fit, evaluated with a *saturated model* [81], yields a p -value of 49%.

The fiducial cross section at particle level is found to be

$$\sigma_{t\bar{t}\gamma\gamma} = 2.42_{-0.53}^{+0.58} \text{ fb} = 2.42_{-0.38}^{+0.46} (\text{stat})_{-0.38}^{+0.35} (\text{syst}) \text{ fb}. \quad (1)$$

The total relative uncertainty of the measurement is approximately 23%, with the dominant contribution coming from the statistical uncertainty of the data, which is about 17%. Systematic uncertainties contribute approximately 15% to the total relative uncertainty. The systematic uncertainties are dominated by the experimental uncertainties related to the jets and the photons, and the uncertainties in the fake-photon background estimates, followed by the normalisation uncertainties of the other $\gamma\gamma$ background contribution. The impact of the different categories of systematic uncertainties is summarised in Table 1 (left column). None of the nuisance parameters are significantly constrained by the fit. Their best-fit values are well within one standard deviation of their initial estimates. The prediction for the fiducial $t\bar{t}\gamma\gamma$ cross section

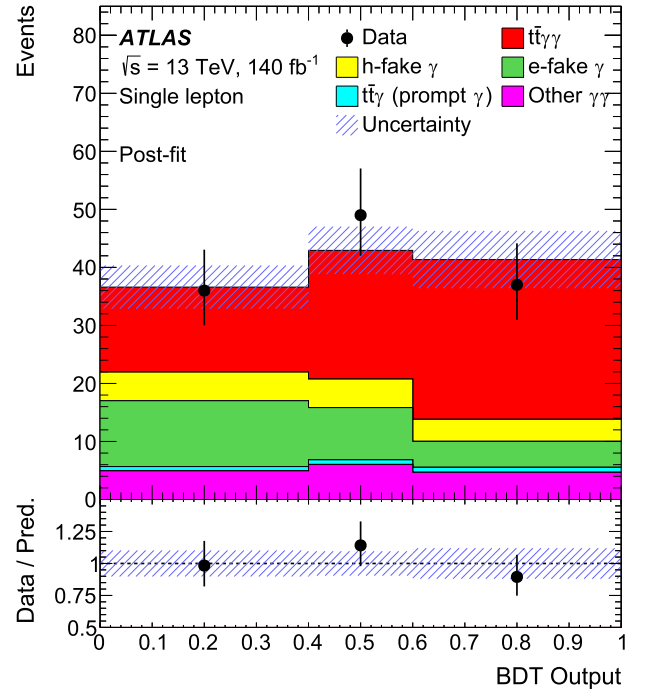


Fig. 3. BDT distribution output after the fit to data. The uncertainty band corresponds to the total uncertainties with correlations among uncertainties taken into account as determined in the fit. The lower part of the plot shows the ratio of the data to the prediction. The ‘Other $\gamma\gamma$ ’ category includes simulated events with two prompt photons from single-top quark, single and diboson processes, $t\bar{t}V$, $t\bar{t}H$, and $t\bar{t}$ samples.

given by the nominal $t\bar{t}\gamma\gamma$ MADGRAPH5_AMC@NLO + PYTHIA 8 LO simulation is $1.53_{-0.52}^{+0.40}(\text{scale})_{-0.03}^{+0.05}(\text{PDF}) \text{ fb}$. The observed significance with respect to the background-only hypothesis is 5.2 standard deviations. The expected significance evaluated with the LO simulation is 3.8 standard deviations, assessed with toy experiments. The expected significance is 5.7 standard deviations with the approximate K -factor of 1.7, described in Section 3, which is used for the prior normalisation of the $t\bar{t}\gamma\gamma$ sample in the distributions before the fit to data. An additional check was performed by fitting the number of events instead of the BDT output. The result, $\sigma_{t\bar{t}\gamma\gamma} = 2.51_{-0.58}^{+0.62} \text{ fb}$, is consistent with the one from the default fit.

The ratio of the cross sections of the $t\bar{t}\gamma\gamma$ process and the $t\bar{t}\gamma$ process ($t\bar{t}\gamma$ production and decay) in the single-lepton channel is additionally extracted at particle level. The input distributions used to measure the $t\bar{t}\gamma$ cross sections are taken from Ref. [13]. The event reconstruction and selection are designed to avoid any statistical overlap with the $t\bar{t}\gamma\gamma$ measurement. The selection criteria at reconstruction level and particle-level phase space definition are analogous to those of the $t\bar{t}\gamma\gamma$ analysis, except that exactly one isolated photon is required instead of two. Neural networks (NNs) are used to enhance the separation of $t\bar{t}\gamma$ production and the various background processes. A four-class NN is used to define a signal region enriched in $t\bar{t}\gamma$ production events and three control regions enriched in $t\bar{t}\gamma$ decay, photon fakes and other events with prompt photons, respectively. The same object selection and the same sources of systematic uncertainties are considered in both measurements. Therefore, the uncertainties related to the object reconstruction, luminosity and pile-up modelling are kept fully correlated between the measurements. The uncertainties related to the modelling and the normalisation of the common processes, which are estimated with the same set of MC samples ($t\bar{t}\gamma$ production, $t\bar{t}\gamma$ decay, $t\bar{t}$, $tW\gamma$, t -channel and s -channel single top quark, $t\bar{t}V$, $V\gamma$, V + jets, inclusive diboson samples) are also correlated among the two measurements. Common background normalisation uncertainties and the uncertainties in the data-

Table 1

Summary of the relative impact of all the systematic uncertainties, in percentage, on the $t\bar{t}\gamma\gamma$ fiducial inclusive cross section and $R_{t\bar{t}\gamma\gamma/\bar{t}\bar{t}\gamma}$ grouped into different categories. The category ‘Jet’ corresponds to the effect of JES, jet resolution and JVT uncertainties, ‘Photon’ and ‘Leptons’ include all experimental uncertainties related to photons and leptons (including trigger uncertainties), respectively.

Source	$\Delta\sigma_{t\bar{t}\gamma\gamma}/\sigma_{t\bar{t}\gamma\gamma}$ [%]	$\Delta R_{t\bar{t}\gamma\gamma/\bar{t}\bar{t}\gamma}/R_{t\bar{t}\gamma\gamma/\bar{t}\bar{t}\gamma}$ [%]
$t\bar{t}\gamma\gamma$ modelling	1.4	1.3
Prompt-photon background norm. & modelling	4.4	5.8
Fake-photon background estimates	6.5	0.5
Fake-lepton background estimate	–	0.9
Jet	9.7	5.9
Photon	6.5	4.0
b -tagging	3.4	1.0
Leptons	1.5	0.3
Luminosity	1.4	0.1
E_{miss}	0.4	1.1
Pile-up	1.6	1.4
MC statistical uncertainties	2.5	2.8
Total systematic uncertainty	15.0	10.0

driven e-fake and h-fake are also correlated. Modelling uncertainties between different processes (e.g. PS uncertainties between $t\bar{t}\gamma$ production and decay and $t\bar{t}\gamma\gamma$) are considered uncorrelated as in the individual analyses.

The ratio of $t\bar{t}\gamma\gamma$ to $t\bar{t}\gamma$ cross section is obtained by fitting simultaneously the $t\bar{t}\gamma\gamma$ BDT output and the variables used in the four regions of the $t\bar{t}\gamma$ measurement. In particular, the output of the corresponding NN classifiers are the input distributions in the $t\bar{t}\gamma$ production and the $t\bar{t}\gamma$ decay regions, while the distributions of the second largest pseudo-continuous b -tagging score are used in the regions enriched in photon fakes and in other prompt photons [13]. In the measurement, the cross-section ratio is treated as the parameter of interest, while the $t\bar{t}\gamma$ cross section is profiled using data. The $t\bar{t}\gamma$ production and $t\bar{t}\gamma$ decay templates are added together, and the normalisation of the combined template is free floating in the fit. A 20% normalisation uncertainty is considered for the $t\bar{t}\gamma$ decay template, which is the pre-fit uncertainty associated with the normalisation of $t\bar{t}\gamma$ decay in the total $t\bar{t}\gamma$ measurement [13]. This value is based on the estimated uncertainty in the NLO K -factor used to correct the normalisation of $t\bar{t}\gamma$ decay LO sample, as obtained in Ref. [14]. This nuisance parameter allows the fit to adjust the fraction of $t\bar{t}\gamma$ production and $t\bar{t}\gamma$ decay events.

The measurement yields $R_{t\bar{t}\gamma\gamma/\bar{t}\bar{t}\gamma} = (3.30^{+0.70}_{-0.65}) \times 10^{-3} = (3.30^{+0.63}_{-0.55} \text{ (stat)} +^{0.32}_{-0.34} \text{ (syst)}) \times 10^{-3}$. The precision of the measurement of about 20% is dominated by the statistical uncertainty of the data, which is approximately 18%, while the total systematic uncertainty is about 10%. The impact of correlated systematic uncertainties partially cancels in the ratio. Specifically, systematic uncertainties that cancel significantly include experimental sources associated with jets, b -tagging, photons, and luminosity, and those arising from data-driven estimates of fake-photon backgrounds. As expected, the relative impact of $t\bar{t}\gamma$ production and decay modelling uncertainties increases compared with the measurement of the $t\bar{t}\gamma\gamma$ cross section, as shown in Table 1 (right column). The measured value and total uncertainty of the $t\bar{t}\gamma$ cross section agree with the result from Ref. [13].

There are no available calculations of the ratio that would allow for a direct comparison with the measured value. As a reference, using the nominal MADGRAPH5_AMC@NLO + PYTHIA 8 samples, the ratio of the fiducial $t\bar{t}\gamma\gamma$ LO cross section to the $t\bar{t}\gamma$ cross section—defined as the sum of the NLO $t\bar{t}\gamma$ production and $t\bar{t}\gamma$ decay contributions, including the NLO/LO K -factor—yields $(2.46^{+0.73}_{-0.94} \text{ (scale)} +^{0.10}_{-0.06} \text{ (PDF)}) \times 10^{-3}$. The scale and PDF uncertainties are evaluated assuming uncorrelated uncertainties between the individual cross sections. This value and its uncertainty should be treated as illustrative, as they are based on a combination of LO and NLO predictions, and no uncertainty is assigned to the K -factor applied to the $t\bar{t}\gamma$ decay contribution.

7. Conclusion

This paper presents the observation of the production of top quark pairs in association with two photons. The measurement is performed using a data sample of proton–proton collisions collected with the ATLAS detector at the LHC at $\sqrt{s} = 13$ TeV, corresponding to a total integrated luminosity of 140 fb^{-1} . The cross-section measured in a fiducial phase space defined at particle level, with kinematic requirements on the photons, lepton, and jets, yields $2.42^{+0.58}_{-0.53} \text{ fb}$, with an observed significance of 5.2 standard deviations. The available MC prediction at LO underestimate the cross section as expected. In the measurement of the ratio of the $t\bar{t}\gamma\gamma$ and the $t\bar{t}\gamma$ processes, several systematic uncertainties—particularly those related to jets, b -tagging, photons, and luminosity—partially cancel out. The ratio, measured in the fiducial phase space, is found to be $(3.30^{+0.70}_{-0.65}) \times 10^{-3}$.

Data availability

The data for this manuscript are not available. The values in the plots and tables associated to this article are stored in HEPDATA (<http://hepdata.cedar.ac.uk>).

Declaration of competing interest

The authors declare that they have no known competing financial interests or personal relationships that could have appeared to influence the work reported in this paper.

Acknowledgements

We thank CERN for the very successful operation of the LHC and its injectors, as well as the support staff at CERN and at our institutions worldwide without whom ATLAS could not be operated efficiently.

The crucial computing support from all WLCG partners is acknowledged gratefully, in particular from CERN, the ATLAS Tier-1 facilities at TRIUMF/SFU (Canada), NDGF (Denmark, Norway, Sweden), CC-IN2P3 (France), KIT/GridKA (Germany), INFN-CNAF (Italy), NL-T1 (Netherlands), PIC (Spain), RAL (UK) and BNL (USA), the Tier-2 facilities worldwide and large non-WLCG resource providers. Major contributors of computing resources are listed in Ref. [82].

We gratefully acknowledge the support of ANPCyT, Argentina; YerPhI, Armenia; ARC, Australia; BMWFW and FWF, Austria; ANAS, Azerbaijan; CNPq and FAPESP, Brazil; NSERC, NRC and CFI, Canada; CERN; ANID, Chile; CAS, MOST and NSFC, China; Minciencias, Colombia; MEYS CR, Czech Republic; DNRF and DNSRC, Denmark; IN2P3-CNRS

and CEA-DRF/IRFU, France; SRNSFG, Georgia; BMFTR, HGF and MPG, Germany; GSRI, Greece; RGC and Hong Kong SAR, China; ICHEP and Academy of Sciences and Humanities, Israel; INFN, Italy; MEXT and JSPS, Japan; CNRST, Morocco; NWO, Netherlands; RCN, Norway; MNiSW, Poland; FCT, Portugal; MNE/IFA, Romania; MSTDI, Serbia; MSSR, Slovakia; ARIS and MVZI, Slovenia; DSI/NRF, South Africa; MI-CIU/AEI, Spain; SRC and Wallenberg Foundation, Sweden; SERI, SNSF and Cantons of Bern and Geneva, Switzerland; NSTC, Taipei; TENMAK, Türkiye; STFC/UKRI, United Kingdom; DOE and NSF, United States of America.

Individual groups and members have received support from BCKDF, CANARIE, CRC and DRAC, Canada; CERN-CZ, FORTE and PRIMUS, Czech Republic; COST, ERC, ERDF, Horizon 2020, ICSC-NextGenerationEU and Marie Skłodowska-Curie Actions, European Union; Investissements d'Avenir Labex, Investissements d'Avenir IDEX and ANR, France; DFG and AvH Foundation, Germany; Herakleitos, Thales and Aristeia programmes co-financed by EU-ESF and the Greek NSRF, Greece; BSF-NSF and MINERVA, Israel; NCN and NAWA, Poland; La Caixa Banking Foundation, CERCA Programme Generalitat de Catalunya and PROMETEO and GenT Programmes Generalitat Valenciana, Spain; Göran Gustafssons Stiftelse, Sweden; The Royal Society and Leverhulme Trust, United Kingdom.

In addition, individual members wish to acknowledge support from CERN: European Organization for Nuclear Research (CERN DOCT); Chile: Agencia Nacional de Investigación y Desarrollo (FONDECYT 1230812, FONDECYT 1240864, Fondecyt 3240661, Fondecyt Regular 1240721); China: [Chinese Ministry of Science and Technology \(MOST-2023YFA1605700, MOST-2023YFA1609300\)](#), [National Natural Science Foundation of China \(NSFC - 12175119, NSFC 12275265\)](#); Czech Republic: [Czech Science Foundation \(GACR - 24-11373S\)](#), Ministry of Education Youth and Sports (ERC-CZ-LL2327, FORTE CZ.02.01.01/00/22_008/0004632), PRIMUS Research Programme (PRIMUS/21/SCI/017); EU: [H2020 European Research Council \(ERC - 101002463\)](#); European Union: [European Research Council \(BARD No. 101116429, ERC - 948254, ERC 101089007\)](#), [European Regional Development Fund \(SMASH COFUND 101081355, SLO ERDF\)](#), [Horizon 2020 Framework Programme \(MUCCA - CHIST-ERA-19-XAI-00\)](#), European Union, Future Artificial Intelligence Research (FAIR-NextGenerationEU PE00000013), Italian Center for High Performance Computing, Big Data and Quantum Computing (ICSC, NextGenerationEU); France: [Agence Nationale de la Recherche \(ANR-21-CE31-0022, ANR-22-EDIR-0002, ANR-24-CE31-0504-01\)](#); Germany: [Baden-Württemberg Stiftung \(BW Stiftung-Postdoc Eliteprogramme\)](#), [Deutsche Forschungsgemeinschaft \(DFG - 469666862, DFG - CR 312/5-2\)](#); China: [Research Grants Council \(GRF\)](#); Italy: [Istituto Nazionale di Fisica Nucleare \(ICSC, NextGenerationEU\)](#), [Ministero dell'Università e della Ricerca \(NextGenEU 153D23001490006 M4C2.1.1, NextGenEU 153D23000820006 M4C2.1.1, NextGenEU 153D23001490006 M4C2.1.1, SOE2024_0000023\)](#); Japan: [Japan Society for the Promotion of Science \(JSPS KAKENHI JP22H01227, JSPS KAKENHI JP22H04944, JSPS KAKENHI JP22KK0227, JSPS KAKENHI JP24K23939, JSPS KAKENHI JP25H00650, JSPS KAKENHI JP25H01291, JSPS KAKENHI JP25K01023\)](#); Norway: [Research Council of Norway \(RCN-314472\)](#); Poland: [Ministry of Science and Higher Education \(IDUB AGH, POB8, D4 no 9722\)](#), [Polish National Science Centre \(NCN 2021/42/E/ST2/00350, NCN OPUS 2023/51/B/ST2/02507, NCN OPUS nr 2022/47/B/ST2/03059, NCN UMO-2019/34/E/ST2/00393, UMO-2022/47/O/ST2/00148, UMO-2023/49/B/ST2/04085, UMO-2023/51/B/ST2/00920, UMO-2024/53/N/ST2/00869\)](#); Portugal: [Foundation for Science and Technology \(FCT\)](#); Spain: [Ministry of Science and Innovation \(MCIN & NextGenEU PCI2022-135018-2, MICIN & FEDER PID2021-125273NB, RYC2019-028510-I, RYC2020-030254-I, RYC2021-031273-I, RYC2022-038164-I\)](#); Sweden: [Carl Trygger Foundation \(Carl Trygger Foundation CTS 22:2312\)](#), [Swedish Research Council \(Swedish Research Council 2023-04654, VR 2021-03651, VR 2022-03845, VR 2022-04683, VR](#)

2023-03403, VR 2024-05451), Knut and Alice Wallenberg Foundation (KAW 2018.0458, KAW 2022.0358, KAW 2023.0366); Switzerland: [Swiss National Science Foundation \(SNSF - PCEFP2_194658\)](#); United Kingdom: [Leverhulme Trust \(Leverhulme Trust RPG-2020-004\)](#), [Royal Society \(NIF-R1-231091\)](#); United States of America: [U.S. Department of Energy \(ECA DE-AC02-76SF00515\)](#), [Neubauer Family Foundation](#).

The ATLAS Collaboration

G. Aad¹⁵², E. Aakvaag¹⁸, B. Abbott¹⁷⁴, S. Abdelhameed¹⁶⁹, K. Abeling⁸², N.J. Abicht⁷⁶, S.H. Abidi⁴³, M. Aboelela⁷¹, A. Aboulhorma⁶⁰, H. Abramowicz²²⁴, Y. Abulaiti¹⁷¹, B.S. Acharya^{100,101,256}, A. Ackermann⁹¹, C.Adam Bourdarios⁵, L. Adamczyk¹³⁴, S.V. Addepalli²¹⁴, M.J. Addison¹⁵¹, J. Adelman¹⁶⁸, A. Adiguzel²⁶, T. Adye¹⁹⁴, A.A. Affolder¹⁹⁶, Y. Afik⁶⁵, M.N. Agaras¹⁴, A. Aggarwal¹⁵⁰, G. Agheorghiesei³⁶, F. Ahmadov^{64,13}, S. Ahuja¹⁴⁵, X. Ai²⁰⁷, G. Aielli^{115,116}, A. Aikot²³⁷, M.Ait Tamlihat⁶⁰, B. Aitbenkhik⁵⁶, M. Akbiyik¹⁵⁰, T.P. A. Åkesson¹⁴⁸, A.V. Akimov²¹⁶, D. Akiyama²⁴², N.N. Akolkar³¹, S. Aktas²⁴⁰, G.L. Alberghi³⁰, J. Albert²³⁹, U. Alberti²², P. Albicocco⁸⁰, G.L. Albouy⁸⁸, S. Alderweireldt⁷⁹, Z.L. Alegria¹⁷⁵, M. Aleksa⁶², I.N. Aleksandrov⁶⁴, C. Alexa³⁵, T. Alexopoulos¹¹, F. Alfonsi³⁰, M. Algren⁸³, M. Alhroob²⁴¹, B. Ali¹⁹², H.M. J. Ali^{141,266}, S. Ali⁴⁵, S.W. Alibocus¹⁴², M. Aliev⁴⁹, G. Alimonti¹⁰⁵, W. Alkakh⁸², C. Allaire⁹⁷, B.M. M. Allbrooke²¹⁷, J.S. Allen¹⁵¹, J.F. Allen⁷⁹, P.P. Allport²³, A. Aloisio^{107,108}, F. Alonso¹⁴⁰, C. Alpigianni²⁰⁵, Z.M. K. Alsolami¹⁴¹, A. Alvarez Fernandez¹⁵⁰, M. Alves Cardoso⁸³, M.G. Alvigi^{107,108}, M. Aly¹⁵¹, Y. Amaral Coutinho¹²⁶, A. Ambler¹⁵⁴, C. Amelung⁶², M. Ameri¹⁵¹, C.G. Ames¹⁵⁹, T. Amezza¹⁸¹, D. Amidei¹⁵⁶, B. Amini⁸¹, K. Amirie²²⁸, A. Amirkhanov⁶⁴, S.P. Amor Dos Santos¹⁸⁴, K.R. Amos²³⁷, D. Amperiadou²²⁵, S. An¹³⁰, C. Anastopoulos²¹⁰, T. Andeen¹², J.K. Anders¹⁴², A.C. Anderson⁸⁷, A. Andreazza^{105,106}, S. Angelidakis¹⁰, A. Angerami⁶⁷, A.V. Anisenkov⁶⁴, A. Annovi¹¹¹, C. Antel⁶², E. Antipov²¹⁶, M. Antonelli⁸⁰, F. Anulli¹¹³, M. Aoki¹³⁰, T. Aoki²²⁶, M.A. Aparo²¹⁷, L. Aperio Bella⁷⁵, M. Apicella⁴⁴, C. Appelt²²⁴, A. Apyan³³, M. Arampatzis¹¹, S.J. Arbiol Val¹³⁶, C. Arcangeletti⁸⁰, A.T.H. Arce⁷⁸, J-F. Arguin¹⁵⁸, S. Argyropoulos²²⁵, J.-H. Arling⁷⁵, O. Arnaez⁵, H. Arnold²¹⁶, G. Artoni^{113,114}, H. Asada¹⁶¹, K. Asai¹⁷², S. Asatryan²⁴⁷, N.A. Asbah⁶², R.A. Ashby Pickering²⁴¹, A.M. Aslam¹⁴⁵, K. Assamagan⁴³, R. Astalos⁴¹, K.S.V. Astrand¹⁴⁸, S. Atashi²³³, R.J. Atkin⁴⁷, H. Atmani⁶¹, P.A. Atlasidha¹⁸², K. Augsten¹⁹², A.D. Aurio¹⁶⁶, V.A. Austrup¹⁵¹, G. Avolio⁶², K. Axiotis⁸³, A. Azzam¹⁴, D. Babal⁴², H. Bachacou¹⁹⁵, K. Bachas^{225,260}, A. Bachi⁵⁵, E. Bachmann⁷⁷, M.J. Backes⁹¹, A. Badae⁶⁵, T.M. Baer¹⁵⁶, P. Bagnaia^{113,114}, M. Bahmani²¹, D. Bahner⁸¹, K. Bai¹⁷⁷, J.T. Baines¹⁹⁴, L. Baines¹⁴⁴, O.K. Baker²⁴⁶, E. Bakos¹⁷, D. Bakshi Gupta⁹, L.E. Balabram Filho¹²⁶, V. Balakrishnan¹⁷⁴, R. Balasubramanian⁵, E.M. Baldwin⁶³, P. Balek¹³⁴, E. Ballabene^{30,29}, F. Balli¹⁹⁵, L.M. Baltes⁹¹, W.K. Balunas⁴⁶, J. Balz¹⁵⁰, I. Bamwidi¹⁷⁰, E. Banas¹³⁶, M. Bandieramonte¹⁸³, A. Bandyopadhyay³¹, S. Bansal³¹, L. Barak²²⁴, M. Barakat⁷⁵, E.L. Barberio¹⁵⁵, D. Barberis²⁰, M. Barbero¹⁵², M.Z. Barel¹⁶⁷, T. Barillari¹⁶⁰, M.-S. Barisits⁶², T. Barklow²¹⁴, P. Baron¹⁹³, D.A. Baron Moreno¹⁵¹, A. Baroncelli⁹⁰, A.J. Barr¹⁸⁰, J.D. Barr¹⁴⁶, F. Barreiro¹⁴⁹, J. Barreiro Guimarães da Costa¹⁵, M.G. Barros Teixeira¹⁸⁴, S. Barsov⁶³, F. Bartels⁹¹, R. Bartoldus²¹⁴, A.E. Barton¹⁴¹, P. Bartos⁴¹, A. Basan¹⁵⁰, M. Baselga⁷⁶, S. Bashiri¹³⁶, A. Bassalat^{97,248}, M.J. Basso²²⁹, S. Bataju⁷¹, R. Bate²³⁸, R.L. Bates⁸⁷, S. Batlamous¹⁴⁹, M. Battaglia¹⁹⁶, D. Battulga²¹, M. Bauge^{113,114}, M. Bauer¹²¹, P. Bauer³¹, L.T. Bayer⁷⁵, L.T. Bazzano Hurrell⁴⁴, J.B. Beacham¹⁶⁰, T. Beau¹⁸¹, J.Y. Beauchamp¹⁴⁰, P.H. Beauchemin²³², P. Bechtel³¹, H.P. Beck^{22,259}, K. Becker²⁴¹, A.J. Beddall¹²⁴, V.A. Bednyakov⁶⁴, C.P. Bee²¹⁶, L.J. Beemster¹⁷, M. Begalli¹²⁸, M. Beggel⁴³, J.K. Behr⁷⁵, J.F. Beier⁶², F. Beisiegel³¹, M. Belfkir¹⁷⁰, G. Bella²²⁴, L. Bellagamba³⁰, A. Bellerive⁵⁵, C.D. Bellgraph⁹⁹, P.

Bellos²³, K. Beloborodov⁶³, I. Benaoumeur²³, D. Benchebkroun⁵⁶, F. Bendebba⁵⁶, Y. Benhammou²²⁴, K.C. Benkendorfer⁸⁹, L. Beresford⁷⁵, M. Beretta⁸⁰, E. Bergeas Kuutmann²³⁵, N. Berger⁵, B. Bergmann¹⁹², J. Beringer¹⁹, G. Bernardi⁶, C. Bernius²¹⁴, F.U. Bernlochner³¹, F. Bernon⁶², A. Berrocal Guardia¹⁴, T. Berry¹⁴⁵, P. Berta¹⁹³, A. Berthold⁷⁷, A. Berti¹⁸⁴, R. Bertrand¹⁵², S. Bethke¹⁶⁰, A. Betti^{113,114}, A.J. Bevan¹⁴⁴, L. Bezio⁸³, N.K. Bhalla⁸¹, S. Bharthuar¹⁶⁰, S. Bhatta²¹⁶, P. Bhattarai²¹⁴, Z.M. Bhatti¹⁷¹, K.D. Bhide⁸¹, V.S. Bhopatkar¹⁷⁵, R.M. Bianchi¹⁸³, G. Bianco^{30,29}, O. Biebel¹⁵⁹, M. Biglietti¹¹⁷, C.S. Billingsley⁷¹, Y. Bimgdi⁶¹, M. Bindj⁸², A. Bingham²⁴⁵, A. Bingul²⁵, C. Bini^{113,114}, G.A. Bird⁴⁶, M. Birman²⁴³, M. Biros¹⁹³, S. Biryukov²¹⁷, T. Bisanz⁷⁶, E. Bisceglie^{30,29}, J.P. Biswal¹⁹⁴, D. Biswas²¹², I. Bloch⁷⁵, A. Blue⁸⁷, U. Blumenschein¹⁴⁴, V.S. Bobrovnikov⁶⁴, L. Boccardo^{85,84}, M. Boehler⁸¹, B. Boehm²⁴⁰, D. Bogavac¹⁴, A.G. Bogdanchikov⁶³, L.S. Boggia¹⁸¹, V. Boisvert¹⁴⁵, P. Bokan⁶², T. Bold¹³⁴, M. Bomben⁶, M. Bona¹⁴⁴, M. Boonekamp¹⁹⁵, A.G. Borbély⁸⁷, I.S. Bordulev⁶³, G. Borissow¹⁴¹, D. Bortoletto¹⁸⁰, D. Boscherini³⁰, M. Bosman¹⁴, K. Bouaouda⁵⁶, N. Bouchhar²³⁷, L. Boudet⁵, J. Boudreau¹⁸³, E.V. Bouhova-Thacker¹⁴¹, D. Boumediene⁶⁶, R. Bouquet^{85,84}, A. Boveia¹⁷³, J. Boyd⁶², D. Boye⁴³, I.R. Boyko⁶⁴, L. Bozianu⁸³, J. Bracinik²³, N. Brahimi⁵, G. Brandt²⁴⁵, O. Brandt⁴⁶, B. Brau¹⁵³, J.E. Brau¹⁷⁷, R. Brener²⁴³, L. Brenner¹⁶⁷, R. Brenner²³⁵, S. Bressler²⁴³, G. Brianti^{119,120}, D. Britton⁸⁷, D. Britzger¹⁶⁰, I. Brock³¹, R. Brock¹⁵⁷, G. Brooijmans⁶⁷, A.J. Brooks⁹⁹, E.M. Brooks²³⁰, E. Brost⁴³, L.M. Brown^{239,229}, L.E. Bruce⁸⁹, T.L. Bruckler¹⁸⁰, P.A. Bruckman de Renstrom¹³⁶, B. Br⁷⁵, A. Bruni³⁰, G. Bruni³⁰, D. Brunner^{73,74}, M. Bruschi³⁰, N. Bruscinò^{113,114}, T. Buanes¹⁸, Q. Buat²⁰⁵, D. Buchin¹⁶⁰, A.G. Buckley⁸⁷, O. Bulekov¹²⁴, B.A. Bullard²¹⁴, S. Burdin¹⁴², C.D. Burgard⁷⁶, A.M. Burger¹³⁹, B. Burghgrave⁹, O. Burlayenko⁸¹, J. Burleson²³⁶, J.C. Burzynski²¹³, E.L. Busch⁶⁷, V. Büscher¹⁵⁰, P.J. Bussey⁸⁷, J.M. Butler³², C.M. Buttar⁸⁷, J.M. Butterworth¹⁴⁶, W. Buttinger¹⁹⁴, C.J. Buxo Vazquez¹⁵⁷, A.R. Buzzykaev⁶⁴, S. Cabrera Urbán²³⁷, L. Cadamuro⁹⁷, H. Cai⁶², Y. Cai^{30,164,29}, Y. Cai¹⁶², V.M.M. Cairo⁶², O. Cakir³, N. Calace⁶², P. Calafiura¹⁹, G. Calderini¹⁸¹, P. Calfayan⁵⁵, L. Calic¹⁴⁸, G. Callea⁸⁷, L.P. Caloba¹²⁶, D. Calvet⁶⁶, S. Calvet⁶⁶, R. Camacho Toro¹⁸¹, S. Camarda⁶², D. Camarero Munoz³³, P. Camarri^{115,116}, C. Camincher²³⁹, M. Campanelli¹⁴⁶, A. Camplani⁶⁸, V. Canale^{107,108}, A.C. Canbay³, E. Canonero¹⁴⁵, J. Cantero²³⁷, Y. Cao²³⁶, F. Capocasa³³, M. Capua^{70,69}, A. Carbone^{105,106}, R. Cardarelli¹¹⁵, J.C.J. Cardenas⁹, M.P. Cardiff⁹³, G. Carducci^{70,69}, T. Carli⁶², G. Carlino¹⁰⁷, J.I. Carlotto¹⁴, B.T. Carlson^{183,261}, E.M. Carlson²³⁹, J. Carmignani¹⁴², L. Carminati^{105,106}, A. Carnelli⁵, M. Carnesale⁶², S. Caron¹⁶⁶, E. Carquin²⁰³, I.B. Carr¹⁵⁵, S. Carrá^{109,110}, G. Carratta^{30,29}, C. Carrion Martinez²³⁷, A.M. Carroll¹⁷⁷, M.P. Casado^{14,252}, P. Casolaro^{107,108}, M. Caspar⁷⁵, F.L. Castillo⁵, L. Castillo Garcia¹⁴, V. Castillo Gimenez²³⁷, N.F. Castro^{184,188}, A. Catinaccio⁶², J.R. Catmore¹⁷⁹, T. Cavaliere⁵, V. Cavaliere⁴³, L.J. Caviedes Betancourt²⁸, E. Celebi¹²⁴, S. Cella⁶², V. Cepaitis⁸³, K. Cerny¹⁷⁶, A.S. Cerqueira¹²⁵, A. Cerri^{111,112,279}, L. Cerrito^{115,116}, F. Cerutti¹⁹, B. Cervato^{105,106}, A. Cervelli³⁰, G. Cesarinì⁸⁰, S.A. Cetin¹²⁴, P.M. Chabrilat¹⁸¹, R. Chakkappai⁹⁷, S. Chakraborty²⁴¹, A. Chambers⁸⁹, J. Chan¹⁹, W.Y. Chan²²⁶, J.D. Chapman⁴⁶, E. Chapon¹⁹⁵, B. Chargeishvili²²¹, D.G. Charlton²³, C. Chauhan¹⁹³, Y. Che¹⁶², S. Chekanov⁷, S.V. Chekulaev²²⁹, G.A. Chelkov^{64,63}, B. Chen²²⁴, B. Chen²³⁹, H. Chen¹⁶², H. Chen⁴³, J. Chen²⁰⁸, J. Chen²¹³, M. Chen¹⁸⁰, S. Chen¹³⁷, S.J. Chen¹⁶², X. Chen²⁰⁸, X. Chen^{16,274}, Z. Chen⁹⁰, C.L. Cheng²⁴⁴, H.C. Cheng⁹³, S. Cheong²¹⁴, A. Cheplakov⁶⁴, E. Cherepanova¹⁶⁷, R. Cherkaoui El Moursli⁶⁰, E. Cheu⁸, K. Cheung⁹⁶, L. Chevalier¹⁹⁵, V. Chiarella⁸⁰, G. Chiarelli¹¹¹, G. Chiodini¹⁰³, A.S. Chisholm²³, A. Chitan³⁵, M. Chitishvili²³⁷, M.V. Chizhov^{64,262}, K. Choi¹², Y. Chou²⁰⁵, E.Y.S. Chow¹⁶⁶, K.L. Chu²⁴³, M.C. Chu⁹³, X. Chu^{15,164}, Z. Chubinizde⁸⁰, J. Chudoba¹⁹¹, J.J. Chwastowski¹³⁶, D. Cieri¹⁶⁰, K.M. Ciesla¹³⁴, V. Cindro¹⁴³, A. Ciocio¹⁹, F. Ciroto^{107,108}, Z.H. Citron²⁴³, M. Citterio¹⁰⁵, D.A. Ciubotaru³⁵, A. Clark⁸³, P.J. Clark⁷⁹, N. Clarke Hall¹⁴⁶, C. Clarry²²⁸, S.E. Clawson⁷⁵, C. Clement^{73,74}, Y. Coadou¹⁵², M. Cobal^{100,102}, A. Cocco⁸⁵, R.F. Coelho Barrue¹⁸⁴, R. Coelho Lopes De Sa¹⁵³, S. Coelli¹⁰⁵, L.S. Colangeli²²⁸, B. Cole⁶⁷, P. Collado Soto¹⁴⁹, J. Collot⁸⁸, R. Coluccia^{103,104}, P. Conde Muñoz^{184,190}, M.P. Connell⁴⁹, S.H. Connell⁴⁹, E.I. Conroy¹⁸⁰, M. Contreras Cossio¹², F. Conventi^{107,276}, A.M. Cooper-Sarkar¹⁸⁰, L. Corazzina^{113,114}, F.A. Corchia^{30,29}, A. Cordeiro Oudot Choi²⁰⁵, L.D. Corpe⁶⁶, M. Corradi^{113,114}, F. Corriveau^{154,270}, A. Cortes-Gonzalez²²⁶, M.J. Costa²³⁷, F. Costanza⁵, D. Costanzo²¹⁰, B.M. Cote¹⁷³, J. Couthures⁵, G. Cowan¹⁴⁵, K. Cranmer²⁴⁴, L. Cremer⁷⁶, D. Cremonini^{30,29}, S. Crépe-Renaudin⁸⁸, F. Crescioli¹⁸¹, T. Cresta^{109,110}, M. Cristinziani²¹², M. Cristoforetti^{119,120}, V. Croft¹⁶⁷, G. Crosetti^{70,69}, A. Cueto¹⁴⁹, H. Cui¹⁴⁶, Z. Cui⁸, B.M. Cunnnett²¹⁷, W.R. Cunningham⁸⁷, F. Curcio²³⁷, J.R. Curran⁷⁹, M.J. Da Cunha Sargedas De Sousa^{85,84}, J.V. Da Fonseca Pinto¹²⁶, C. Da Via¹⁵¹, W. Dabrowski¹³⁴, T. Dado⁶², S. Dahbi²¹⁹, T. Dai¹⁵⁶, D. Dal Santo²², C. Dallapiccola¹⁵³, M. Dam⁶⁸, G. D'amen⁴³, V. D'Amico¹⁵⁹, J. Damp¹⁵⁰, J.R. Dandoy⁵⁵, M. D'Andrea^{85,84}, D. Dannheim⁶², G. D'anniballe^{111,112}, M. Danninger²¹³, V. Dao²¹⁶, G. Darbo⁸⁵, S.J. Das⁴³, F. Dattola⁷⁵, S. D'Auria^{105,106}, A. D'Avanzo^{107,108}, T. Davidek¹⁹³, J. Davidson²⁴¹, I. Dawson¹⁴⁴, K. De⁹, C. De Almeida Rossi²²⁸, R. De Asmundis¹⁰⁷, N. De Biase⁷⁵, S. De Castro^{30,29}, N. De Groot¹⁶⁶, P. de Jong¹⁶⁷, H. De la Torre¹⁶⁸, A. De Maria¹⁶², A. De Salvo¹¹³, U. De Santis^{115,116}, F. De Santis^{103,104}, A. De Santo²¹⁷, J.B. De Vivie De Regie⁸⁸, J. Debevc¹⁴³, D.V. Dedovich⁶⁴, J. Degens¹⁴², A.M. Deiana⁷¹, J. Del Peso¹⁴⁹, L. Delagrèze¹⁸¹, F. Deliot¹⁹⁵, C.M. Delitzsch⁷⁶, M. Della Pietra^{107,108}, D. Della Volpe⁸³, A. Dell'Acqua⁶², L. Dell'Asta^{105,106}, M. Delmastro⁵, C.C. Delogu¹⁵⁰, P.A. Delsart⁸⁸, S. Demers²⁴⁶, M. Demichev⁶⁴, S.P. Denisov⁶³, H. Denizli^{24,255}, L. D'Eramo⁶⁶, D. Derendarz¹³⁶, F. Derue¹⁸¹, P. Dervan¹⁴², A.M. Desai¹, K. Desch³¹, F.A. Di Bello^{85,84}, A. Di Ciaccio^{115,116}, L. Di Ciaccio⁵, A. Di Domenico^{113,114}, C. Di Donato^{107,108}, A. Di Girolamo⁶², G. Di Gregorio⁶², A. Di Luca^{119,120}, B. Di Micco^{117,118}, R. Di Nardo^{117,118}, K.F. Di Petrillo⁶⁵, M. Diamantopoulou⁵⁵, F.A. Dias¹⁶⁷, M.A. Diaz^{197,198}, A.R. Didenko⁶⁴, M. Didenko²³⁷, S.D. Diefenbacher¹⁹, E.B. Diehl¹⁵⁶, S. Díez Cornell⁷⁵, C. Diez Pardo²¹², C. Dimitriadi²¹⁵, A. Dimitrievska²³, A. Dimri²¹⁶, Y. Ding⁹⁰, J. Dingfelder³¹, T. Dingley¹⁸⁰, I-M Dinu³⁵, S.J. Dittmeier⁹², F. Dittus⁶², M. Divisek¹⁹³, B. Dixit¹⁴², F. Djama¹⁵², T. Djobava²²¹, C. Doglioni^{151,148}, A. Dohnalova⁴¹, Z. Dolezal¹⁹³, K. Domijan¹³⁴, K.M. Dona⁶⁵, M. Donadelli¹²⁸, B. Dong¹⁵⁷, J. Donini⁶⁶, A. D'Onofrio^{107,108}, M. D'Onofrio¹⁴², J. Dopke¹⁹⁴, A. Doria¹⁰⁷, N. Dos Santos Fernandes¹⁸⁴, I.A. Dos Santos Luz¹²⁹, P. Dougan¹⁵¹, M.T. Dova¹⁴⁰, A.T. Doyle⁸⁷, M.P. Drescher⁸², E. Dreyer²⁴³, I. Drivas-Koulouris¹¹, M. Drnevich¹⁷¹, D. Du⁹⁰, T.A. du Pree¹⁶⁷, Z. Duan¹⁶², M. Dubau⁵, F. Dubinin⁶⁴, M. Dubovsky⁴¹, E. Duchovni²⁴³, G. Duckeck¹⁵⁹, P.K. Duckett¹⁴⁶, O.A. Ducu³⁵, D. Duda⁷⁹, A. Dudarev⁶², M.M. Dudek¹³⁶, E.R. Duden³³, M. D'uffizi¹⁵¹, L. Duflo⁹⁷, M. Dührssen⁶², I. Duminica⁴⁰, A.E. Dumitriu³⁵, M. Dunford⁹¹, K. Dunne^{73,74}, A. Duperrin¹⁵², H. Duran Yildiz³, A. Durglishvili²²⁰, D. Duvnjak⁵⁵, G.I. Dyckes¹⁹, M. Dyndal¹³⁴, B.S. Dziedzic⁶², Z.O. Earnshaw²¹⁷, G.H. Eberwein¹⁸⁰, B. Eckerova⁴¹, S. Eggebrecht⁸², E. Egidio Purcino De Souza¹²⁹, G. Eigen¹⁸, K. Einsweiler¹⁹, T. Ekelof²³⁵, P.A. Ekman¹⁴⁸, S. El Farkh⁵⁷, Y. El Ghazali⁹⁰, H. El Jarrari⁶², A. El Moussaouy⁵⁶, D. Elitez⁶², M. Ellert²³⁵, F. Ellinghaus²⁴⁵, T.A. Elliot¹⁴⁵, N. Ellis⁶², J. Elmsheuser⁴³, M. Elsayy¹⁶⁹, M. Elsing⁶², D. Emelianov¹⁹⁴, Y. Enari¹³⁰, I. Ene¹⁹, S. Epari¹⁵⁸, D. Ernani Martins Neto¹³⁶, F. Ernst⁶², M. Errenst²⁴⁵, M. Escalier⁹⁷, C. Escobar²³⁷, E. Etzion²²⁴, G. Evans^{184,185}, H. Evans⁹⁹, L.S. Evans⁷⁵, A. Ezhilov⁶³, S. Ezzarqouni⁵⁶, F. Fabbri^{30,29}, L. Fabbri^{30,29}, G. Facini¹⁴⁶, V. Fadeyev¹⁹⁶, R.M. Fakhruddinov⁶³, D. Fakoudis¹⁵⁰, S. Falciano¹¹³, L.F. Falda Ulhoa Coelho¹⁸⁴, F. Fallavollita¹⁶⁰, G. Falsetti^{70,69},

J. Faltova¹⁹³, C. Fan²³⁶, K.Y. Fan⁹⁴, Y. Fan¹⁵, Y. Fang^{15,164}, M. Fanti^{105,106}, M. Faraj^{100,101}, Z. Farazpay¹⁴⁷, A. Farbin⁹, A. Farilla¹¹⁷, K. Farman²¹⁹, T. Faroouque¹⁵⁷, J.N. Farr²⁴⁶, S.M. Farrington^{194,79}, F. Fassi⁶⁰, D. Fassouliotis¹⁰, L. Fayard⁹⁷, P. Federic¹⁹³, P. Federicova¹⁹¹, O.L. Fedin^{63,63}, M. Feickert²⁴⁴, L. Feligioni¹⁵², D.E. Fellers¹⁹, C. Feng²⁰⁶, Y. Feng¹⁵, Z. Feng¹⁶⁷, M.J. Fenton²³³, L. Ferencz⁷⁵, B. Fernandez Barbadillo¹⁴¹, P. Fernandez Martinez⁹⁸, M.J.V. Fernoux¹⁵², J. Ferrando¹⁴¹, A. Ferrari²³⁵, P. Ferrari^{167,166}, R. Ferrari¹⁰⁹, D. Ferrere⁸³, C. Ferretti¹⁵⁶, M.P. Fewell¹, D. Fiacco^{113,114}, F. Fiedler¹⁵⁰, P. Fiedler¹⁹², S. Filimonov⁶⁴, M.S. Filip^{35,263}, A. Filipčić¹⁴³, E.K. Filmer²²⁹, F. Filthaut¹⁶⁶, M.C.N. Fiolhais^{184,186,249}, L. Fiorini²³⁷, W.C. Fisher¹⁵⁷, T. Fitschen¹⁵¹, P.M. Fitzhugh¹⁹⁵, I. Fleck²¹², P. Fleischmann¹⁵⁶, T. Flick²⁴⁵, M. Flores⁵⁰, L.R. Flores Castillo⁹³, L. Flores Sanz De Acedo⁶², F.M. Follega^{119,120}, N. Fomin⁴⁶, J.H. Foo²²⁸, A. Formica¹⁹⁵, A.C. Forti¹⁵¹, E. Fortin⁶², A.W. Fortman¹⁹, L. Foster¹⁹, L. Fountas^{10,253}, D. Fournier⁹⁷, H. Fox¹⁴¹, P. Francavilla^{111,112}, S. Francescato⁸⁹, S. Franchellucci⁸³, M. Franchini^{30,29}, S. Franchino⁹¹, D. Francis⁶², L. Franco¹⁶⁶, L. Franconi⁷⁵, M. Franklin⁸⁹, G. Frattari³³, Y.Y. Frid²²⁴, J. Friend⁸⁷, N. Fritzsche⁶², A. Froch⁸³, D. Froidevaux⁶², J.A. Frost¹⁸⁰, Y. Fu¹⁵⁷, S. Fuenzalida Garrido²⁰³, M. Fujimoto¹⁵², K.Y. Fung⁹³, E. Furtado De Simas Filho¹²⁹, M. Furukawa²²⁶, J. Fuster²³⁷, A. Gaa⁸², A. Gabrielli^{30,29}, A. Gabrielli²²⁸, P. Gadov⁶², G. Gagliardi^{85,84}, L.G. Gagnon¹⁹, S. Gaid¹³², S. Galantzan²²⁴, J. Gallagher¹, E.J. Gallas¹⁸⁰, A.L. Gallen²³⁵, B.J. Gallop¹⁹⁴, K.K. Gan¹⁷³, S. Ganguly²²⁶, Y. Gao⁷⁹, A. Garabaglu²⁰⁵, F.M. Garay Walls^{197,198}, C. García²³⁷, A.Garcia Alonso¹⁶⁷, A.G.Garcia Caffaro²⁴⁶, J.E. García Navarro²³⁷, M.A.Garcia Ruiz²⁸, M. Garcia-Sciveres¹⁹, G.L. Gardner¹⁸², R.W. Gardner⁶⁵, N. Garelli²³², R.B. Garg²¹⁴, J.M. Gargan⁷⁹, C.A. Garner²²⁸, C.M. Garvey⁴⁷, V.K. Gassmann²³², G. Gaudio¹⁰⁹, V. Gautam¹⁴, P. Gauzzi^{113,114}, J. Gavrancovic¹⁴³, I.L. Gavrilenko¹⁸⁴, A. Gavriluk⁶³, C. Gay²³⁸, G. Gaycken¹⁷⁷, E.N. Gazis¹¹, A. Gekow¹⁷³, C. Gemme⁸⁵, M.H. Genest⁸⁸, A.D. Gentry¹⁶⁵, S. George¹⁴⁵, T. Gerialis⁷², A.A. Gerwin¹⁷⁴, P. Gessinger-Befurt⁶², M.E. Geyik²⁴⁵, M. Ghani²⁴¹, K. Ghorbanian¹⁴⁴, A. Ghosal²¹², A. Ghosh²³³, A. Ghosh⁸, B. Giacobbe³⁰, S. Giagu^{113,114}, T. Giani¹⁶⁷, A. Giannini⁹⁰, S.M. Gibson¹⁴⁵, M. Gignac¹⁹⁶, D.T. Gil¹³⁵, A.K. Gilbert¹³⁴, B.J. Gilbert⁶⁷, D. Gillberg⁵⁵, G. Gilles¹⁶⁷, D.M. Gingrich^{2,275}, M.P. Giordani^{100,102}, P.F. Giraud¹⁹⁵, G. Giugliarelli^{100,102}, D. Giugni¹⁰⁵, F. Giuliani^{115,116}, I. Gkialas^{10,253}, L.K. Gladilin⁶³, C. Glasman¹⁴⁹, M. Glazewska²², R.M. Gleason²³³, G. Glemža⁷⁵, M. Glisic¹⁷⁷, I. Gnesi⁷⁰, Y. Go⁴³, M. Goblirsch-Kolb⁶², B. Gocke⁷⁶, D. Godin¹⁵⁸, B. Gokturk²⁴, S. Goldfarb¹⁵⁵, T. Golling⁸³, M.G.D. Gololo⁴⁹, D. Golubkov⁶³, J.P. Gombas¹⁵⁷, A. Gomes^{184,185}, G. Gomes Da Silva²¹², A.J. Gomez Delegido⁶², R. Gonçalves¹⁸⁴, L. Gonella²³, A. Gongadze²²², F. Gonnella²³, J.L. Gonski²¹⁴, R.Y. González Andana⁷⁹, S. González de la Hoz²³⁷, M.V. Gonzalez Rodriguez⁷⁵, R. Gonzalez Suarez²³⁵, S. Gonzalez-Sevilla⁸³, L. Goossens⁶², B. Gorini⁶², E. Gorini^{103,104}, A. Gorišek¹⁴³, T.C. Gosart¹⁸², A.T. Goshaw⁷⁸, M.I. Gostkin⁶⁴, S. Goswami¹⁷⁵, C.A. Gottardo⁶², S.A. Gotz¹⁵⁹, M. Gouighri⁵⁷, A.G. Goussiou²⁰⁵, N. Govender⁴⁹, R.P. Grabarczyk¹⁸⁰, I. Grabowska-Bold¹³⁴, K. Graham⁵⁵, E. Gramstad¹⁷⁹, S. Grancagnolo^{103,104}, C.M. Grant¹, P.M. Gravila³⁹, F.G. Gravili^{103,104}, H.M. Gray¹⁹, M. Greco¹⁶⁰, M.J. Green¹, C. Greife³¹, A.S. Grefsrud¹⁸, I.M. Gregor⁷⁵, K.T. Greif²³³, P. Grenier²¹⁴, S.G. Grewe¹⁶⁰, A.A. Grillo¹⁹⁶, K. Grimm⁴⁵, S. Grinstein^{14,267}, J.-F. Grivaz⁹⁷, E. Gross²⁴³, J. Grosse-Knetter⁸², L. Guan¹⁵⁶, G. Guerrieri⁶², R. Guevara¹⁷⁹, R. Gugel¹⁵⁰, J.A.M. Guhit¹⁵⁶, A. Guida²¹, E. Guillon²⁴¹, S. Guindon⁶², F. Guo^{15,164}, J. Guo²⁰⁸, L. Guo⁷⁵, L. Guo^{163,265}, Y. Guo¹⁵⁶, A. Gupta⁷⁶, R. Gupta¹⁸³, S. Gupta³³, S. Gurbuz³¹, S.S. Gurdasani⁷⁵, G. Gustavino^{113,114}, P. Gutierrez¹⁷⁴, L.F. Gutierrez Zagazeta¹⁸², M. Gutsche⁷⁷, C. Gutschow¹⁴⁶, C. Gwenlan¹⁸⁰, C.B. Gwilliam¹⁴², E.S. Haaland¹⁷⁹, A. Haas¹⁷¹, M. Habedank⁸⁷, C. Haber¹⁹, H.K. Hadavand⁹, A. Haddad⁶⁶, A. Hadeef⁷⁷, A.I. Hagan¹⁴¹, J.J. Hahn²¹², E.H. Haines¹⁴⁶, M. Haleem²⁴⁰, J. Haley¹⁷⁵, G.D. Hallewell¹⁵², K. Hamano²³⁹, H. Hamdaoui²³⁵, M. Hamer³¹, S.E.D. Hammoud⁹⁷, E.J. Hampshire¹⁴⁵, J. Han²⁰⁶, L. Han¹⁶², L. Han⁹⁰, S. Han¹⁵, K. Hanagaki¹³⁰, M. Hance¹⁹⁶, D.A. Hangal⁶⁷, H. Hanif²¹³, M.D. Hank¹⁸², J.B. Hansen⁶⁸, P.H. Hansen⁶⁸, D. Harada⁸³, T. Harenberg²⁴⁵, S. Harkusha²⁴⁷, M.L. Harris¹⁵³, Y.T. Harris³¹, J. Harrison¹⁴, N.M. Harrison¹⁷³, P.F. Harrison²⁴¹, M.L.E. Hart¹⁴⁶, N.M. Hartman¹⁶⁰, N.M. Hartmann¹⁵⁹, R.Z. Hasan^{145,194}, Y. Hasegawa²¹¹, F. Haslbeck¹⁸⁰, S. Hassan¹⁸, R. Hauser¹⁵⁷, M. Haviernik¹⁹³, C.M. Hawkes²³, R.J. Hawkings⁶², Y. Hayashi²²⁶, D. Hayden¹⁵⁷, C. Hayes¹⁵⁶, R.L. Hayes¹⁶⁷, C.P. Hays¹⁸⁰, J.M. Hays¹⁴⁴, H.S. Hayward¹⁴², M. He^{15,164}, Y. He⁷⁵, Y. He¹⁴⁶, N.B. Heatley¹⁴⁴, V. Hedberg¹⁴⁸, C. Heidegger⁸¹, K.K. Heidegger⁸¹, J. Heilman⁵⁵, S. Heim⁷⁵, T. Heim¹⁹, J.G. Heinlein¹⁸², J.J. Heinrich¹⁷⁷, L. Heinrich¹⁶⁰, J. Hejbal¹⁹¹, M. Helbig⁷⁷, A. Held²⁴⁴, S. Hellesund¹⁸, C.M. Helling²³⁸, S. Hellman^{73,74}, A.M. Henriques Correia⁶², H. Herde¹⁴⁸, Y. Hernández Jiménez²¹⁶, L.M. Herrmann³¹, T. Herrmann⁷⁷, G. Herten⁸¹, R. Hertenberger¹⁵⁹, L. Hervas⁶², M.E. Hespings¹⁵⁰, N.P. Hessey²²⁹, J. Hessler¹⁶⁰, M. Hidaoui⁵⁷, N. Hidic¹⁹³, E. Hill²²⁸, T.S. Hillersoy¹⁸, S.J. Hillier²³, J.R. Hinds¹⁵⁷, F. Hinterkeuser³¹, M. Hirose¹⁷⁸, S. Hirose²³¹, D. Hirschbuehl²⁴⁵, T.G. Hitchings¹⁵¹, B. Hiti¹⁴³, J. Hobbs²¹⁶, R. Hobincu³⁸, N. Hod²⁴³, A.M. Hodges²³⁶, M.C. Hodgkinson²¹⁰, B.H. Hodgkinson¹⁸⁰, A. Hoecker⁶², D.D. Hofer¹⁵⁶, J. Hofer²³⁷, M. Holzbock⁶², L.B.A.H. Hommels⁴⁶, V. Homsak¹⁸⁰, B.P. Honan¹⁵¹, J.J. Hong⁹⁹, T.M. Hong¹⁸³, B.H. Hooberman²³⁶, W.H. Hopkins⁷, M.C. Hoppesch²³⁶, Y. Horii¹⁶¹, M.E. Horstmann¹⁶⁰, S. Hou²¹⁹, M.R. Housenga²³⁶, J. Howarth⁸⁷, J. Hoya⁷, M. Hrabovsky¹⁷⁶, T. Hryn'ova⁵, P.J. Hsu⁹⁶, S.-C. Hsu²⁰⁵, T. Hsu⁹⁷, M. Hu¹⁹, Q. Hu⁹⁰, S. Huang⁴⁶, X. Huang^{15,164}, Y. Huang¹⁹³, Y. Huang¹⁶³, Y. Huang¹⁵, Z. Huang⁹⁷, Z. Hubacek¹⁹², F. Huegging³¹, T.B. Huffman¹⁸⁰, M. Hufnagel Maranha De Faria¹²⁵, C.A. Hugli⁷⁵, M. Huhtinen⁶², S.K. Huiberts¹⁸, R. Hulken¹⁵⁴, C.E. Hultquist¹⁹, D.L. Humphreys¹⁵³, N. Huseynov¹³, J. Huston¹⁵⁷, J. Huth⁸⁹, L. Huth⁷⁵, R. Hyneman⁸, G. Iacobucci⁸³, G. Iakovidis⁴³, L. Iconomidou-Fayard⁹⁷, J.P. Iddon⁶², P. Iengo^{107,108}, R. Iguchi²²⁶, Y. Iiyama²²⁶, T. Iizawa²²⁶, Y. Ikegami¹³⁰, D. Iliadis²²⁵, N. Ilic²²⁸, H. Imam⁵⁶, G. Inacio Goncalves¹²⁸, S.A. Infante Cabanas¹⁹⁹, T. Ingebretsen Carlson^{73,74}, J.M. Inglis¹⁴⁴, G. Introzzi^{109,110}, M. Iodice¹¹⁷, V. Ippolito^{113,114}, R.K. Irwin¹⁴², M. Ishino²²⁶, W. Islam²⁴⁴, C. Issever²¹, S. Istin^{24,281}, K. Itabashi¹³⁰, H. Ito²⁴², R. Iuppa^{119,120}, A. Ivina²⁴³, V. Izzo¹⁰⁷, P. Jacka¹⁹², P. Jackson¹, P. Jain⁷⁵, K. Jakobs⁸¹, T. Jakoubek²⁴³, J. Jamieson⁸⁷, W. Jang²²⁶, S. Jankovych¹⁹³, M. Javurkova¹⁵³, P. Jawahar¹⁵¹, L. Jeanty¹⁷⁷, J. Jejelava^{220,272}, P. Jenni^{81,62}, C.E. Jessiman⁵⁵, C. Jia²⁰⁶, H. Jia²³⁸, J. Jia²¹⁶, X. Jia^{160,164}, Z. Jia¹⁶², C. Jiang⁷⁹, Q. Jiang⁹⁴, S. Jiggins⁷⁵, M. Jimenez Ortega²³⁷, J. Jimenez Pena¹⁴, S. Jin¹⁶², A. Jinaru³⁵, O. Jinnouchi²⁰⁴, P. Johansson²¹⁰, K.A. Johns⁸, J.W. Johnson¹⁹⁶, F.A. Jolly⁷⁵, D.M. Jones²¹⁷, E. Jones⁷⁵, K.S. Jones⁹, P. Jones⁴⁶, R.W.L. Jones¹⁴¹, T.J. Jones¹⁴², H.L. Joos⁸², R. Joshi¹⁷³, J. Jovicevic¹⁷, X. Ju¹⁹, J.J. Junggeburth⁶², T. Junkermann⁹¹, A. Juste Rozas^{14,267}, M.K. Juzek¹³⁶, S. Kabana²⁰², A. Kaczmarska¹³⁶, S.A. Kadir²¹⁴, M. Kado¹⁶⁰, H. Kagan¹⁷³, M. Kagan²¹⁴, A. Kahn¹⁸², C. Kahra¹⁵⁰, T. Kaji²²⁶, E. Kajomovitz²²³, N. Kakati²⁴³, N. Kakoty¹⁴, I. Kalaitzidou⁸¹, S. Kandel⁹, N. Kanellos¹¹, N.J. Kang¹⁹⁶, D. Kar⁵⁴, E. Karentzos³¹, K. Karki⁹, O. Karkout¹⁶⁷, S.N. Karpov⁶⁴, Z.M. Karpova⁶⁴, V. Kartvelishvili¹⁴¹, A.N. Karyukhin⁶³, E. Kasimi²²⁵, J. Katzy⁷⁵, S. Kaur⁵⁵, K. Kawade²¹¹, M.P. Kawale¹⁷⁴, C. Kawamoto¹³⁷, T. Kawamoto⁹⁰, E.F. Kay⁶², F.I. Kaya²³², S. Kazakos¹⁵⁷, V.F. Kazanin⁶³, J.M. Keaveney⁴⁷, R. Keeler²³⁹, G.V. Kehris⁸⁹, J.S. Keller⁵⁵, J.M. Kelly²³⁹, J.J. Kempster²¹⁷, O. Kepka¹⁹¹, J. Kerr²³⁰, B.P. Kerridge¹⁹⁴, B.P. Kersevan¹⁴³, L. Keszeghova⁴¹, R.A. Khan¹⁸³, A. Khanov¹⁷⁵, A.G. Kharlamov⁶³, T. Kharlamova⁶³, E.E. Khoda²⁰⁵, M. Kholodenko¹⁸⁴, T.J. Khoo²¹, G.

Khoraiuli²⁴⁰, Y. Khoualaki⁵⁶, J. Khubua^{1,221}, Y.A.R. Khwaira¹⁸¹, B. Kibirige⁵⁴, D. Kim⁷, D.W. Kim^{73,74}, Y.K. Kim⁶⁵, N. Kimura¹⁴⁶, M.K. Kingston⁸², A. Kirchoff⁸², C. Kirfel³¹, F. Kirfel³¹, J. Kirl¹⁹⁴, A.E. Kiryunin¹⁶⁰, S. Kita²³¹, O. Kivernyk³¹, M. Klassen²³², C. Klein⁵⁵, L. Klein²⁴⁰, M.H. Klein⁷¹, S.B. Klein⁸³, U. Klein¹⁴², A. Klimentov⁴³, T. Klioutchnikova⁶², P. Kluit¹⁶⁷, S. Kluth¹⁶⁰, E. Kneringer¹²¹, T.M. Knight²²⁸, A. Knue⁷⁶, M. Kobel⁷⁷, D. Kobylanski²⁴³, S.F. Koch¹⁸⁰, M. Kocian²¹⁴, P. Kodyš¹⁹³, D.M. Koeck¹⁷⁷, T. Koffas⁵⁵, O. Kolay⁷⁷, I. Koletsou⁵, T. Komarek¹³⁶, K. Köneke⁸², A.X.Y. Kong¹, T. Kono¹⁷², N. Konstantinidis¹⁴⁶, P. Kontaxakis⁸³, B. Konya¹⁴⁸, R. Kopeliansky⁶⁷, S. Kopyerny¹³⁴, K. Korcyl¹³⁶, K. Kordas^{225,250}, A. Korn¹⁴⁶, S. Korn⁸², I. Korolkov¹⁴, N. Korotkova⁶³, B. Kortman¹⁶⁷, O. Kortner¹⁶⁰, S. Kortner¹⁶⁰, W.H. Kostecka¹⁶⁸, M. Kostov⁴¹, V.V. Kostyukhin²¹², A. Kotschev⁶², A. Kotwal⁷⁸, A. Koulouris⁶², A. Kourkoumelis^{109,110}, C. Kourkoumelis¹⁰, E. Kourlitis¹⁶⁰, O. Kovanda¹⁷⁷, R. Kowalewski²³⁹, W. Kozanecki¹⁷⁷, A.S. Kozhin⁶³, V.A. Kramarenko⁶³, G. Kramerberger¹⁴³, P. Kramer³¹, M.W. Krasny¹⁸¹, A. Krasznahorkay¹⁵³, A.C. Kraus¹⁶⁸, J.W. Kraus²⁴⁵, J.A. Kremer⁷⁵, N.B. Krenkel²¹², T. Kresse⁷⁷, L. Kretschmann²⁴⁵, J. Kretzschmar¹⁴², P. Krieger²²⁸, K. Krizka²³, K. Kroeninger⁷⁶, H. Kroha¹⁶⁰, J. Kroll¹⁹¹, J. Kroll¹⁸², K.S. Krowpman¹⁵⁷, U. Kruchonak⁶⁴, H. Kr³¹, N. Krumnack¹²³, M.C. Kruse⁷⁸, O. Kuchinskaya⁶⁴, S. Kuday³, S. Kuehn⁶², R. Kuesters⁸¹, T. Kuhl⁷⁵, V. Kukhtin⁶⁴, Y. Kulchitsky⁶⁴, S. Kuleshov^{200,198}, J. Kull¹, E.V. Kumar¹⁵⁹, M. Kumar⁵⁴, N. Kumari⁷⁵, P. Kumari²³⁰, A. Kupco¹⁹¹, A. Kupich⁶³, O. Kuprash⁸¹, H. Kurashige¹³³, L.L. Kurchaninov²²⁹, O. Kurdysh⁵, Y.A. Kurochkin⁶³, A. Kurova⁶³, M. Kuze²⁰⁴, A.K. Kvam¹⁵³, J. Kvita¹⁷⁶, N.G. Kyriacou²⁰⁵, C. Lacasta²³⁷, F. Lacava^{113,114}, H. Lacker²¹, D. Lacour¹⁸¹, N.N. Lad¹⁴⁶, E. Ladygin⁶⁴, A. Lafarge⁶⁶, B. Laforge¹⁸¹, T. Lagouri²⁴⁶, F.Z. Lahbabi⁵⁶, S. Lai^{82,62}, W.S. Lai¹⁴⁶, J.E. Lambert²³⁹, S. Lammers⁹⁹, W. Lampl⁸, C. Lampoudis^{225,250}, G. Lamprinou¹⁵⁰, A.N. Lancaster¹⁶⁸, E. Lançon⁴³, U. Landgraf⁸¹, M.P.J. Landon¹⁴⁴, V.S. Lang⁸¹, O.K.B. Langrekken¹⁷⁹, A.J. Lankford²³³, F. Lanni⁶², K. Lantzschi³¹, A. Lanza¹⁰⁹, M. Lanzac Berrocal²³⁷, J.F. Laporte¹⁹⁵, T. Lari¹⁰⁵, D. Larsen¹⁸, L. Larson¹², F. Lasagni Manghi³⁰, M. Lassnig⁶², S.D. Lawlor²¹⁰, R. Lazaridou²³³, M. Lazzaroni^{105,106}, H.D.M. Le¹⁵⁷, E.M. Le Boulicaut²⁴⁶, L.T. Le Pottier¹⁹, B. Leban^{30,29}, F. Ledroit-Guillon⁸⁸, T.F. Lee²³⁰, L.L. Leeuw⁴⁹, M. Lefebvre²³⁹, C. Leggett¹⁹, G. Lehmann Miotto⁶², M. Leigh⁸³, W.A. Leight¹⁵³, W. Leinonen¹⁶⁶, A. Leisos^{225,264}, M.A.L. Leite¹²⁷, C.E. Leitgeb²¹, R. Leitner¹⁹³, K.J.C. Leney⁷¹, T. Lenz³¹, S. Leone¹¹¹, C. Leonidopoulos⁷⁹, A. Leopold²¹⁵, J.H. Lepage Bourbonnais⁵⁵, R. Les¹⁵⁷, C.G. Lester⁴⁶, M. Levchenko⁶³, J. Levêque⁵, L.J. Levinson²⁴³, G. Levrin^{30,29}, M.P. Lewicki¹³⁶, C. Lewis²⁰⁵, D.J. Lewis⁵, L. Lewitt²¹⁰, A. Li⁴³, B. Li²⁰⁶, C. Li¹⁵⁶, C-Q Li¹⁶⁰, H. Li²⁰⁶, H. Li¹⁵¹, H. Li¹⁶, H. Li⁹⁰, H. Li²⁰⁶, J. Li²⁰⁸, K. Li¹⁵, L. Li²⁰⁸, R. Li²⁴⁶, S. Li^{15,164}, S. Li^{209,208}, T. Li⁶², X. Li¹⁵⁴, Y. Li¹⁵, Z. Li²²⁶, Z. Li^{15,164}, Z. Li⁹⁰, S. Liang^{15,164}, Z. Liang¹⁵, M. Liberatore¹⁹⁵, B. Liberti¹¹⁵, G.B. Libotte¹²⁸, K. Lie⁹⁵, J. Lieber Marin¹²⁹, H. Lien⁹⁹, H. Lin¹⁵⁶, S.F. Lin²¹⁶, L. Linden¹⁵⁹, R.E. Lindley⁸, J.H. Lindon⁶², J. Ling⁸⁹, E. Lipeles¹⁸², A. Lipniacka¹⁸, A. Lister²³⁸, J.D. Little⁹⁹, B. Liu¹⁵, B.X. Liu¹⁶³, D. Liu^{209,208}, D. Liu¹⁹⁶, E.H.L. Liu²³, P.K.K. Liu¹⁷¹, K. Liu²⁰⁹, K. Liu^{209,208}, M. Liu⁹⁰, M.Y. Liu⁹⁰, J.J. Liu¹⁵, Q. Liu^{209,205,208}, S. Liu²¹⁶, X. Liu⁹⁰, X. Liu²⁰⁶, Y. Liu^{163,164}, Y.L. Liu²⁰⁶, Y.W. Liu²¹⁶, Z. Liu^{97,90}, S.L. Lloyd¹⁴⁴, E.M. Lobodzinska⁷⁵, P. Loch⁸, E. Lodhi²²⁸, K. Lohwasser²¹⁰, E. Loiacono⁷⁵, J.D. Lomas²³, J.D. Long⁶⁷, I. Longarini²³³, R. Longo²³⁶, A. Lopez Solis¹⁴, N.A. Lopez-canelas⁸, N. Lorenzo Martinez⁵, A.M. Lory¹⁵⁹, M. Losada¹⁶⁹, G. Löschecke Centeno⁵, X. Lou^{73,74}, X. Lou^{15,164}, A. Lounis⁹⁷, P.A. Love¹⁴¹, M. Lu⁹⁷, S. Lu¹⁸², Y.J. Lu²¹⁹, H.J. Lubatti²⁰⁵, C. Luci^{113,114}, F.L. Lucio Alves¹⁶², F. Luehring⁹⁹, B.S. Lunday¹⁸², O. Lundberg²¹⁵, J. Lunde⁶², N.A. Luongo⁷, M.S. Lutz⁶², A.B. Lux³², D. Lynn⁴³, R. Lysak¹⁹¹, V. Lysenko¹⁹², E. Lytken¹⁴⁸, V. Lyubushkin⁶⁴, T. Lyubushkina⁶⁴, M.M. Lyukova²¹⁶, H. Ma⁴³, K. Ma⁹⁰, L.L. Ma²⁰⁶, W. Ma⁹⁰, Y. Ma¹⁷⁵, J.C. MacDonald¹⁵⁰, P.C. Machado De Abreu Farias¹²⁹, D. Macina⁶², R. Madar⁶⁶, T. Madula¹⁴⁶, J. Maeda¹³³, T. Maeno⁴³, P.T. Mafa^{49,254}, H. Maguire²¹⁰, M. Maheshwari⁴⁶, V. Maiboroda⁹⁷, A. Maio^{184,185,187}, K. Maj¹³⁴, O. Majersky⁷⁵, S. Majewski¹⁷⁷, R. Makhmanazarov⁶³, N. Makovec⁹⁷, V. Maksimovic¹⁷, B. Malaescu¹⁸¹, J. Malamant¹⁷⁹, Pa Malecki¹³⁶, V.P. Maleev⁶³, F. Malek^{88,258}, M. Mali¹⁴³, D. Malito¹⁴⁵, U. Mallik^{1,122}, A. Maloizel⁶, S. Maltezos¹¹, A. Malvezzi Lopes¹²⁸, S. Malysukov⁶⁴, J. Mamuzic¹⁴³, G. Mancini⁸⁰, M.N. Mancini³³, G. Manco^{109,110}, J.P. Mandalia¹⁴⁴, S.S. Mandary²¹⁷, I. Mandi¹⁴³, L. Manhaes de Andrade Filho¹²⁵, I.M. Maniatis²⁴³, J. Manjarres Ramos¹³⁹, D.C. Mankad²⁴³, A. Mann¹⁵⁹, T. Manoussos⁶², M.N. Mantinan⁶⁵, S. Manzoni⁶², L. Mao²⁰⁸, X. Mapekula⁴⁹, A. Marantis²²⁵, R.R. Marcelo Gregorio¹⁴⁴, G. Marchiori⁶, C. Marcon¹⁰⁵, E. Maricic¹⁷, M. Marinescu⁷⁵, S. Marius⁷⁵, M. Marjanovic¹⁷⁴, A. Markhoos⁸¹, M. Markovitch⁹⁷, M.K. Maroun¹⁵³, M.C. Mari²¹³, G.T. Marsden¹⁵¹, E.J. Marshall¹⁴¹, Z. Marshall¹⁹, S. Marti-Garcia²³⁷, J. Martin¹⁴⁶, T.A. Martin¹⁹⁴, V.J. Martin⁷⁹, B. Martin dit Latour¹⁸, L. Martinelli^{113,114}, M. Martinez^{14,267}, P. Martinez Agullo²³⁷, V.I. Martinez Outschoorn¹⁵³, P. Martinez Suarez⁶², S. Martin-Haugh¹⁹⁴, G. Martinovicova¹⁹³, V.S. Martoiu³⁵, A.C. Martyniuk¹⁴⁶, A. Marzin⁶², D. Mascione^{119,120}, L. Masetti¹⁵⁰, J. Masik¹⁵¹, A.L. Maslennikov⁶⁴, S.L. Mason⁶⁷, P. Massarotti^{107,108}, P. Mastrandrea^{111,112}, A. Mastroberardino^{70,69}, T. Masubuchi¹⁷⁸, T.T. Mathew¹⁷⁷, J. Matousek¹⁹³, D.M. Mattern⁷⁶, J. Maurer³⁵, T. Maurin⁸⁷, A.J. Maury⁹⁷, B. Maček¹⁴³, C. Mavungu Tsava¹⁵², D.A. Maximov⁶³, A.E. May¹⁵¹, E. Mayer⁶⁶, R. Mazini⁵⁴, I. Maznas¹⁶⁸, S.M. Mazza¹⁹⁶, E. Mazzeo⁶², J.P. Mc Gowan²³⁹, S.P. Mc Kee¹⁵⁶, C.A. Mc Lean⁷, C.C. McCracken²³⁸, E.F. McDonald¹⁵⁵, A.E. McDougall¹⁶⁷, L.F. Mcelhinney¹⁴¹, J.A. Mcfayden²¹⁷, R.P. McGovern¹⁸², R.P. Mckenzie⁵⁴, T.C. Mclachlan⁷⁵, D.J. Mclaughlin¹⁴⁶, S.J. McMahon¹⁹⁴, C.M. Mcpartland¹⁴², R.A. McPherson^{239,270}, S. Mehlhase¹⁵⁹, A. Mehta¹⁴², D. Melini²³⁷, B.R. Castillo Garcia⁵⁴, A.H. Melo⁸², F. Meloni⁷⁵, A.M. Mendes Jacques Da Costa¹⁵¹, L. Meng¹⁴¹, S. Menke¹⁶⁰, M. Mentink⁶², E. Meoni^{70,69}, G. Mercado¹⁶⁸, S. Merianos²²⁵, C. Merlassino^{100,102}, C. Meroni^{105,106}, J. Metcalfe⁷, A.S. Mete⁷, E. Meuser¹⁵⁰, C. Meyer⁹⁹, J-P Meyer¹⁹⁵, Y. Miao¹⁶², R.P. Middleton¹⁹⁴, M. Mihovilovic⁹⁷, L. Mijovic⁷⁹, G. Mikenberg²⁴³, M. Mikestikova¹⁹¹, M. Mikuz¹⁴³, H. Mildner¹⁵⁰, A. Milic⁶², D.W. Miller⁶⁵, E.H. Miller²¹⁴, A. Milov²⁴³, D.A. Milstead^{73,74}, T. Min¹⁶², A.A. Minaenko⁶³, I.A. Minashvili²²¹, A.I. Mincer¹⁷¹, B. Mindur¹³⁴, M. Mineev⁶⁴, Y. Mino¹³⁷, L.M. Mir¹⁴, M. Miralles Lopez⁸⁷, M. Mironova¹⁹, M. Missio¹⁶⁶, A. Mitra²⁴¹, V.A. Mitsou²³⁷, Y. Mitsumori¹⁶¹, O. Miu²²⁸, P.S. Miyagawa¹⁴⁴, T. Mkrtychyan⁹¹, M. Mlinarevic¹⁴⁶, T. Mlinarevic¹⁴⁶, M. Mlynarikova¹⁹³, L. Mlynarska¹³⁴, C. Mo²⁰⁸, S. Mobius²², M.H. Mohamed Farook¹⁶⁵, S. Mohapatra⁶⁷, M.F. Mohd Soberi⁷⁹, S. Mohiuddin¹⁷⁵, G. Mokgatswane⁵⁴, L. Moleri²⁴³, U. Molinari¹⁸⁰, L.G. Mollier²², B. Mondal¹⁹¹, S. Mondal¹⁹², K. Mönig⁷⁵, E. Monnier¹⁵², L. Monsonis Romero²³⁷, J. Montejo Berlingen¹⁴, A. Montella^{73,74}, M. Montella¹⁷³, F. Montereali^{117,118}, F. Monticelli¹⁴⁰, S. Monzani^{100,102}, A. Moranco Tarda⁶⁸, N. Morange⁹⁷, A.L. Moreira De Carvalho⁷⁵, M. Moreno Llacer²³⁷, C. Moreno Martinez⁸³, J.M. Moreno Perez²⁸, P. Moretti⁸⁵, S. Morgenstern⁶², M. Morii⁸⁹, M. Morinaga²²⁶, M. Moritsu¹³⁸, F. Morodei^{113,114}, P. Moschovakos⁶², B. Moser⁸¹, M. Mosidze²²¹, T. Moskalets⁷¹, P. Moskvitina¹⁶⁶, J. Moss⁴⁵, P. Moszkowicz¹³⁴, A. Moussa⁵⁹, Y. Moyal²⁴³, H. Moyano Gomez¹⁴, E.J.W. Moyses¹⁵³, T.G. Mroz¹³⁶, O. Mtintsilana⁵⁴, S. Muanza¹⁵², M. Mucha³¹, J. Mueller¹⁸³, R. Müller⁶², G.A. Mullier²³⁵, A.J. Mullin⁴⁶, J.J. Mullin⁷⁸, A.C. Mullins⁷¹, A.E. Mulski⁸⁹, D.P. Mungo²²⁸, D. Munoz Perez²³⁷, F.J. Munoz Sanchez¹⁵¹, W.J. Murray^{241,194}, M. Muškinja¹⁴³, C. Mwewa⁷⁵, A.G. Myagkov^{63,63}, A.J. Myers⁹, G. Myers¹⁵⁶, M. Myska¹⁹², B.P. Nachman²¹⁴, K. Nagai¹⁸⁰, K. Nagano¹³⁰

R. Nagasaka²²⁶, J.L. Nagle^{43,278}, E. Nagy¹⁵², A.M. Nairz⁶², Y. Nakahama¹³⁰, K. Nakamura¹³⁰, K. Nakkalil⁶, A. Nandi⁹², H. Nanjo¹⁷⁸, E.A. Narayanan⁷¹, Y. Narukawa²²⁶, I. Naryshkin⁶³, L. Nasella^{105,106}, S. Nasri¹⁷⁰, C. Nass³¹, G. Navarro²⁷, A. Nayaz²¹, P.Y. Nechaeva⁶³, S. Nechaeva^{30,29}, F. Nechansky¹⁹¹, L. Nedic¹⁸⁰, T.J. Neep²³, A. Negri^{109,110}, M. Negrini³⁰, C. Nellist¹⁶⁷, C. Nelson¹⁵⁴, K. Nelson¹⁵⁶, S. Nemecek¹⁹¹, M. Nessi^{62,83}, M.S. Neubauer²³⁶, J. Newell¹⁴², P.R. Newman²³, Y.W.Y. Ng²³⁶, B. Ngair¹⁶⁹, H.D.N. Nguyen¹⁵⁸, J.D. Nichols¹⁷⁴, R.B. Nickerson¹⁸⁰, R. Nicolaidou¹⁹⁵, J. Nielsen¹⁹⁶, M. Niemeyer⁸², J. Niermann⁶², N. Nikiforov⁶², V. Nikolaenko^{63,63}, I. Nikolic-Audit¹⁸¹, P. Nilsson⁴³, I. Ninca⁷⁵, G. Ninio²²⁴, A. Nisati¹¹³, R. Nisius¹⁶⁰, N. Nitika^{100,102}, J.-E. Nitschke⁷⁷, E.K. Nkadimeng⁴⁸, T. Nobe²²⁶, D. Noll¹⁹, T. Nommensen²¹⁸, M.B. Norfolk²¹⁰, B.J. Norman⁵⁵, L.C. Nosler¹⁹, M. Noury⁵⁶, J. Novak¹⁴³, T. Novak¹⁴³, R. Novotny¹⁹², L. Nozka¹⁷⁶, K. Ntekas²³³, D. Ntounis²¹⁴, N.M.J. Nunes De Moura Junior¹²⁶, J. Ocariz¹⁸¹, I. Ochoa¹⁸⁴, S. Oerdek^{75,268}, J.T. Offermann⁶⁵, A. Ogradnik¹⁹³, A. Oh¹⁵¹, C.C. Ohm²¹⁵, H. Oide¹³⁰, M.L. Ojeda⁶², Y. Okumura²²⁶, L.F.Oleiro Seabra¹⁸⁴, I. Oleksiyuk⁸³, G. Oliveira Correa¹⁴, D. Oliveira Damazio⁴³, J.L. Oliver²³³, R. Omar⁹⁹, Ö.O. Öncel⁸¹, A.P. O'Neill²², A. Onofre^{184,188,251}, P.U.E. Onyisi¹², M.J. Oreglia⁶⁵, D. Orestano^{117,118}, R. Orlandini^{117,118}, R.S. Orr²²⁸, L.M. Osojnak⁶⁷, Y. Osumi¹⁶¹, G. Otero y Garzon⁴⁴, H. Otono¹³⁸, M. Ouchrif⁵⁹, F. Ould-Saada¹⁷⁹, T. Ovsinnikova²⁰⁵, M. Owen⁸⁷, R.E. Owen¹⁹⁴, V.E. Ozcan²⁴, F. Ozturk¹³⁶, N. Ozturk⁹, S. Ozturk¹²⁴, H.A. Pacey¹⁸⁰, K. Pachal²²⁹, A. Pacheco Pages¹⁴, C. Padilla Aranda¹⁴, G. Padovano^{113,114}, S. Pagan Griso¹⁹, G. Palacino⁹⁹, A. Palazzo^{103,104}, J. Pampel³¹, J. Pan²⁴⁶, T. Pan⁹³, D.K. Panchal¹², C.E. Pandini⁸⁸, J.G. Panduro Vazquez¹⁹⁴, H.D. Pandya¹, H. Pang¹⁹⁵, P. Pani⁷⁵, G. Panizzo^{100,102}, L. Panwar¹⁸¹, L. Paolozzi⁸³, S. Parajuli²³⁶, A. Paramonov⁷, C. Paraskevopoulos⁸⁰, D. Paredes Hernandez⁹⁴, A. Pareti^{109,110}, K.R. Park⁶⁷, T.H. Park¹⁶⁰, F. Parodi^{85,84}, J.A. Parsons⁶⁷, U. Parzefall⁸¹, B. Pascual Dias⁶⁶, L. Pascual Dominguez¹⁴⁹, E. Pasqualucci¹¹³, S. Passaggio⁸⁵, F. Pastore¹⁴⁵, P. Patel¹³⁶, U.M. Patel⁷⁸, J.R. Pater¹⁵¹, T. Pauly⁶², F. Pauwels¹⁹³, C.I. Pazos²³², M. Pedersen¹⁷⁹, R. Pedro¹⁸⁴, S.V. Peleganchuk⁶³, O. Penc¹⁹¹, E.A. Pender⁷⁹, S. Peng¹⁶, G.D. Penn²⁴⁶, K.E. Pinski¹⁵⁹, M. Penzin⁶³, B.S. Peralva¹²⁸, A.P. Pereira Peixoto²⁰⁵, L. Pereira Sanchez²¹⁴, D.V. Perepelitsa^{43,278}, G. Perera¹⁵³, E. Perez Codina⁶², M. Perganti¹¹, H. Pernegger⁶², S. Perrella^{113,114}, K. Peters⁷⁵, R.F.Y. Peters¹⁵¹, B.A. Petersen⁶², T.C. Petersen⁶⁸, E. Petit¹⁵², V. Petousis¹⁹², A.R. Petri^{105,106}, C. Petridou^{225,250}, T. Petru¹⁹³, A. Petrukhin²¹², M. Pettee¹⁹, A. Petukhov¹²⁴, K. Petukhova⁶², R. Pezoa²⁰³, L. Pezzotti^{30,29}, G. Pezzullo²⁴⁶, L. Pfaffenbichler⁶², A.J. Pfeifer¹²¹, T.M. Pham²⁴⁴, T. Pham¹⁵⁵, P.W. Phillips¹⁹⁴, G. Piacquadio²¹⁶, E. Pianori¹⁹, F. Piazza¹⁷⁷, R. Piegaia⁴⁴, D. Pietreanu³⁵, A.D. Pilkington¹⁵¹, M. Pinamonti^{100,102}, J.L. Pinfold², B.C. Pinheiro Pereira¹⁸⁴, J. Pinol Bel¹⁴, A.E. Pinto Pinoargote¹⁸¹, L. Pintucci^{100,102}, K.M. Piper²¹⁷, A. Pirttikoski⁸³, D.A. Pizzi⁵⁵, L. Pizzimento⁹⁴, A. Plebani⁴⁶, M.-A. Pleier⁴³, V. Pleskot¹⁹³, E. Plotnikova⁶⁴, G. Poddar¹⁴⁴, R. Poettgen¹⁴⁸, L. Poggioli¹⁸¹, S. Polacek¹⁹³, G. Polesello¹⁰⁹, A. Poley²¹³, A. Polini³⁰, C.S. Pollard²⁴¹, Z.B. Pollock¹⁷³, E. Pompa Pacchi¹⁷⁴, N.I. Pond¹⁴⁶, D. Ponomarenko⁹⁹, L. Pontecorvo⁶², S. Popa³⁴, G.A. Popeneciu³⁷, A. Poreba⁶², D.M. Portillo Quintero²²⁹, S. Pospisil¹⁹², M.A. Postill²¹⁰, P. Postolache³⁶, K. Potamianos²⁴¹, P.A. Potepa¹³⁴, I.N. Potrap⁶⁴, C.J. Potter⁴⁶, H. Potti²¹⁸, J. Poveda²³⁷, M.E. Pozo Astigarraga⁶², R. Pozzi⁶², A. Prades Ibanez^{115,116}, S.R. Pradhan²¹⁰, J. Pretel²³⁹, D. Price¹⁵¹, M. Primavera¹⁰³, L. Primomo^{100,102}, M.A. Principe Martin¹⁴⁹, R. Privara¹⁷⁶, T. Procter¹³⁵, M.L. Proffitt²⁰⁵, N. Proklova¹⁸², K. Prokofiev⁹⁵, G. Proto¹⁶⁰, J. Proudfoot⁷, M. Przybycien¹³⁴, W.W. Przygoda¹³⁵, A. Psallidas⁷², J.E. Puddefoot²¹⁰, D. Pudza⁸⁰, H.I. Purnell¹, D. Pyatizbyantseva¹⁶⁶, J. Qian¹⁵⁶, R. Qian¹⁵⁷, D. Qichen¹⁸⁰, Y. Qin¹⁴, T. Qiu⁷⁹, A. Quadt⁸², M. Quetsch-Maitland¹⁵¹, G. Quetant⁸³, R.P. Quinn²³⁸, G. Rabanal Bolanos⁸⁹, D. Rafanoharana¹⁶⁰, F. Raffaelli^{115,116}, F. Ragusa^{105,106}, J.L. Rainbolt⁶⁵, S. Rajagopalan⁴³, E. Ramakoti⁶⁴, L. Rambelli^{85,84}, I.A. Ramirez-Berend⁵⁵, K. Ran^{75,164}, D.S. Rankin¹⁸², N.P. Rapheeha⁵⁴, H. Rasheed³⁵, D.F. Rassloff⁹¹, A. Rastogi¹⁹, S. Rave¹⁵⁰, S. Ravera^{85,84}, B. Ravina⁶², I. Ravinovich²⁴³, M. Raymond⁶², A.L. Read¹⁷⁹, N.P. Readioff²¹⁰, D.M. Rebuffi^{109,110}, A.S. Reed⁸⁷, K. Reeves³³, J.A. Reidelsturz²⁴⁵, D. Reikher⁶², A. Rej⁷⁶, C. Rembser⁶², H. Ren⁹⁰, M. Renda³⁵, F. Renner⁷⁵, A.G. Rennie⁸⁷, A.L. Rescia^{85,84}, S. Resconi¹⁰⁵, M. Ressegotti^{85,84}, S. Rettie¹⁶⁷, W.F. Rettie⁵⁵, M.M. Revering⁴⁶, E. Reynolds¹⁴⁹, O.L. Rezanova⁶⁴, P. Reznicek¹⁹³, H. Riani⁵⁹, N. Ribarik⁷⁸, B. Ricci^{100,102}, E. Ricci^{119,120}, R. Richter¹⁶⁰, S. Richter^{73,74}, E. Richter-Was¹³⁵, M. Ridel¹⁸¹, S. Ridouani⁵⁹, P. Rieck¹⁷¹, P. Riedler⁶², E.M. Riefel^{73,74}, J.O. Rieger¹⁶⁷, M. Rijssenbeek²¹⁶, M. Rimoldi⁶², L. Rinaldi^{30,29}, P. Rincke^{235,82}, G. Ripellino²³⁵, I. Riu¹⁴, J.C. Rivera Vergara²³⁹, F. Rizatdinova¹⁷⁵, E. Rizvi¹⁴⁴, B.R. Roberts¹⁹, S.S. Roberts¹⁹⁶, D. Robinson⁴⁶, M. Robles Manzano¹⁵⁰, A. Robson⁸⁷, A. Rocchi^{115,116}, C. Roda^{111,112}, S. Rodriguez Bosca⁶², Y. Rodriguez Garcia²⁷, A.M. Rodriguez Vera¹⁶⁸, S. Roe⁶², J.T. Roemer⁶², O. Röhne¹⁷⁹, R.A. Rojas⁶², C.P.A. Roland¹⁸¹, A. Romaniouk¹²¹, E. Romano^{109,110}, M. Romano³⁰, A.C. Romero Hernandez²³⁶, N. Rompotis¹⁴², L. Roos¹⁸¹, S. Rosati¹¹³, B.J. Rosser⁶⁵, E. Rossi¹⁸⁰, E. Rossi^{107,108}, L.P. Rossi⁸⁹, L. Rossini⁸¹, R. Rosten¹⁷³, M. Rotaru³⁵, B. Rottler⁸¹, D. Rousseau⁹⁷, D. Rouso⁷⁵, S. Roy-Garand²²⁸, A. Rozanov¹⁵², Z.M.A. Rozario⁸⁷, Y. Rozen²²³, A. Rubio Jimenez²³⁷, V.H. Ruelas Rivera²¹, T.A. Ruggieri¹, A. Ruggiero¹⁸⁰, A. Ruiz-Martinez²³⁷, A. Rummeler⁶², Z. Rurikova⁸¹, N.A. Rusakovich⁶⁴, S. Ruscelli⁷⁶, H.L. Russell²³⁹, G. Russo^{113,114}, J.P. Rutherford⁸, S. Rutherford Colmenares⁴⁶, M. Rybar¹⁹³, P. Rybczynski¹³⁴, A. Ryzhov⁷¹, J.A. Sabater Iglesias⁸³, H.F.-W. Sadrozinski¹⁹⁶, F. Safai Tehrani¹¹³, S. Saha¹, M. Sahinson¹²⁴, B. Sahoo²⁴³, A. Saibel²³⁷, B.T. Saifuddin¹⁷⁴, M. Saimpert¹⁹⁵, G.T. Saito¹²⁷, M. Saito²²⁶, T. Saito²²⁶, A. Sala^{105,106}, A. Salnikov²¹⁴, J. Salt²³⁷, A. Salvador Salas²²⁴, F. Salvatore²¹⁷, A. Salzburger⁶², D. Sammel⁸¹, E. Sampson¹⁴¹, D. Sampsonidis^{225,250}, D. Sampsonidou¹⁷⁷, J. Sánchez²³⁷, V. Sanchez Sebastian²³⁷, H. Sandaker¹⁷⁹, C.O. Sander⁷⁵, J.A. Sandesara²⁴⁴, M. Sandhoff²⁴⁵, C. Sandoval²⁸, L. Sanfilippo⁹¹, D.P.C. Sankey¹⁹⁴, T. Sano¹³⁷, A. Sansoni⁸⁰, M. Santana Queiroz²⁰, L. Santi⁶², C. Santoni⁶⁶, H. Santos^{184,185}, A. Santra²⁴³, E. Sanzani^{30,29}, K.A. Saoucha¹³², J.G. Saraiva^{184,187}, J. Sardain⁸, O. Sasaki¹³⁰, K. Sato²³¹, C. Sauer⁶², E. Sauvan⁵, P. Savard^{228,275}, R. Sawada²²⁶, C. Sawyer¹⁹⁴, L. Sawyer¹⁴⁷, C. Sbarra³⁰, A. Sbrizzi^{30,29}, T. Scanlon¹⁴⁶, J. Schaarschmidt²⁰⁵, U. Sch¹⁵⁰, A.C. Schaffer^{97,71}, D. Schaile¹⁵⁹, R.D. Schamberger²¹⁶, C. Scharf²¹, M.M. Schefer²², V.A. Schegelsky⁶³, D. Scheirich¹⁹³, M. Schernau²⁰², C. Scheulen⁸³, C. Schiavi^{85,84}, M. Schioppa^{70,69}, B. Schlag²¹⁴, S. Schlenker⁶², J. Schmeing²⁴⁵, E. Schmidt¹⁶⁰, M.A. Schmidt²⁴⁵, K. Schmieden¹⁵⁰, C. Schmitt¹⁵⁰, N. Schmitt¹⁵⁰, S. Schmitt⁷⁵, N.A. Schneider¹⁵⁹, L. Schoeffel¹⁹⁵, A. Schoening⁹², P.G. Scholer⁵⁵, E. Schopf²¹², M. Schott³¹, S. Schramm⁸³, T. Schroer⁸³, H.-C. Schultz-Coulon⁹¹, M. Schumacher⁸¹, B.A. Schumm¹⁹⁶, Ph. Schune¹⁹⁵, H.R. Schwartz⁸, A. Schwartzman²¹⁴, T.A. Schwarz¹⁵⁶, Ph. Schwemling¹⁹⁵, R. Schwienhorst¹⁵⁷, F.G. Sciaccia²², A. Sciandra⁴³, G. Sciolla³³, F. Scuri¹¹¹, C.D. Sebastiani⁶², K. Sedlaczek¹⁶⁸, S.C. Seidel¹⁶⁵, A. Seiden¹⁹⁶, B.D. Seidlitz⁶⁷, C. Seitz⁷⁵, J.M. Seixas¹²⁶, G. Sekhniaidze¹⁰⁷, L. Selem⁸⁸, N. Semprini-Cesari^{30,29}, A. Semushin²⁴⁷, D. Sengupta⁸³, V. Senthilkumar²³⁷, L. Serin⁹⁷, M. Sessa^{107,108}, H. Severini¹⁷⁴, F. Sforza^{85,84}, A. Sfyrla⁸³, Q. Sha¹⁵, E. Shabalina⁸², H. Shaddix¹⁶⁸, A.H. Shah⁴⁶, R. Shaheen²¹⁵, J.D. Shahinian¹⁸², M. Shamim⁶², L.Y. Shan¹⁵, M. Shapiro¹⁹, A. Sharma⁶², A.S. Sharma²³⁸, P. Sharma⁴³, P.B. Shatalov⁶³, K. Shaw²¹⁷, S.M. Shaw¹⁵¹, Q. Shen¹⁵, D.J. Sheppard²¹³, P. Sherwood¹⁴⁶, L. Shi¹⁴⁶, X. Shi¹⁵, S. Shimizu¹³⁰, C.O. Shimmin²⁴⁶, I.P.J. Shipsey^{1,180}, S. Shirabe¹³⁸, M. Shiyakova^{64,269}, M.J. Shochet⁶⁵, D.R. Shope¹⁷⁹, B. Shrestha¹⁷⁴, S. Shrestha^{173,280},

I. Shreyber⁶⁴, M.J. Shroff²³⁹, P. Sicho¹⁹¹, A.M. Sickles²³⁶, E. Sideras Haddad^{54,234}, A.C. Sidley¹⁶⁷, A. Sidoti³⁰, F. Siegert⁷⁷, Dj Sijacki¹⁷, F. Sili¹⁴⁰, J.M. Silva⁷⁹, I. Silva Ferreira¹²⁶, M.V. Silva Oliveira⁴³, S.B. Silverstein⁷³, S. Simion⁹⁷, R. Simoniello⁶², E.L. Simpson¹⁵¹, H. Simpson²¹⁷, L.R. Simpson⁷, S. Simsek¹²⁴, S. Sindhu⁸², P. Sinervo²²⁸, S.N. Singh³³, S. Singh⁴³, S. Sinha⁷⁵, S. Sinha¹⁵¹, M. Sioli^{30,29}, K. Sioulas¹⁰, I. Siral⁶², E. Sitnikova⁷⁵, J. Sj^{73,74}, A. Skaf⁸², E. Skorda²³, P. Skubic¹⁷⁴, M. Slawinska¹³⁶, I. Slazyk¹⁸, I. Sliuser¹⁷⁹, V. Smakhtin²⁴³, B.H. Smart¹⁹⁴, S.Yu Smirnov¹⁹⁸, Y. Smirnov¹²⁴, L.N. Smirnova^{63,63}, O. Smirnova¹⁴⁸, A.C. Smith⁶⁷, D.R. Smith²³³, J.L. Smith¹⁵¹, M.B. Smith⁵⁵, R. Smith²¹⁴, H. Smitmanns¹⁵⁰, M. Smizanska¹⁴¹, K. Smolek¹⁹², P. Smolyanskiy¹⁹², A.A. Snesarev⁶⁴, H.L. Snoek¹⁶⁷, S. Snyder⁴³, R. Sobie^{239,270}, A. Soffer²²⁴, C.A. Solans Sanchez⁶², E.Yu Soldatov⁶⁴, U. Soldevila²³⁷, A.A. Solodkov⁵⁴, S. Solomon³³, A. Soloshenko⁶⁴, K. Solovieva⁸¹, O.V. Solovyanov⁶⁶, P. Sommer⁷⁷, A. Sonay¹⁴, A. Sopczak¹⁹², A.L. Soppio⁴², F. Sopkova⁹¹, J.D. Sorenson¹⁶⁵, I.R. Sotarriva Alvarez²⁰⁴, V. Sothilingam⁹², O.J. Soto Sandoval^{199,198}, S. Sottocornola⁹⁹, R. Soualah¹³¹, Z. Soumami⁶⁰, D. South⁷⁵, N. Soybelman²⁴³, S. Spagnolo^{103,104}, M. Spalla¹⁶⁰, D. Sperlich⁸¹, B. Spisso^{107,108}, D.P. Spiteri⁸⁷, L. Splendori¹⁵², M. Spousta¹⁹³, E.J. Staats⁵⁵, R. Stamen⁹¹, E. Stanecka¹³⁶, W. Stanek-Maslouska⁷⁵, M.V. Stange⁷⁷, B. Stanislaus¹⁹, M.M. Stanitzki⁷⁵, B. Stapf⁷⁵, E.A. Starchenko⁶³, G.H. Stark¹⁹⁶, J. Stark¹³⁹, P. Staroba¹⁹¹, P. Starovoitov¹³², R. Staszewski¹³⁶, C. Stauch¹⁵⁹, G. Stavropoulos⁷², A. Steff⁶², A. Stein¹⁵⁰, P. Steinberg⁴³, B. Stelzer^{213,229}, H.J. Stelzer¹⁸³, O. Stelzer²²⁹, H. Stenzel⁸⁶, T.J. Stevenson²¹⁷, G.A. Stewart⁶², J.R. Stewart¹⁷⁵, G. Stoicea³⁵, M. Stolarski¹⁸⁴, S. Stonjek¹⁶⁰, A. Straessner⁷⁷, J. Strandberg²¹⁵, S. Strandberg^{73,74}, M. Stratmann²⁴⁵, M. Strauss¹⁷⁴, T. Strebler¹⁵², P. Strizenc⁴², R. Str⁴⁰, D.M. Strom¹⁷⁷, R. Stroyanowski⁷¹, A. Strubig^{73,74}, S.A. Stucci⁴³, B. Stugu¹⁸, J. Stupak¹⁷⁴, N.A. Styles⁷⁵, D. Su²¹⁴, S. Su⁹⁰, X. Su⁹⁰, D. Suchy⁴¹, A.D. Ponnusudhakar⁸², K. Sugizaki¹⁸², V.V. Sulini⁶³, D.M.S. Sultan¹⁸⁰, L. Sultanaliyeva³¹, S. Sultansoy⁴, S. Sun²⁴⁴, W. Sun¹⁵, O. Sunneborn Gudnadottir²³⁵, N. Sur¹⁴⁸, M.R. Sutton²¹⁷, M. Svatos¹⁹¹, P.N. Swallow⁴⁶, M. Swiatlowski²²⁹, T. Swirski²⁴⁰, A. Swoboda⁶², I. Sykora⁴¹, M. Sykora¹⁹³, T. Sykora¹⁹³, D. Ta¹⁵⁰, K. Tackmann^{75,268}, A. Taffard²³³, R. Tafirout²²⁹, Y. Takubo¹³⁰, M. Talby¹⁵², A.A. Talyshev⁶³, K.C. Tam⁹⁴, N.M. Tamir²²⁴, A. Tanaka²²⁶, J. Tanaka²²⁶, R. Tanaka⁹⁷, M. Tanasini²¹⁶, Z. Tao²³⁸, S. Tapia Araya²⁰³, S. Tapprogge¹⁵⁰, A. Tarek Abouelfadl Mohamed⁶², S. Tarem²²³, K. Tariq¹⁵, G. Tarna⁶², G.F. Tartarelli¹⁰⁵, M.J. Tartarin¹³⁹, P. Tas¹⁹³, M. Tasevsky¹⁹¹, E. Tassi^{70,69}, A.C. Tate²³⁶, Y. Tayalati^{60,61}, G.N. Taylor¹⁵⁵, W. Taylor²³⁰, R.J. Taylor Vara²³⁷, A.S. Tegetmeier¹³⁹, P. Teixeira-Dias¹⁴⁵, J.J. Teoh²²⁸, K. Terashi²²⁶, J. Terron¹⁴⁹, S. Terzo¹⁴, M. Testa⁸⁰, R.J. Teuscher^{228,270}, A. Thaler¹²¹, O. Theiner⁸³, T. Theveneaux-Pelzer¹⁵², D.W. Thomas¹⁴⁵, J.P. Thomas²³, E.A. Thompson¹⁹, P.D. Thompson²³, E. Thomson¹⁸², R.E. Thornberry⁷¹, C. Tian⁹⁰, Y. Tian⁸³, V. Tikhomirov¹²⁴, Yu A. Tikhonov⁶⁴, S. Timoshenko⁶³, D. Timoshyn¹⁹³, E.X.L. Ting¹, P. Tipton²⁴⁶, A. Tishelman-Charny⁴³, K. Todome²⁰⁴, S. Todorova-Nova¹⁹³, L. Toffolin^{100,102}, M. Togawa¹³⁰, J. Tojo¹³⁸, S. Tokar⁴¹, O. Toldaiev⁹⁹, G. Tolkachev¹⁵², M. Tomoto¹³⁰, L. Tompkins^{214,257}, E. Torrence¹⁷⁷, H. Torres¹³⁹, E. Torró Pastor²³⁷, M. Toscani⁴⁴, C. Toscirri⁶⁵, M. Tost¹², D.R. Tovey²¹⁰, T. Trefzger²⁴⁰, P.M. Tricarico¹⁴, A. Tricoli⁴³, I.M. Trigger²²⁹, S. Trincaz-Duvoid¹⁸¹, D.A. Trischuk³³, A. Tropina⁶⁴, L. Truong⁴⁹, M. Trzebinski¹³⁶, A. Trzupek¹³⁶, F. Tsai²¹⁶, M. Tsai¹⁵⁶, A. Tsiamis²²⁵, P.V. Tsiarehsha⁶⁴, S. Tsigaridas²²⁹, A. Tsigiridis^{225,264}, V. Tsiskaridze²²⁰, E.G. Tskhadadze²²⁰, Y. Tsujikawa¹³⁷, I.I. Tsukerman⁶³, V. Tsulaia¹⁹, S. Tsuno¹³⁰, K. Tsurii¹⁷², D. Tsybychev²¹⁶, Y. Tu⁹⁴, A. Tudorache³⁵, V. Tudorache³⁵, S.B. Tuncay¹⁸⁰, S. Turchikhin^{85,84}, I. Turk Cakir³, R. Turra¹⁰⁵, T. Turtuvshin^{64,271}, P.M. Tuts⁶⁷, S. Tzamarias^{225,250}, Y. Uematsu¹³⁰, F. Ukegawa²³¹, P.A. Ulloa

Poblete^{199,198}, E.N. Umaka⁴³, G. Unal⁶², A. Undrus⁴³, G. Unel²³³, J. Urban⁴², P. Urrejola²⁰¹, G. Usai⁹, R. Ushioda²²⁷, M. Usman¹⁵⁸, F. Ustuner⁷⁹, Z. Uysal¹²⁴, V. Vacek¹⁹², B. Vachon¹⁵⁴, T. Vafeiadis⁶², A. Vaitkus¹⁴⁶, C. Valderanis¹⁵⁹, E. Valdes Santurio^{73,74}, M. Valente⁶², S. Valentinetti^{30,29}, A. Valero²³⁷, E. Valiente Moreno²³⁷, A. Vallier¹³⁹, J.A. Valls Ferrer²³⁷, D.R. Van Arneeman¹⁶⁷, A. Van Der Graaf⁷⁶, H.Z. Van Der Schyf⁵⁴, P. Van Gemmeren⁷, M. Van Rijnbach⁶², S. Van Stroud¹⁴⁶, I. Van Vulpen¹⁶⁷, P. Vana¹⁹³, M. Vanadia^{115,116}, U.M. Vande Voorde²¹⁵, W. Vandelli⁶², E.R. Vandewall¹⁷⁵, D. Vannicola²²⁴, L. Vannoli⁸⁰, R. Vari¹¹³, M. Varma²⁴⁶, E.W. Varnes⁸, C. Varni¹⁶⁸, D. Varouchas⁹⁷, L. Varriale²³⁷, K.E. Varvell²¹⁸, M.E. Vasile³⁵, L. Vaslin¹³⁰, M.D. Vassilev²¹⁴, A. Vasyukov⁶⁴, L.M. Vaughan¹⁷⁵, R. Vavricka¹⁹³, T. Vazquez Schroeder¹⁴, J. Veatch⁴⁵, V. Vecchio¹⁵¹, M.J. Veen¹⁵³, I. Veliscek⁴³, I. Velkovska¹⁴³, L.M. Veloce²²⁸, F. Veloso^{184,186}, S. Veneziano¹¹³, A. Ventura^{103,104}, A. Verbytskyi¹⁶⁰, M. Verducci^{111,112}, C. Vergis¹⁴⁴, M. Verissimo De Araujo¹²⁶, W. Verkerke¹⁶⁷, J.C. Vermeulen¹⁶⁷, C. Vernieri²¹⁴, M. Vessella²³³, M.C. Vetterli^{213,275}, A. Vgenopoulos¹⁵⁰, N. Viaux Maira^{203,273}, T. Vickey²¹⁰, O.E. Vickey Boeriu²¹⁰, G.H.A. Viehhauser¹⁸⁰, L. Vigani⁹², M. Vigil¹⁶⁰, M. Villa^{30,29}, M. Villaplana Perez²³⁷, E.M. Villhauer⁶⁵, E. Vilucchi⁸⁰, M. Vincent²³⁷, M.G. Vinciter⁵⁵, A. Visibile¹⁶⁷, A. Visive¹⁶⁷, C. Vittori⁶², I. Vivarelli^{30,29}, M.I. Vivas Alborno⁷⁵, E. Voevodina¹⁶⁰, F. Vogel¹⁵⁰, J.C. Voigt⁷⁷, P. Vokac¹⁹², Yu Volkotrub¹³⁵, L. Vomberg³¹, E. Von Toerne³¹, B. Vormwald⁶², K. Voroeb⁷⁸, M. Vos²³⁷, K. Voss²¹², M. Vozak⁶², L. Vozdecky¹⁷⁴, N. Vranjes¹⁷, M. Vranjes Milosavljevic¹⁷, M. Vreeswijk¹⁶⁷, N.K. Vu^{209,208}, R. Vuillermet⁶², O. Vujanovic¹⁵⁰, I. Vukotic⁶⁵, I.K. Vyas⁵⁵, J.F. Wack⁴⁶, S. Wada²³¹, C. Wagner²¹⁴, J.M. Wagner¹⁹, W. Wagner²⁴⁵, S. Wahdan²⁴⁵, H. Wahlberg¹⁴⁰, C.H. Waits¹⁷⁴, J. Walder¹⁹⁴, R. Walker¹⁵⁹, K. Walkingshaw Pass⁸⁷, W. Walkowiak²¹², A. Wall¹⁸², E.J. Wallin¹⁴⁸, T. Wamorkar¹⁹, K. Wandall-Christensen²³⁷, A. Wang³⁰, A.Z. Wang¹⁹⁶, C. Wang¹⁵⁰, C. Wang¹², H. Wang¹⁹, J. Wang⁹⁵, P. Wang¹⁵¹, P. Wang¹⁴⁶, R. Wang⁸⁹, R. Wang⁷, S.M. Wang²¹⁹, S. Wang¹⁵, T. Wang¹⁶⁶, T. Wang⁹⁰, W.T. Wang¹⁸⁰, W. Wang¹⁵, X. Wang²³⁶, X. Wang²⁰⁸, X. Wang⁷⁵, Y. Wang¹⁶², Y. Wang⁹⁰, Z. Wang¹⁵⁶, Z. Wang²⁰⁹, Z. Wang¹⁵⁶, C. Wanotayaroj¹³⁰, A. Warburton¹⁵⁴, A.L. Warnerbring²¹², S. Waterhouse¹⁴⁵, A.T. Watson²³, B.H. Watson⁷⁹, M.F. Watson²³, E. Watton⁸⁷, G. Watts²⁰⁵, M.M. Waugh¹⁴⁶, J.M. Webb⁸¹, C. Weber⁴³, H.A. Weber²¹, M.S. Weber²², S.M. Weber⁹¹, C. Wei⁹⁰, Y. Wei⁸¹, A.R. Weidberg¹⁸⁰, E.J. Weik¹⁷¹, J. Weingarten⁷⁶, C. Weiser⁸¹, C.J. Wells⁷⁵, T. Wenaus⁴³, T. Wengler⁶², N.S. Wenke¹⁶⁰, N. Vermes³¹, M. Wessels⁹¹, A.M. Wharton¹⁴¹, A.S. White⁸⁹, A. White⁹, M.J. White¹, D. Whiteson²³³, L. Wickremasinghe¹⁷⁸, W. Wiedenmann²⁴⁴, M. Wieler¹⁹⁴, R. Wierda²¹⁵, C. Wiglesworth⁶⁸, H.G. Wilkens⁶², J.J.H. Wilkinson⁴⁶, D.M. Williams⁶⁷, H.H. Williams¹⁸², S. Williams⁴⁶, S. Willocq¹⁵³, B.J. Wilson¹⁵¹, D.J. Wilson¹⁵¹, P.J. Windischhofer⁶⁵, F.I. Winkel¹⁴⁴, F. Winklmeier¹⁷⁷, B.T. Winter⁸¹, M. Wittgen²¹⁴, M. Wobisch¹⁴⁷, T. Wojtkowski⁸⁸, Z. Wolffs¹⁶⁷, J. Wollrath⁶², M.W. Wolter¹³⁶, H. Wolters^{184,186}, M.C. Wong¹⁹⁶, E.L. Woodward⁶⁷, S.D. Worm⁷⁵, B.K. Wosiek¹³⁶, K.W. Woźniak¹³⁶, S. Wozniewski⁸², K. Wraight⁸⁷, C. Wu²²⁸, C. Wu²³, J. Wu²²⁶, M. Wu¹⁶³, M. Wu¹⁶⁶, S.L. Wu²⁴⁴, S. Wu^{15,277}, X. Wu⁹⁰, Y.Q. Wu²²⁸, Y. Wu⁹⁰, Z. Wu⁵, Z. Wu¹⁶², J. Wuerzinger¹⁶⁰, T.R. Wyatt¹⁵¹, B.M. Wynne⁷⁹, S. Xella⁶⁸, L. Xia¹⁶², M. Xia¹⁶, M. Xie⁹⁰, A. Xiong¹⁷⁷, J. Xiong¹⁹, D. Xu¹⁵, H. Xu⁹⁰, L. Xu⁹⁰, R. Xu¹⁸², T. Xu¹⁵⁶, Y. Xu²⁰⁵, Z. Xu⁷⁹, R. Xue¹⁸³, B. Yabsley²¹⁸, S. Yacoub⁴⁷, Y. Yamaguchi¹³⁰, E. Yamashita²²⁶, H. Yamauchi²³¹, T. Yamazaki¹⁹, Y. Yamazaki¹³³, S. Yan⁸⁷, Z. Yan¹⁵³, H.J. Yang^{208,209}, H.T. Yang⁹⁰, S. Yang⁹⁰, T. Yang⁹⁵, X. Yang⁶², X. Yang¹⁵, Y. Yang²²⁶, Y. Yang⁹⁰, W.-M. Yao¹⁹, C.L. Yardley²¹⁷, J. Ye¹⁵, S. Ye⁴³, X. Ye⁹⁰, Y. Yeh¹⁴⁶, I. Yeletsikh⁶⁴, B. Yeo²⁰, M.R. Yexley¹⁴⁶, T.P. Yildirim¹⁸⁰, K. Yorita²⁴², C.J. S. Young⁶², C. Young²¹⁴, N.D. Young¹⁷⁷, Y.

Yu⁹⁰, J. Yuan^{15,164}, M. Yuan¹⁵⁶, R. Yuan^{209,208}, L. Yue¹⁴⁶, M. Zaazoua⁹⁰, B. Zabinski¹³⁶, I. Zahir⁵⁶, A. Zaid^{85,84}, Z.K. Zak¹³⁶, T. Zakareishvili²³⁷, S. Zambito⁸³, J.A. Zamora Saa²⁰⁰, J. Zang²²⁶, R. Zanzottera^{105,106}, O. Zaplatilek¹⁹², C. Zeitnitz²⁴⁵, H. Zeng¹⁵, J.C. Zeng²³⁶, D.T. Zenger Jr³³, O. Zenin⁶³, T. Ženiš⁴¹, S. Zenz¹⁴⁴, D. Zerwas⁹⁷, M. Zhai^{15,164}, D.F. Zhang²¹⁰, G. Zhang^{15,277}, J. Zhang²⁰⁶, J. Zhang⁷, K. Zhang^{15,164}, L. Zhang⁹⁰, L. Zhang¹⁶², P. Zhang^{15,164}, R. Zhang¹⁶², S. Zhang¹³⁹, T. Zhang²²⁶, Y. Zhang²⁰⁵, Y. Zhang¹⁴⁶, Y. Zhang⁹⁰, Y. Zhang¹⁶², Z. Zhang²⁰⁶, Z. Zhang⁹⁷, H. Zhao²⁰⁵, T. Zhao²⁰⁶, Y. Zhao⁵⁵, Z. Zhao⁹⁰, Z. Zhao⁹⁰, A. Zhemchugov⁶⁴, J. Zheng¹⁶², K. Zheng²³⁶, X. Zheng⁹⁰, Z. Zheng²¹⁴, D. Zhong²³⁶, B. Zhou¹⁵⁶, H. Zhou⁸, N. Zhou²⁰⁸, Y. Zhou¹⁶, Y. Zhou¹⁶², Y. Zhou⁸, C.G. Zhu²⁰⁶, J. Zhu¹⁵⁶, X. Zhu²⁰⁹, Y. Zhu²⁰⁸, Y. Zhu⁹⁰, X. Zhuang¹⁵, K. Zhukov⁹⁹, N.I. Zimine⁶⁴, J. Zinsler⁹², M. Ziolkowski²¹², L. Živković¹⁷, A. Zoccoli^{30,29}, K. Zoch⁸⁹, A. Zografos⁶², T.G. Zorbas²¹⁰, O. Zormpa⁷², L. Zwaliński⁶²

Affiliation Notes

¹Deceased

Collaboration Institutes

- ¹ Department of Physics, University of Adelaide, Adelaide, Australia
- ² Department of Physics, University of Alberta, Edmonton, AB, Canada
- ³ Department of Physics, Ankara University, Ankara, Türkiye
- ⁴ Division of Physics, TOBB University of Economics and Technology, Ankara, Türkiye
- ⁵ LAPP, Université Savoie Mont Blanc, CNRS/IN2P3, Annecy, France
- ⁶ APC, Université Paris Cité, CNRS/IN2P3, Paris, France
- ⁷ High Energy Physics Division, Argonne National Laboratory, Argonne, IL, United States of America
- ⁸ Department of Physics, University of Arizona, Tucson, AZ, United States of America
- ⁹ Department of Physics, University of Texas at Arlington, Arlington, TX, United States of America
- ¹⁰ Physics Department, National and Kapodistrian University of Athens, Athens, Greece
- ¹¹ Physics Department, National Technical University of Athens, Zografou, Greece
- ¹² Department of Physics, University of Texas at Austin, Austin, TX, United States of America
- ¹³ Institute of Physics, Azerbaijan Academy of Sciences, Baku, Azerbaijan
- ¹⁴ Institut de Física d'Altes Energies (IFAE), Barcelona Institute of Science and Technology, Barcelona, Spain
- ¹⁵ Institute of High Energy Physics, Chinese Academy of Sciences, Beijing, China
- ¹⁶ Physics Department, Tsinghua University, Beijing, China
- ¹⁷ Institute of Physics, University of Belgrade, Belgrade, Serbia
- ¹⁸ Department for Physics and Technology, University of Bergen, Bergen, Norway
- ¹⁹ Physics Division, Lawrence Berkeley National Laboratory, Berkeley, CA, United States
- ²⁰ University of California, Berkeley, CA, United States of America
- ²¹ Institut für Physik, Humboldt Universität zu Berlin, Berlin, Germany
- ²² Albert Einstein Center for Fundamental Physics and Laboratory for High Energy Physics, University of Bern, Bern, Switzerland
- ²³ School of Physics and Astronomy, University of Birmingham, Birmingham, United Kingdom
- ²⁴ Department of Physics, Bogazici University, Istanbul, Türkiye
- ²⁵ Department of Physics Engineering, Gaziantep University, Gaziantep, Türkiye
- ²⁶ Department of Physics, Istanbul University, Istanbul, Türkiye

- ²⁷ Facultad de Ciencias y Centro de Investigaciones, Universidad Antonio Nariño, Bogotá, Colombia
- ²⁸ Departamento de Física, Universidad Nacional de Colombia, Bogotá, Colombia
- ²⁹ Dipartimento di Fisica e Astronomia A. Righi, Università di Bologna, Bologna, Italy
- ³⁰ INFN Sezione di Bologna, Italy
- ³¹ Physikalisches Institut, Universität Bonn, Bonn, Germany
- ³² Department of Physics, Boston University, Boston, MA, United States of America
- ³³ Department of Physics, Brandeis University, Waltham, MA, United States of America
- ³⁴ Transilvania University of Brasov, Brasov, Romania
- ³⁵ Horia Hulubei National Institute of Physics and Nuclear Engineering, Bucharest, Romania
- ³⁶ Department of Physics, Alexandru Ioan Cuza University of Iasi, Iasi, Romania
- ³⁷ Physics Department, National Institute for Research and Development of Isotopic and Molecular Technologies, Cluj-Napoca, Romania
- ³⁸ National University of Science and Technology Politehnica, Bucharest, Romania
- ³⁹ West University in Timisoara, Timisoara, Romania
- ⁴⁰ Faculty of Physics, University of Bucharest, Bucharest, Romania
- ⁴¹ Faculty of Mathematics, Physics and Informatics, Comenius University, Bratislava, Slovak Republic
- ⁴² Department of Subnuclear Physics, Institute of Experimental Physics, Slovak Academy of Sciences, Kosice, Slovak Republic
- ⁴³ Physics Department, Brookhaven National Laboratory, Upton, NY, United States of America
- ⁴⁴ Facultad de Ciencias Exactas y Naturales, Departamento de Física, Instituto de Física de Buenos Aires (IFIBA), CONICET, Universidad de Buenos Aires, Buenos Aires, Argentina
- ⁴⁵ California State University, CA, United States of America
- ⁴⁶ Cavendish Laboratory, University of Cambridge, Cambridge, United Kingdom
- ⁴⁷ Department of Physics, University of Cape Town, Cape Town, South Africa
- ⁴⁸ iThemba Labs, Western Cape, South Africa
- ⁴⁹ Department of Mechanical Engineering Science, University of Johannesburg, Johannesburg, South Africa
- ⁵⁰ National Institute of Physics, University of the Philippines Diliman, Philippines
- ⁵¹ Department of Physics, Stellenbosch University, Matieland, South Africa
- ⁵² Department of Physics, University of South Africa, Pretoria, South Africa
- ⁵³ University of Zululand, KwaDlangezwa, South Africa
- ⁵⁴ School of Physics, University of the Witwatersrand, Johannesburg, South Africa
- ⁵⁵ Department of Physics, Carleton University, Ottawa, ON, Canada
- ⁵⁶ Faculté des Sciences Ain Chock, Université Hassan II de Casablanca, Morocco
- ⁵⁷ Faculté des Sciences, Kénitra, Université Ibn-Tofail, Morocco
- ⁵⁸ Faculté des Sciences Semailia, Université Cadi Ayyad, LPHEA-Marrakech, Morocco
- ⁵⁹ Faculté des Sciences, LPMR, Université Mohamed Premier, Oujda, Morocco
- ⁶⁰ Faculté des sciences, Université Mohammed V, Rabat, Morocco
- ⁶¹ Institute of Applied Physics, Mohammed VI Polytechnic University, Ben Guerir, Morocco
- ⁶² CERN, Geneva, Switzerland
- ⁶³ Affiliated with an institute formerly covered by a cooperation agreement with CERN
- ⁶⁴ Affiliated with an international laboratory covered by a cooperation agreement with CERN

- ⁶⁵ Enrico Fermi Institute, University of Chicago, Chicago, IL, United States of America
- ⁶⁶ LPC, Université Clermont Auvergne, CNRS/IN2P3, Clermont-Ferrand, France
- ⁶⁷ Nevis Laboratory, Columbia University, Irvington, NY, United States of America
- ⁶⁸ Niels Bohr Institute, University of Copenhagen, Copenhagen, Denmark
- ⁶⁹ Dipartimento di Fisica, Università della Calabria, Rende, Italy
- ⁷⁰ INFN Gruppo Collegato di Cosenza, Laboratori Nazionali di Frascati, Italy
- ⁷¹ Physics Department, Southern Methodist University, Dallas, TX, United States of America
- ⁷² National Centre for Scientific Research Demokritos, Agia Paraskevi, Greece
- ⁷³ Department of Physics, Stockholm University, Sweden
- ⁷⁴ Oskar Klein Centre, Stockholm, Sweden
- ⁷⁵ Deutsches Elektronen-Synchrotron DESY, Hamburg and Zeuthen, Germany
- ⁷⁶ Fakultät Physik, Technische Universität Dortmund, Dortmund, Germany
- ⁷⁷ Institut für Kern- und Teilchenphysik, Technische Universität Dresden, Dresden, Germany
- ⁷⁸ Department of Physics, Duke University, Durham, NC, United States of America
- ⁷⁹ SUPA - School of Physics and Astronomy, University of Edinburgh, Edinburgh, United Kingdom
- ⁸⁰ INFN e Laboratori Nazionali di Frascati, Frascati, Italy
- ⁸¹ Physikalisches Institut, Albert-Ludwigs-Universität Freiburg, Freiburg, Germany
- ⁸² II. Physikalisches Institut, Georg-August-Universität Göttingen, Göttingen, Germany
- ⁸³ Département de Physique Nucléaire et Corpusculaire, Université de Genève, Genève, Switzerland
- ⁸⁴ Dipartimento di Fisica, Università di Genova, Genova, Italy
- ⁸⁵ INFN Sezione di Genova, Italy
- ⁸⁶ II. Physikalisches Institut, Justus-Liebig-Universität Giessen, Giessen, Germany
- ⁸⁷ SUPA - School of Physics and Astronomy, University of Glasgow, Glasgow, United Kingdom
- ⁸⁸ LPSC, Université Grenoble Alpes, CNRS/IN2P3, Grenoble INP, Grenoble, France
- ⁸⁹ Laboratory for Particle Physics and Cosmology, Harvard University, Cambridge, MA, United States of America
- ⁹⁰ Department of Modern Physics and State Key Laboratory of Particle Detection and Electronics, University of Science and Technology of China, Hefei, China
- ⁹¹ Kirchhoff-Institut für Physik, Ruprecht-Karls-Universität Heidelberg, Heidelberg, Germany
- ⁹² Physikalisches Institut, Ruprecht-Karls-Universität Heidelberg, Heidelberg, Germany
- ⁹³ Department of Physics, Chinese University of Hong Kong, Shatin, N.T., Hong Kong
- ⁹⁴ Department of Physics, University of Hong Kong, Hong Kong
- ⁹⁵ Department of Physics, Institute for Advanced Study, Hong Kong University of Science and Technology, Clear Water Bay, Kowloon, Hong Kong, China
- ⁹⁶ Department of Physics, National Tsing Hua University, Hsinchu, Taiwan
- ⁹⁷ IJCLab, Université Paris-Saclay, CNRS/IN2P3, 91405, Orsay, France
- ⁹⁸ Centro Nacional de Microelectrónica (IMB-CNM-CSIC), Barcelona, Spain
- ⁹⁹ Department of Physics, Indiana University, Bloomington, IN, United States of America
- ¹⁰⁰ INFN Gruppo Collegato di Udine, Sezione di Trieste, Udine, Italy
- ¹⁰¹ ICTP, Trieste, Italy
- ¹⁰² Dipartimento Politecnico di Ingegneria e Architettura, Università di Udine, Udine, Italy
- ¹⁰³ INFN Sezione di Lecce, Italy
- ¹⁰⁴ Dipartimento di Matematica e Fisica, Università del Salento, Lecce, Italy
- ¹⁰⁵ INFN Sezione di Milano, Italy
- ¹⁰⁶ Dipartimento di Fisica, Università di Milano, Milano, Italy
- ¹⁰⁷ INFN Sezione di Napoli, Italy
- ¹⁰⁸ Dipartimento di Fisica, Università di Napoli, Napoli, Italy
- ¹⁰⁹ INFN Sezione di Pavia, Italy
- ¹¹⁰ Dipartimento di Fisica, Università di Pavia, Pavia, Italy
- ¹¹¹ INFN Sezione di Pisa, Italy
- ¹¹² Dipartimento di Fisica E. Fermi, Università di Pisa, Pisa, Italy
- ¹¹³ INFN Sezione di Roma, Italy
- ¹¹⁴ Dipartimento di Fisica, Sapienza Università di Roma, Roma, Italy
- ¹¹⁵ INFN Sezione di Roma Tor Vergata, Italy
- ¹¹⁶ Dipartimento di Fisica, Università di Roma Tor Vergata, Roma, Italy
- ¹¹⁷ INFN Sezione di Roma Tre, Italy
- ¹¹⁸ Dipartimento di Matematica e Fisica, Università Roma Tre, Roma, Italy
- ¹¹⁹ INFN-TIFPA, Italy
- ¹²⁰ Università degli Studi di Trento, Trento, Italy
- ¹²¹ Department of Astro and Particle Physics, Universität Innsbruck, Innsbruck, Austria
- ¹²² University of Iowa, Iowa City, IA, United States of America
- ¹²³ Department of Physics and Astronomy, Iowa State University, Ames, IA, United States of America
- ¹²⁴ Istinye University, Sariyer, Istanbul, Türkiye
- ¹²⁵ Departamento de Engenharia Elétrica, Universidade Federal de Juiz de Fora (UFJF), Juiz de Fora, Brazil
- ¹²⁶ COPPE/EE/IF, Universidade Federal do Rio De Janeiro, Rio de Janeiro, Brazil
- ¹²⁷ Instituto de Física, Universidade de São Paulo, São Paulo, Brazil
- ¹²⁸ Rio de Janeiro State University, Rio de Janeiro, Brazil
- ¹²⁹ Federal University of Bahia, Bahia, Brazil
- ¹³⁰ KEK, High Energy Accelerator Research Organization, Tsukuba, Japan
- ¹³¹ Khalifa University of Science and Technology, Abu Dhabi, United Arab Emirates
- ¹³² University of Sharjah, Sharjah, United Arab Emirates
- ¹³³ Graduate School of Science, Kobe University, Kobe, Japan
- ¹³⁴ Faculty of Physics and Applied Computer Science, AGH University of Krakow, Krakow, Poland
- ¹³⁵ Marian Smoluchowski Institute of Physics, Jagiellonian University, Krakow, Poland
- ¹³⁶ Institute of Nuclear Physics, Polish Academy of Sciences, Krakow, Poland
- ¹³⁷ Faculty of Science, Kyoto University, Kyoto, Japan
- ¹³⁸ Research Center for Advanced Particle Physics, Department of Physics, Kyushu University, Fukuoka, Japan
- ¹³⁹ L2IT, Université de Toulouse, CNRS/IN2P3, UPS, Toulouse, France
- ¹⁴⁰ Instituto de Física La Plata, Universidad Nacional de La Plata and CONICET, La Plata, Argentina
- ¹⁴¹ Physics Department, Lancaster University, Lancaster, United Kingdom
- ¹⁴² Oliver Lodge Laboratory, University of Liverpool, Liverpool, United Kingdom
- ¹⁴³ Department of Experimental Particle Physics, Department of Physics, Jožef Stefan Institute, University of Ljubljana, Ljubljana, Slovenia
- ¹⁴⁴ Department of Physics and Astronomy, Queen Mary University of London, London, United Kingdom
- ¹⁴⁵ Department of Physics, Royal Holloway University of London, Egham, United Kingdom
- ¹⁴⁶ Department of Physics and Astronomy, University College London, London, United Kingdom

- 147 Louisiana Tech University, Ruston, LA, United States of America
 148 Fysiska institutionen, Lunds universitet, Lund, Sweden
 149 Departamento de Física Teórica C-15 and CIAFF, Universidad Autónoma de Madrid, Madrid, Spain
 150 Institut für Physik, Universität Mainz, Mainz, Germany
 151 School of Physics and Astronomy, University of Manchester, Manchester, United Kingdom
 152 CPPM, Aix-Marseille Université, CNRS/IN2P3, Marseille, France
 153 Department of Physics, University of Massachusetts, Amherst, MA, United States of America
 154 Department of Physics, McGill University, Montreal, QC, Canada
 155 School of Physics, University of Melbourne, Victoria, Australia
 156 Department of Physics, University of Michigan, Ann Arbor, MI, United States of America
 157 Department of Physics and Astronomy, Michigan State University, East Lansing, MI, United States of America
 158 Group of Particle Physics, University of Montreal, Montreal, QC, Canada
 159 Fakultät für Physik, Ludwig-Maximilians-Universität München, München, Germany
 160 Max-Planck-Institut für Physik (Werner-Heisenberg-Institut), München, Germany
 161 Graduate School of Science and Kobayashi-Maskawa Institute, Nagoya University, Nagoya, Japan
 162 Department of Physics, Nanjing University, Nanjing, China
 163 School of Science, Shenzhen Campus of Sun Yat-sen University, China
 164 University of Chinese Academy of Science (UCAS), Beijing, China
 165 Department of Physics and Astronomy, University of New Mexico, Albuquerque, NM, United States of America
 166 Institute for Mathematics, Astrophysics and Particle Physics, Nikhef, Radboud University, Nijmegen, Netherlands
 167 Nikhef National Institute for Subatomic Physics and University of Amsterdam, Amsterdam, the Netherlands
 168 Department of Physics, Northern Illinois University, DeKalb, IL, United States of America
 169 New York University Abu Dhabi, Abu Dhabi, United Arab Emirates
 170 United Arab Emirates University, Al Ain, United Arab Emirates
 171 Department of Physics, New York University, New York, NY, United States of America
 172 Ochanomizu University, Bunkyo-ku, Otsuka, Tokyo, Japan
 173 Ohio State University, Columbus, OH, United States of America
 174 Department of Physics and Astronomy, Homer L. Dodge, University of Oklahoma, Norman, OK, United States of America
 175 Department of Physics, Oklahoma State University, Stillwater, OK, United States of America
 176 Joint Laboratory of Optics, Palacký University, Olomouc, Czech Republic
 177 Institute for Fundamental Science, University of Oregon, Eugene, OR, United States of America
 178 Graduate School of Science, University of Osaka, Osaka, Japan
 179 Department of Physics, University of Oslo, Oslo, Norway
 180 Department of Physics, Oxford University, Oxford, United Kingdom
 181 LPNHE, Sorbonne Université, Université Paris Cité, CNRS/IN2P3, Paris, France
 182 Department of Physics, University of Pennsylvania, Philadelphia, PA, United States of America
 183 Department of Physics and Astronomy, University of Pittsburgh, Pittsburgh, PA, United States of America
 184 Laboratório de Instrumentação e Física Experimental de Partículas - LIP, Lisboa, Portugal
 185 Departamento de Física, Faculdade de Ciências, Universidade de Lisboa, Lisboa, Portugal
 186 Departamento de Física, Universidade de Coimbra, Coimbra, Portugal
 187 Centro de Física Nuclear da Universidade de Lisboa, Lisboa, Portugal
 188 Departamento de Física, Escola de Ciências, Universidade do Minho, Braga, Portugal
 189 Departamento de Física Teórica y del Cosmos, Universidad de Granada, Granada, Spain
 190 Departamento de Física, Instituto Superior Técnico, Universidade de Lisboa, Lisboa, Portugal
 191 Institute of Physics, Czech Academy of Sciences, Prague, Czech Republic
 192 Czech Technical University, Prague Prague, Czech Republic
 193 Faculty of Mathematics and Physics, Charles University, Prague, Czech Republic
 194 Particle Physics Department, Rutherford Appleton Laboratory Didcot, United Kingdom
 195 IRFU, CEA, Université Paris-Saclay, Gif-sur-Yvette, France
 196 Santa Cruz Institute for Particle Physics, University of California Santa Cruz, Santa Cruz, CA, United States of America
 197 Departamento de Física, Pontificia Universidad Católica de Chile, Santiago, Chile
 198 Millennium Institute for Subatomic physics at high energy frontier (SAPHIR), Santiago, Chile
 199 Departamento de Física, Instituto de Investigación Multidisciplinario en Ciencia y Tecnología, Universidad de La Serena, Chile
 200 Department of Physics, Universidad Andres Bello, Santiago, Chile
 201 Universidad San Sebastian, Recoleta, Chile
 202 Instituto de Alta Investigación, Universidad de Tarapacá, Arica, Chile
 203 Departamento de Física, Universidad Técnica Federico Santa María, Valparaíso, Chile
 204 Department of Physics, Institute of Science, Tokyo, Japan
 205 Department of Physics, University of Washington, Seattle, WA, United States of America
 206 Institute of Frontier and Interdisciplinary Science and Key Laboratory of Particle Physics and Particle Irradiation (MOE), Shandong University, Qingdao, China
 207 School of Physics, Zhengzhou University, China
 208 School of Physics and Astronomy, State Key Laboratory of Dark Matter Physics, Key Laboratory for Particle Astrophysics and Cosmology (MOE), Shanghai Jiao Tong University, SKLPPC, Shanghai, China
 209 State Key Laboratory of Dark Matter Physics, Tsung-Dao Lee Institute, Shanghai Jiao Tong University, Shanghai, China
 210 Department of Physics and Astronomy, University of Sheffield, Sheffield, United Kingdom
 211 Department of Physics, Shinshu University, Nagano, Japan
 212 Department Physik, Universität Siegen, Siegen, Germany
 213 Department of Physics, Simon Fraser University, Burnaby, BC, Canada
 214 SLAC National Accelerator Laboratory, Stanford, CA, United States of America
 215 Department of Physics, Royal Institute of Technology, Stockholm, Sweden
 216 Departments of Physics and Astronomy, Stony Brook University, Stony Brook, NY, United States of America
 217 Department of Physics and Astronomy, University of Sussex, Brighton, United Kingdom
 218 School of Physics, University of Sydney, Sydney, Australia
 219 Institute of Physics, Academia Sinica, Taipei, Taiwan
 220 E. Andronikashvili Institute of Physics, Iv. Javakhishvili, Tbilisi State University, Tbilisi, Georgia
 221 High Energy Physics Institute, Tbilisi State University, Tbilisi, Georgia
 222 University of Georgia, Tbilisi, Georgia
 223 Department of Physics, Israel Institute of Technology, Technion Haifa, Israel
 224 Raymond & Beverly Sackler School of Physics and Astronomy, Tel Aviv University, Tel Aviv, Israel

- 225 Department of Physics, Aristotle University of Thessaloniki, Thessaloniki, Greece
- 226 International Center for Elementary Particle Physics, Department of Physics, University of Tokyo, Tokyo, Japan
- 227 Graduate School of Science and Technology, Tokyo Metropolitan University, Tokyo, Japan
- 228 Department of Physics, University of Toronto, Toronto, ON, Canada
- 229 TRIUMF, Vancouver, BC, Canada
- 230 Department of Physics and Astronomy, York University, Toronto, ON, Canada
- 231 Division of Physics and Tomonaga Center, Faculty of Pure and Applied Sciences, the History of the Universe, University of Tsukuba, Tsukuba, Japan
- 232 Department of Physics and Astronomy, Tufts University, Medford, MA, United States of America
- 233 Department of Physics and Astronomy, University of California Irvine, Irvine, CA, United States of America
- 234 University of West Attica, Athens, Greece
- 235 Department of Physics and Astronomy, University of Uppsala, Uppsala, Sweden
- 236 Department of Physics, University of Illinois, Urbana, IL, United States of America
- 237 Centro Mixto, Instituto de Física Corpuscular (IFIC), Universidad de Valencia - CSIC, Valencia, Spain
- 238 Department of Physics, University of British Columbia, Vancouver, BC, Canada
- 239 Department of Physics and Astronomy, University of Victoria, Victoria, BC, Canada
- 240 Fakultät für Physik und Astronomie, Julius-Maximilians-Universität Würzburg, Würzburg, Germany
- 241 Department of Physics, University of Warwick, Coventry, United Kingdom
- 242 Waseda University, Tokyo, Japan
- 243 Department of Particle Physics and Astrophysics, Weizmann Institute of Science, Rehovot, Israel
- 244 Department of Physics, University of Wisconsin, Madison, WI, United States of America
- 245 Fachgruppe Physik, Fakultät für Mathematik und Naturwissenschaften, Bergische Universität Wuppertal, Wuppertal, Germany
- 246 Department of Physics, Yale University, New Haven, CT, United States of America
- 247 Yerevan Physics Institute, Yerevan, Armenia
- 248 An-Najah National University, Nablus, Palestine
- 249 Borough of Manhattan Community College, City University of New York, New York, NY, United States of America
- 250 Center for Interdisciplinary Research and Innovation (CIRI-AUTH), Thessaloniki, Greece
- 251 Centre of Physics, Universities of Minho and Porto (CF-UM-UP), Portugal
- 252 Departament de Física, Universitat Autònoma de Barcelona, Barcelona, Spain
- 253 Department of Financial and Management Engineering, University of the Aegean, Chios, Greece
- 254 Department of Mathematical Sciences, University of South Africa, Johannesburg, South Africa
- 255 Department of Physics, Bolu Abant İzzet Baysal University, Bolu, Türkiye
- 256 Department of Physics, King's, College London London, United Kingdom
- 257 Department of Physics, Stanford University, Stanford, CA, United States of America
- 258 Department of Physics, Stellenbosch University, South Africa
- 259 Department of Physics, University of Fribourg, Fribourg, Switzerland
- 260 Department of Physics, University of Thessaly, Greece
- 261 Department of Physics, Westmont College, Santa Barbara, United States of America
- 262 Faculty of Physics, Sofia University, 'St. Kliment Ohridski', Sofia, Bulgaria
- 263 Faculty of Physics, University of Bucharest, Romania
- 264 Hellenic Open University, Patras, Greece
- 265 Henan University, China
- 266 Imam Mohammad Ibn Saud Islamic University, Saudi Arabia
- 267 Institució Catalana de Recerca i Estudis Avançats, ICREA, Barcelona, Spain
- 268 Institut für Experimentalphysik, Universität Hamburg, Hamburg, Germany
- 269 Institute for Nuclear Research and Nuclear Energy (INRNE), Bulgarian Academy of Sciences, Sofia, Bulgaria
- 270 Institute of Particle Physics (IPP), Canada
- 271 Institute of Physics and Technology, Mongolian Academy of Sciences, Ulaanbaatar, Mongolia
- 272 Institute of Theoretical Physics, Ilia State University, Tbilisi, Georgia
- 273 Millennium Institute for Subatomic physics at high energy frontier (SAPHIR), Santiago, Chile
- 274 The Collaborative Innovation Center of Quantum Matter (CICQM), Beijing, China
- 275 TRIUMF, Vancouver, BC, Canada
- 276 Università di Napoli Parthenope, Napoli, Italy
- 277 University of Chinese Academy of Sciences (UCAS), Beijing, China
- 278 Department of Physics, University of Colorado Boulder, Colorado, United States of America
- 279 University of Sienna, Italy
- 280 Washington College, Chestertown, MD, United States of America
- 281 Physics Department, Yeditepe University, Istanbul, Türkiye

References

- [1] U. Baur, A. Juste, L.H. Orr, D. Rainwater, Probing electroweak top quark couplings at hadron colliders, *Phys. Rev. D* 71 (2005) 054013. [arXiv:hep-ph/0412021](https://arxiv.org/abs/hep-ph/0412021), <https://doi.org/10.1103/PhysRevD.71.054013>
- [2] A.O. Bouzas, F. Larios, Electromagnetic dipole moments of the top quark, *Phys. Rev. D* 87 (7) (2013) 074015. [arXiv:1212.6575](https://arxiv.org/abs/1212.6575), <https://doi.org/10.1103/PhysRevD.87.074015>
- [3] M. Schulze, Y. Soreq, Pinning down electroweak dipole operators of the top quark, *Eur. Phys. J. C* 76 (8) (2016) 466. [arXiv:1603.08911](https://arxiv.org/abs/1603.08911), <https://doi.org/10.1140/epjc/s10052-016-4263-x>
- [4] B.B. Olga, F. Maltoni, I. Tsinikos, E. Vryonidou, C. Zhang, Probing top quark neutral couplings in the standard model effective field theory at NLO in QCD, *JHEP* 05 (2016) 052. [arXiv:1601.08193](https://arxiv.org/abs/1601.08193), [https://doi.org/10.1007/JHEP05\(2016\)052](https://doi.org/10.1007/JHEP05(2016)052)
- [5] CDF Collaboration, T. Aaltonen, et al., CDF, Evidence for $t\bar{t}\gamma$ production and measurement of $\sigma_{t\bar{t}\gamma}/\sigma_{t\bar{t}}$, *Phys. Rev. D* 84 (2011) 031104. [arXiv:1106.3970](https://arxiv.org/abs/1106.3970), <https://doi.org/10.1103/PhysRevD.84.031104>
- [6] ATLAS Collaboration, Observation of top-quark pair production in association with a photon and measurement of the $t\bar{t}\gamma$ production cross section in pp collisions at $\sqrt{s} = 7$ TeV using the ATLAS detector, *Phys. Rev. D* 91 (2015) 072007. [arXiv:1502.00586](https://arxiv.org/abs/1502.00586), <https://doi.org/10.1103/PhysRevD.91.072007>
- [7] ATLAS Collaboration, Measurement of the $t\bar{t}\gamma$ production cross section in proton-proton collisions at $\sqrt{s} = 8$ TeV with the ATLAS detector, *JHEP* 11 (2017) 086. [arXiv:1706.03046](https://arxiv.org/abs/1706.03046), [https://doi.org/10.1007/JHEP11\(2017\)086](https://doi.org/10.1007/JHEP11(2017)086)
- [8] CMS Collaboration, Measurement of the semileptonic $t\bar{t} + \gamma$ production cross section in pp collisions at $\sqrt{s} = 8$ TeV, *JHEP* 10 (2017) 006. [arXiv:1706.08128](https://arxiv.org/abs/1706.08128), [https://doi.org/10.1007/JHEP10\(2017\)006](https://doi.org/10.1007/JHEP10(2017)006)
- [9] ATLAS Collaboration, Measurements of inclusive and differential fiducial cross-sections of $t\bar{t}\gamma$ production in leptonic final states at $\sqrt{s} = 13$ TeV in ATLAS, *Eur. Phys. J. C* 79 (2019) 382. [arXiv:1812.01697](https://arxiv.org/abs/1812.01697), <https://doi.org/10.1140/epjc/s10052-019-6849-6>
- [10] ATLAS Collaboration, Measurements of inclusive and differential cross-sections of combined $t\bar{t}\gamma$ and $tW\gamma$ production in the $e\mu$ channel at 13 TeV with the ATLAS detector, *JHEP* 09 (2020) 049. [arXiv:2007.06946](https://arxiv.org/abs/2007.06946), [https://doi.org/10.1007/JHEP09\(2020\)049](https://doi.org/10.1007/JHEP09(2020)049)
- [11] CMS Collaboration, Measurement of the inclusive and differential $t\bar{t}\gamma$ cross sections in the single-lepton channel and EFT interpretation at $\sqrt{s} = 13$ TeV, *JHEP* 12 (2021) 180. [arXiv:2107.01508](https://arxiv.org/abs/2107.01508), [https://doi.org/10.1007/JHEP12\(2021\)180](https://doi.org/10.1007/JHEP12(2021)180)
- [12] CMS Collaboration, Measurement of the inclusive and differential $t\bar{t}\gamma$ cross sections in the dilepton channel and effective field theory interpretation in proton-proton collisions at $\sqrt{s} = 13$ TeV, *JHEP* 05 (2022) 091. [arXiv:2201.07301](https://arxiv.org/abs/2201.07301), [https://doi.org/10.1007/JHEP05\(2022\)091](https://doi.org/10.1007/JHEP05(2022)091)
- [13] ATLAS Collaboration, Measurements of inclusive and differential cross-sections of $t\bar{t}\gamma$ production in pp collisions at $\sqrt{s} = 13$ TeV with the ATLAS detector, *JHEP* 10 (2024) 191. [arXiv:2403.09452](https://arxiv.org/abs/2403.09452), [https://doi.org/10.1007/JHEP10\(2024\)191](https://doi.org/10.1007/JHEP10(2024)191)

- [14] ATLAS Collaboration, Measurement of the charge asymmetry in top-quark pair production in association with a photon with the ATLAS experiment, *Phys. Lett. B* 843 (2023) 137848. [arXiv:2212.10552](https://arxiv.org/abs/2212.10552), <https://doi.org/10.1016/j.physletb.2023.137848>
- [15] D. Pagani, H.-S. Shao, I. Tsiniokos, M. Zaro, Automated EW corrections with isolated photons: $t\bar{t}\gamma$, $t\bar{t}\gamma\gamma$ and $t\bar{t}j$ as case studies, *JHEP* 09 (2021) 155. [arXiv:2106.02059](https://arxiv.org/abs/2106.02059), [https://doi.org/10.1007/JHEP09\(2021\)155](https://doi.org/10.1007/JHEP09(2021)155)
- [16] D. Stremmer, M. Worek, Associated production of a top-quark pair with two isolated photons at the LHC through NLO in QCD, *JHEP* 08 (2023) 179. [arXiv:2306.16968](https://arxiv.org/abs/2306.16968), [https://doi.org/10.1007/JHEP08\(2023\)179](https://doi.org/10.1007/JHEP08(2023)179)
- [17] D. Stremmer, M. Worek, Complete NLO corrections to top-quark pair production with isolated photons, *JHEP* 07 (2024) 091. [arXiv:2403.03796](https://arxiv.org/abs/2403.03796), [https://doi.org/10.1007/JHEP07\(2024\)091](https://doi.org/10.1007/JHEP07(2024)091)
- [18] S.M. Etesami, E.D. Roknabadi, Probing the nonstandard top-gluon couplings through $t\bar{t}\gamma\gamma$ production at the LHC, *Phys. Rev. D* 100 (1) (2019) 015023. [arXiv:1810.07477](https://arxiv.org/abs/1810.07477), <https://doi.org/10.1103/PhysRevD.100.015023>
- [19] ATLAS Collaboration, Luminosity determination in pp collisions at $\sqrt{s} = 13$ TeV using the ATLAS detector at the LHC, *Eur. Phys. J. C* 83 (2023) 982. [arXiv:2212.09379](https://arxiv.org/abs/2212.09379), <https://doi.org/10.1140/epjc/s10052-023-11747-w>
- [20] ATLAS Collaboration, The ATLAS experiment at the CERN large hadron collider, *JINST* 3 (2008) S08003. <https://doi.org/10.1088/1748-0221/3/08/S08003>
- [21] G. Avoni, et al., The new LUCID-2 detector for luminosity measurement and monitoring in ATLAS, *JINST* 13 (2018) P07017. <https://doi.org/10.1088/1748-0221/13/07/P07017>
- [22] ATLAS Collaboration, Performance of the ATLAS trigger system in 2015, *Eur. Phys. J. C* 77 (2017) 317. [arXiv:1611.09661](https://arxiv.org/abs/1611.09661), <https://doi.org/10.1140/epjc/s10052-017-4852-3>
- [23] ATLAS Collaboration, Software and computing for Run 3 of the ATLAS experiment at the LHC, *Eur. Phys. J. C* 85 (2025) 234. [arXiv:2404.06335](https://arxiv.org/abs/2404.06335), <https://doi.org/10.1140/epjc/s10052-024-13701-w>
- [24] ATLAS Collaboration, The ATLAS simulation infrastructure, *Eur. Phys. J. C* 70 (2010) 823. [arXiv:1005.4568](https://arxiv.org/abs/1005.4568), <https://doi.org/10.1140/epjc/s10052-010-1429-9>
- [25] S. Agostinelli, et al., GEANT4 – a simulation toolkit, *Nucl. Instrum. Meth. A* 506 (2003) 250. [https://doi.org/10.1016/S0168-9002\(03\)01368-8](https://doi.org/10.1016/S0168-9002(03)01368-8)
- [26] P. Nason, A new method for combining NLO QCD with shower Monte Carlo algorithms, *JHEP* 11 (2004) 040. [arXiv:hep-ph/0409146](https://arxiv.org/abs/hep-ph/0409146), <https://doi.org/10.1088/1126-6708/2004/11/040>
- [27] S. Frixione, G. Ridolfi, P. Nason, A positive-weight next-to-leading-order Monte Carlo for heavy flavour hadroproduction, *JHEP* 09 (2007) 126. [arXiv:0707.3088](https://arxiv.org/abs/0707.3088), <https://doi.org/10.1088/1126-6708/2007/09/126>
- [28] S. Frixione, P. Nason, C. Oleari, Matching NLO QCD computations with parton shower simulations: the POWHEG method, *JHEP* 11 (2007) 070. [arXiv:0709.2092](https://arxiv.org/abs/0709.2092), <https://doi.org/10.1088/1126-6708/2007/11/070>
- [29] S. Alioli, P. Nason, C. Oleari, E. Re, A general framework for implementing NLO calculations in shower Monte Carlo programs: the POWHEG BOX, *JHEP* 06 (2010) 043. [arXiv:1002.2581](https://arxiv.org/abs/1002.2581), [https://doi.org/10.1007/JHEP06\(2010\)043](https://doi.org/10.1007/JHEP06(2010)043)
- [30] J. Alwall, R. Frederix, S. Frixione, V. Hirschi, F. Maltoni, O. Mattelaer, H.-S. Shao, T. Stelzer, P. Torrielli, M. Zaro, The automated computation of tree-level and next-to-leading order differential cross sections, and their matching to parton shower simulations, *JHEP* 07 (2014) 079. [arXiv:1405.0301](https://arxiv.org/abs/1405.0301), [https://doi.org/10.1007/JHEP07\(2014\)079](https://doi.org/10.1007/JHEP07(2014)079)
- [31] T. Sjöstrand, S. Ask, J.R. Christiansen, R. Corke, N. Desai, P. Ilten, S. Mrenna, S. Prestel, C.O. Rasmussen, P.Z. Skands, An introduction to PYTHIA 8.2, *Comput. Phys. Commun.* 191 (2015) 159. [arXiv:1410.3012](https://arxiv.org/abs/1410.3012), <https://doi.org/10.1016/j.cpc.2015.01.024>
- [32] ATLAS Collaboration, ATLAS Pythia 8 tunes to 7 TeV data, *ATL-PHYS-PUB-2014-021*, 2014. <https://cds.cern.ch/record/1966419>
- [33] NNPDF Collaboration, R.D. Ball, et al., Parton distributions with LHC data, *Nucl. Phys. B* 867 (2013) 244. [arXiv:1207.1303](https://arxiv.org/abs/1207.1303), <https://doi.org/10.1016/j.nuclphysb.2012.10.003>
- [34] D.J. Lange, The EvtGen particle decay simulation package, *Nucl. Instrum. Meth. A* 462 (2001) 152. [https://doi.org/10.1016/S0168-9002\(01\)00089-4](https://doi.org/10.1016/S0168-9002(01)00089-4)
- [35] T. Gleisberg, S. Höche, F. Krauss, M. Schönherr, S. Schumann, F. Siegert, J. Winter, Event generation with SHERPA 1.1, *JHEP* 02 (2009) 007. [arXiv:0811.4622](https://arxiv.org/abs/0811.4622), <https://doi.org/10.1088/1126-6708/2009/02/007>
- [36] S. Höche, F. Krauss, S. Schumann, F. Siegert, QCD matrix elements and truncated showers, *JHEP* 05 (2009) 053. [arXiv:0903.1219](https://arxiv.org/abs/0903.1219), <https://doi.org/10.1088/1126-6708/2009/05/053>
- [37] S. Schumann, F. Krauss, A parton shower algorithm based on Catani–Seymour dipole factorisation, *JHEP* 03 (2008) 038. [arXiv:0709.1027](https://arxiv.org/abs/0709.1027), <https://doi.org/10.1088/1126-6708/2008/03/038>
- [38] T. Sjöstrand, S. Mrenna, P. Skands, A brief introduction to PYTHIA 8.1, *Comput. Phys. Commun.* 178 (2008) 852–867. [arXiv:0710.3820](https://arxiv.org/abs/0710.3820), <https://doi.org/10.1016/j.cpc.2008.01.036>
- [39] ATLAS Collaboration, The Pythia 8 A3 tune description of ATLAS minimum bias and inelastic measurements incorporating the Donnachie–Landshoff diffractive model, *ATL-PHYS-PUB-2016-017*, 2016. <https://cds.cern.ch/record/2206965>
- [40] NNPDF Collaboration, R.D. Ball, et al., Parton distributions for the LHC Run II, *JHEP* 04 (2015) 040. [arXiv:1410.8849](https://arxiv.org/abs/1410.8849), [https://doi.org/10.1007/JHEP04\(2015\)040](https://doi.org/10.1007/JHEP04(2015)040)
- [41] C. Bierlich, S. Chakraborty, N. Desai, L. Gellersen, I. Helenius, P. Ilten, L. Lönnblad, S. Mrenna, S. Prestel, C.T. Preuss, T. Sjöstrand, P. Skands, M. Utheim, R. Verheyen, A comprehensive guide to the physics and usage of PYTHIA 8.3, *SciPost Phys. Codeb.* (2022) 8. [arXiv:2203.11601](https://arxiv.org/abs/2203.11601), <https://doi.org/10.21468/SciPostPhysCodeb.8>
- [42] S. Frixione, Isolated photons in perturbative QCD, *Phys. Lett. B* 429 (1998) 369–374. [arXiv:hep-ph/9801442](https://arxiv.org/abs/hep-ph/9801442), [https://doi.org/10.1016/S0370-2693\(98\)00454-7](https://doi.org/10.1016/S0370-2693(98)00454-7)
- [43] S. Frixione, E. Laenen, P. Motylinski, B.R. Webber, Angular correlations of lepton pairs from vector boson and top quark decays in Monte Carlo simulations, *JHEP* 04 (2007) 081. [arXiv:hep-ph/0702198](https://arxiv.org/abs/hep-ph/0702198), <https://doi.org/10.1088/1126-6708/2007/04/081>
- [44] P. Artoisenet, R. Frederix, O. Mattelaer, R. Rietkerk, Automatic spin-entangled decays of heavy resonances in Monte Carlo simulations, *JHEP* 03 (2013) 015. [arXiv:1212.3460](https://arxiv.org/abs/1212.3460), [https://doi.org/10.1007/JHEP03\(2013\)015](https://doi.org/10.1007/JHEP03(2013)015)
- [45] ATLAS Collaboration, Studies on top-quark Monte Carlo modelling for Top2016, *ATL-PHYS-PUB-2016-020*, 2016. <https://cds.cern.ch/record/2216168>
- [46] M. Czakon, A. Mitov, Top++: a program for the calculation of the top-pair cross-section at hadron colliders, *Comput. Phys. Commun.* 185 (2014) 2930. [arXiv:1112.5675](https://arxiv.org/abs/1112.5675), <https://doi.org/10.1016/j.cpc.2014.06.021>
- [47] N. Kidonakis, Two-loop soft anomalous dimensions for single top quark associated production with a W^- or H^- , *Phys. Rev. D* 82 (2010) 054018. [arXiv:1005.4451](https://arxiv.org/abs/1005.4451), <https://doi.org/10.1103/PhysRevD.82.054018>
- [48] N. Kidonakis, Next-to-next-to-leading logarithm resummation for s-channel single top quark production, *Phys. Rev. D* 81 (2010) 054028. [arXiv:1001.5034](https://arxiv.org/abs/1001.5034), <https://doi.org/10.1103/PhysRevD.81.054028>
- [49] N. Kidonakis, Next-to-next-to-leading-order collinear and soft gluon corrections for t-channel single top quark production, *Phys. Rev. D* 83 (2011) 091503. [arXiv:1103.2792](https://arxiv.org/abs/1103.2792), <https://doi.org/10.1103/PhysRevD.83.091503>
- [50] D. de Florian, et al., LHC Higgs Cross Section Working Group, Handbook of LHC Higgs Cross Sections: 4. Deciphering the Nature of the Higgs Sector (2017). [arXiv:1610.07922](https://arxiv.org/abs/1610.07922), <https://doi.org/10.23731/CYRM-2017-002>
- [51] J.M. Campbell, R.K. Ellis, Update on vector boson pair production at hadron colliders, *Phys. Rev. D* 60 (1999) 113006. [arXiv:hep-ph/9905386](https://arxiv.org/abs/hep-ph/9905386), <https://doi.org/10.1103/PhysRevD.60.113006>
- [52] ATLAS Collaboration, Measurement of W^\pm and Z-boson production cross sections in pp collisions at $\sqrt{s} = 13$ TeV with the ATLAS detector, *Phys. Lett. B* 759 (2016) 601. [arXiv:1603.09222](https://arxiv.org/abs/1603.09222), <https://doi.org/10.1016/j.physletb.2016.06.023>
- [53] ATLAS Collaboration, Performance of the ATLAS muon triggers in Run 2, *JINST* 15 (2020) P09015. [arXiv:2004.13447](https://arxiv.org/abs/2004.13447), <https://doi.org/10.1088/1748-0221/15/09/P09015>
- [54] ATLAS Collaboration, Performance of electron and photon triggers in ATLAS during LHC Run 2, *Eur. Phys. J. C* 80 (2020) 47. [arXiv:1909.00761](https://arxiv.org/abs/1909.00761), <https://doi.org/10.1140/epjc/s10052-019-7500-2>
- [55] ATLAS Collaboration, Operation of the ATLAS trigger system in Run 2, *JINST* 15 (2020) P10004. [arXiv:2007.12539](https://arxiv.org/abs/2007.12539), <https://doi.org/10.1088/1748-0221/15/10/P10004>
- [56] ATLAS Collaboration, The ATLAS inner detector trigger performance in pp collisions at 13 TeV during LHC Run 2, *Eur. Phys. J. C* 82 (2022) 206. [arXiv:2107.02485](https://arxiv.org/abs/2107.02485), <https://doi.org/10.1140/epjc/s10052-021-09920-0>
- [57] ATLAS Collaboration, Vertex Reconstruction Performance of the ATLAS Detector at $\sqrt{s} = 13$ TeV, *ATL-PHYS-PUB-2015-026*, 2015. <https://cds.cern.ch/record/2037717>
- [58] ATLAS Collaboration, Electron and photon performance measurements with the ATLAS detector using the 2015–2017 LHC proton–proton collision data, *JINST* 14 (2019) P2006. [arXiv:1908.00005](https://arxiv.org/abs/1908.00005), <https://doi.org/10.1088/1748-0221/14/12/P2006>
- [59] ATLAS Collaboration, Muon reconstruction and identification efficiency in ATLAS using the full Run 2 pp collision data set at $\sqrt{s} = 13$ TeV, *Eur. Phys. J. C* 81 (2021) 578. [arXiv:2012.00578](https://arxiv.org/abs/2012.00578), <https://doi.org/10.1140/epjc/s10052-021-09233-2>
- [60] ATLAS Collaboration, Evidence for the associated production of the Higgs boson and a top quark pair with the ATLAS detector, *Phys. Rev. D* 97 (2018) 072003. [arXiv:1712.08891](https://arxiv.org/abs/1712.08891), <https://doi.org/10.1103/PhysRevD.97.072003>
- [61] M. Cacciari, G.P. Salam, G. Soyez, The anti- k_t jet clustering algorithm, *JHEP* 04 (2008) 063. [arXiv:0802.1189](https://arxiv.org/abs/0802.1189), <https://doi.org/10.1088/1126-6708/2008/04/063>
- [62] M. Cacciari, G.P. Salam, G. Soyez, FastJet user manual, *Eur. Phys. J. C* 72 (2012) 1896. [arXiv:1111.6097](https://arxiv.org/abs/1111.6097), <https://doi.org/10.1140/epjc/s10052-012-1896-2>
- [63] ATLAS Collaboration, Jet reconstruction and performance using particle flow with the ATLAS detector, *Eur. Phys. J. C* 77 (2017) 466. [arXiv:1703.10485](https://arxiv.org/abs/1703.10485), <https://doi.org/10.1140/epjc/s10052-017-5031-2>
- [64] ATLAS Collaboration, Jet energy scale and resolution measured in proton–proton collisions at $\sqrt{s} = 13$ TeV with the ATLAS detector, *Eur. Phys. J. C* 81 (2021) 689. [arXiv:2007.02645](https://arxiv.org/abs/2007.02645), <https://doi.org/10.1140/epjc/s10052-021-09402-3>
- [65] ATLAS Collaboration, Performance of pile-up mitigation techniques for jets in pp collisions at $\sqrt{s} = 8$ TeV using the ATLAS detector, *Eur. Phys. J. C* 76 (2016) 581. [arXiv:1510.03823](https://arxiv.org/abs/1510.03823), <https://doi.org/10.1140/epjc/s10052-016-4395-z>
- [66] ATLAS Collaboration, ATLAS flavour-tagging algorithms for the LHC Run 2 pp collision dataset, *Eur. Phys. J. C* 83 (2023) 681. [arXiv:2211.16345](https://arxiv.org/abs/2211.16345), <https://doi.org/10.1140/epjc/s10052-023-11699-1>
- [67] ATLAS Collaboration, The performance of missing transverse momentum reconstruction and its significance with the ATLAS detector using 140 fb^{-1} of $\sqrt{s} = 13$ TeV pp collisions, *Eur. Phys. J. C* 85 (2025) 606. [arXiv:2402.05858](https://arxiv.org/abs/2402.05858), <https://doi.org/10.1140/epjc/s10052-025-14062-8>
- [68] ATLAS Collaboration, Electron and photon efficiencies in LHC Run 2 with the ATLAS experiment, *JHEP* 05 (2024) 162. [arXiv:2308.13362](https://arxiv.org/abs/2308.13362), [https://doi.org/10.1007/JHEP05\(2024\)162](https://doi.org/10.1007/JHEP05(2024)162)
- [69] CDF Collaboration, Measurement of $\sigma(BW \rightarrow e\nu)$ and $\sigma(BZ^0 \rightarrow e^+e^-)$ in $p\bar{p}$ collisions at $\sqrt{s} = 1800$ GeV, *Phys. Rev. D* 44 (1991) 29–52. <https://doi.org/10.1103/PhysRevD.44.29>
- [70] J. Butterworth, et al., PDF4LHC recommendations for LHC Run II, *J. Phys. G* 43 (2016) 023001. [arXiv:1510.03865](https://arxiv.org/abs/1510.03865), <https://doi.org/10.1088/0954-3899/43/2/023001>

- [71] M. Bähr, et al., Herwig++ physics and manual, *Eur. Phys. J. C* 58 (2008) 639. [arXiv:0803.0883](https://arxiv.org/abs/0803.0883), <https://doi.org/10.1140/epjc/s10052-008-0798-9>
- [72] J. Bellm, et al., Herwig 7.0/Herwig++ 3.0 release note, *Eur. Phys. J. C* 76 (4) (2016) 196. [arXiv:1512.01178](https://arxiv.org/abs/1512.01178), <https://doi.org/10.1140/epjc/s10052-016-4018-8>
- [73] ATLAS Collaboration, Improvements in $t\bar{t}$ modelling using NLO+PS Monte Carlo generators for Run 2, ATL-PHYS-PUB-2018-009, 2018. <https://cds.cern.ch/record/2630327>.
- [74] ATLAS Collaboration, Observation of $W\gamma\gamma$ triboson production in proton–proton collisions at $\sqrt{s} = 13$ TeV with the ATLAS detector, *Phys. Lett. B* 848 (2024) 138400. [arXiv:2308.03041](https://arxiv.org/abs/2308.03041), <https://doi.org/10.1016/j.physletb.2023.138400>
- [75] ATLAS Collaboration, ATLAS b -jet identification performance and efficiency measurement with $t\bar{t}$ events in pp collisions at $\sqrt{s} = 13$ TeV, *Eur. Phys. J. C* 79 (2019) 970. [arXiv:1907.05120](https://arxiv.org/abs/1907.05120), <https://doi.org/10.1140/epjc/s10052-019-7450-8>
- [76] ATLAS Collaboration, Measurement of the c -jet mistagging efficiency in $t\bar{t}$ events using pp collision data at $\sqrt{s} = 13$ TeV collected with the ATLAS detector, *Eur. Phys. J. C* 82 (2022) 95. [arXiv:2109.10627](https://arxiv.org/abs/2109.10627), <https://doi.org/10.1140/epjc/s10052-021-09843-w>
- [77] ATLAS Collaboration, Calibration of the light-flavour jet mistagging efficiency of the b -tagging algorithms with Z +jets events using 139 fb^{-1} of ATLAS proton–proton collision data at $\sqrt{s} = 13$ TeV, *Eur. Phys. J. C* 83 (2023) 728. [arXiv:2301.06319](https://arxiv.org/abs/2301.06319), <https://doi.org/10.1140/epjc/s10052-023-11736-z>
- [78] T. Chen, C. Guestrin, XGBoost: a scalable tree boosting system, in: Proceedings of the 22nd ACM SIGKDD International Conference on Knowledge Discovery and Data Mining, ACM, 2016, p. 785–794. <https://doi.org/10.1145/2939672.2939785>
- [79] M. Cacciari, G.P. Salam, G. Soyez, The catchment area of jets, *JHEP* 04 (2008) 005. [arXiv:0802.1188](https://arxiv.org/abs/0802.1188), <https://doi.org/10.1088/1126-6708/2008/04/005>
- [80] G. Cowan, K. Cranmer, E. Gross, O. Vitells, Asymptotic formulae for likelihood-based tests of new physics, *Eur. Phys. J. C* 71 (2011) 1554. [arXiv:1007.1727](https://arxiv.org/abs/1007.1727), <https://doi.org/10.1140/epjc/s10052-011-1554-0>
- [81] S. Baker, R.D. Cousins, Clarification of the use of CHI-square and likelihood functions in fits to histograms, *Nucl. Instrum. Meth.* 221 (2) (1984) 437–442. [https://doi.org/10.1016/0167-5087\(84\)90016-4](https://doi.org/10.1016/0167-5087(84)90016-4)
- [82] ATLAS Collaboration, ATLAS Computing Acknowledgements, ATL-SOFT-PUB-2025-001, 2025. <https://cds.cern.ch/record/2922210>.